Journal of Human Evolution xxx (2012) 1–30

Contents lists available at SciVerse ScienceDirect

Journal of Human Evolution

journal homepage: www.elsevier.com/locate/jhevol

The environmental context for the origins of modern human diversity: A synthesis of regional variability in African climate 150,000–30,000 years ago

Margaret Whiting Blome [a,*], Andrew S. Cohen [a], Christian A. Tryon [b], Alison S. Brooks [c], Joellen Russell [a]

[a] Department of Geosciences, University of Arizona, 1040 E 4th St., Tucson, AZ 85712, USA
[b] Center for the Study of Human Origins, Department of Anthropology, New York University, 25 Waverly Place, NYC, NY 10003, USA
[c] Department of Anthropology, George Washington University, 2110 G St., NW, Washington, DC 20052, USA

ARTICLE INFO

Article history:
Received 17 March 2011
Accepted 24 January 2012

Keywords:
Paleoclimate
Pleistocene
Homo sapiens
Demography
Population dispersal

ABSTRACT

We synthesize African paleoclimate from 150 to 30 ka (thousand years ago) using 85 diverse datasets at a regional scale, testing for coherence with North Atlantic glacial/interglacial phases and northern and southern hemisphere insolation cycles. Two major determinants of circum-African climate variability over this time period are supported by principal components analysis: North Atlantic sea surface temperature (SST) variations and local insolation maxima. North Atlantic SSTs correlated with the variability found in most circum-African SST records, whereas the variability of the majority of terrestrial temperature and precipitation records is explained by local insolation maxima, particularly at times when solar radiation was intense and highly variable (e.g., 150–75 ka). We demonstrate that climates varied with latitude, such that periods of relatively increased aridity or humidity were asynchronous across the northern, eastern, tropical and southern portions of Africa. Comparisons of the archaeological, fossil, or genetic records with generalized patterns of environmental change based solely on northern hemisphere glacial/interglacial cycles are therefore imprecise.

We compare our refined climatic framework to a database of 64 radiometrically-dated paleoanthropological sites to test hypotheses of demographic response to climatic change among African hominin populations during the 150–30 ka interval. We argue that at a continental scale, population and climate changes were asynchronous and likely occurred under different regimes of climate forcing, creating alternating opportunities for migration into adjacent regions. Our results suggest little relation between large scale demographic and climate change in southern Africa during this time span, but strongly support the hypothesis of hominin occupation of the Sahara during discrete humid intervals ~135–115 ka and 105–75 ka. Hominin populations in equatorial and eastern Africa may have been buffered from the extremes of climate change by locally steep altitudinal and rainfall gradients and the complex and variable effects of increased aridity on human habitat suitability in the tropics. Our data are consistent with hominin migrations out of Africa through varying exit points from ~140–80 ka.

Introduction

Fossil and genetic data are consistent with an African origin of *Homo sapiens* by 195,000 years ago (ka) (Ingman et al., 2000; Clark et al., 2003; White et al., 2003; McDougall et al., 2005; Gonder et al., 2007). Numerous studies have emphasized the diversity in morphology, life history, and genetic signatures likely present among populations of Middle and Late Pleistocene hominins, some of which dispersed from Africa in the Late Pleistocene, replacing existing hominin populations in parts of Eurasia and eventually colonizing Australia and North and South America. The variability among the source populations within Africa is compounded by local demographic changes and range expansions or contractions, as well as the persistence of ancestral or sister taxa (Lahr and Foley, 1998; Howell, 1999; Excoffier, 2002; Forster, 2004; Harding and McVean, 2004; Eswaran et al., 2005; Prugnolle et al., 2005; Trinkaus, 2005; Garrigan and Hammer, 2006; Garrigan et al., 2007; Smith et al., 2007; Bräuer, 2008; Pearson, 2008; Crevecoeur et al., 2009; Gunz et al., 2009; Hammer et al., 2011; Harvati et al.,

* Corresponding author.
E-mail addresses: mwblom@email.arizona.edu, meg_blome@yahoo.com (M.W. Blome).

0047-2484/$ – see front matter © 2012 Elsevier Ltd. All rights reserved.
doi:10.1016/j.jhevol.2012.01.011

2011). Middle Stone Age (MSA) archaeological sites provide the strongest record of the behavior of early African populations of *H. sapiens*, and these sites record pronounced spatial and temporal variation not seen in earlier periods (McBrearty and Brooks, 2000; Henshilwood and Marean, 2003; Marean and Assefa, 2005; Jacobs et al., 2008a; Shea, 2011).

Paleoenvironmental history and variability during the Middle and Late Pleistocene may have played a crucial role in shaping the biological diversity, distribution and behavior of *H. sapiens* populations during this period. Environmental change is a causal mechanism for the dispersal and isolation of animal populations, and the accumulation of variation through drift resulting from geographic isolation (allopatry) is a central cause of biological divergence and speciation (e.g., Barraclough and Nee, 2001; Mayr, 2001). Human behavioral change occurs as a result of a range of causal factors and we do not advocate strict environmental determinism. However, recent and ancient human forager subsistence, technology, land use, and some social behaviors show clear relationships with environment (Kelly, 1995; Binford, 2001; Kuhn and Stiner, 2001; Marlowe, 2005), and archaeological changes at some Middle Stone Age (MSA) sites have been interpreted as behavioral responses to variation in resource structure and availability as a result of environmental shifts (Ambrose and Lorenz, 1990; Marean et al., 2007; McCall, 2007). Our objective here is to synthesize available African Middle and Late Pleistocene paleoclimatic and paleoanthropological records relevant to early populations of *H. sapiens*. Although a number of studies have focused on providing the environmental context for subsequent hominin dispersals out of Africa (cf. Carto et al., 2009; Osbourne et al., 2008; Vaks et al., 2007; but see; Basell, 2008; Cowling et al., 2008; Drake et al., 2008), recent genetic evidence has also indicated the importance of Pleistocene population dispersal within Africa and its importance in shaping modern human genetic diversity (e.g., Reed and Tishkoff, 2006; Behar et al., 2008; Tishkoff et al., 2009; Verdu et al., 2009; see also Hammer et al., 2011). Our goal therefore is to explore climatic variability within Africa during this time period to better understand both the context of intra-African hominin population dispersal and conditions relevant to out-of-Africa scenarios.

We emphasize the importance of considering different temporal and spatial frameworks for interpreting the role of climate change in human evolution, and these can be conceived of as occupying a continuum from macro-scale to micro-scale approaches. Macro-scale approaches include those that examine continental scale changes across long time intervals (e.g., Potts, 1998; deMenocal, 2004) or use coarse temporal frameworks such as the Marine Isotope Stage boundaries and glacial/interglacial variation (e.g., Lahr and Foley, 1998; Marean and Assefa, 2005; Basell, 2008; Crowley and Hyde, 2008). At the other end of the continuum are micro-scale approaches that seek to understand the response of small populations to environmental change over relatively short periods recorded at a single archaeological site or depositional basin (e.g., Potts et al., 1999). We are not suggesting that either macro-scale or micro-scale approaches are 'better', but rather that the scale of the available data should match the scale of the questions being asked.

Following other recent efforts (e.g., Fisher et al., 2010; Marean et al., 2010; Drake et al., 2011), we employ what might be termed a 'meso-scale' approach in the examination of sub-continental variation in paleoclimate and the human fossil and archaeological records. To do so, we synthesize paleoclimate data from diverse datasets of varying degrees of temporal and spatial resolution, divided into three broad categories: (1) cores from offshore marine sites, whose age models are largely constrained by the global oxygen isotope time scale. These provide relatively continuous data sampled over a large area, and provide key data on sea surface temperatures and ocean circulation patterns, changes in terrestrial vegetation patterns and relative aridity; (2) cores from a number of African lakes, particularly Lake Malawi and Lake Tanganyika. As well as the impact crater lakes Tswaing and Bosumtwi, which provide relatively continuous records of watershed and regional environmental change; (3) a number of other terrestrial sedimentary archives, including caves, rockshelters, and open-air archaeological sites that provide temporally discontinuous, often highly local records of climatic and environmental change. We compare these climatic and environmental data to a database of published, radiometrically dated hominin fossil- or artifact-bearing deposits to test whether these changes are coincident with demographic changes in Pleistocene African hominin populations.

We focus on the 150–30 ka time interval for theoretical and practical reasons. This time period is important as it includes much of the early history of *H. sapiens*, and from an archaeological perspective, it includes the shift from MSA to Later Stone Age (LSA) technologies, an important change that may signal changes in human cognition or demography (cf. Klein, 2009; Powell et al., 2009). Pragmatically, 150 ka marks the beginning of the time interval for which statistically significant numbers of detailed, well-constrained records are available from both the oceanic sites surrounding Africa and for a number of the key lake records such as Lake Malawi. In addition, the paleoclimate records for the past 30 kyr (thousand years) in Africa have long been a focus of earlier reviews (e.g., Street and Grove, 1979; Nicholson and Flohn, 1980). Because we are aggregating datasets of varying degrees of temporal resolution, often particularly poor for the archaeological record, we examine paleoclimate change using 5 kyr intervals and paleoanthropological change using estimated 10 kyr intervals, as detailed below.

Research questions and hypotheses

We synthesize African paleoclimate and paleoanthropological data from 150 to 30 ka, and use these data to test a number of hypotheses.

Pleistocene tropical African precipitation history is coincident with glacial/interglacial history

Many important recent works have used the Marine Isotope Stage (MIS) boundaries as a framework to explore the relation between Pleistocene African environmental change and human evolution (Lahr and Foley, 1998; Marean and Assefa, 2005; Barham and Mitchell, 2008; Basell, 2008). Such an approach has the potential to provide a common global temporal and environmental framework for exploring variation in Africa and elsewhere, but its utility would be severely compromised if African climates do not vary in phase with recognized MIS boundaries. We therefore test the extent to which changes in African paleoclimates are coincident with changes predicted by MIS boundaries derived from North Atlantic and North Pole data.

Pleistocene African climate change is coincident with Northern and Southern Hemisphere insolation cycles on a continent-wide basis

A number of recent studies (e.g., deMenocal and Rind, 1993; Kingston, 2007; Trauth et al., 2009) have emphasized the importance of monsoon intensity driven by precession-modulated insolation for tropical African climates. This hypothesis predicts that climatic change follows ~19–23 kyr cycles rather than the temporally variable MIS boundaries, and that the impact of this cyclicity is strongly expressed across Africa. We test the extent to

Please cite this article in press as: Blome, M.W., et al., The environmental context for the origins of modern human diversity: A synthesis of regional variability in African climate 150,000–30,000 years ago, Journal of Human Evolution (2012), doi:10.1016/j.jhevol.2012.01.011

which changes in African paleoclimate are coincident with changes predicted by Northern and Southern Hemisphere insolation cycles.

Pleistocene tropical African precipitation history is the result of the complex interaction of a number of factors, including atmospheric dynamics

Neither MIS boundaries nor precessional cycles likely account for all elements of climate change in Africa (deMenocal et al., 1993; deMenocal and Rind, 1993), and we thus explore other possible mechanisms including the paleo-position of the Westerlies and the Intertropical Convergence Zone (ITCZ). If the location of the Westerlies is a major driver of African climate, then the paleo-humidity records of North and South Africa should co-vary through time. Changes in the average ITCZ position over extended time periods may explain long-term moisture variation between ~20°N and 15°S (Tropical and/or East Africa) over the 150–30 ka time interval.

Climate change is asynchronous across Africa

Africa is large, spanning more than 70° of latitude. Given its size, it is perhaps unsurprising that a number of recent studies suggest that periods of climate change may be out of phase among different regions of Africa (e.g., Cohen et al., 2007; Scholz et al., 2007). We test this hypothesis by comparing climate change in Africa among four latitudinally-defined regions (North Africa and the Levant, East Africa, tropical Africa, southern Africa). This spatial component is often overlooked or insufficiently stressed in studies combining archaeological and environmental datasets.

Changes in climate impacted the distribution of Pleistocene African hominin populations

Genetic and fossil data suggest demographic changes among Pleistocene African populations of *H. sapiens*, including fluctuations in size and increases in ancient lineage diversity that may be linked to environmental change (Lahr and Foley, 1998; Excoffier, 2002; Ambrose, 2003; Prugnolle et al., 2005; Mellars, 2006; Basell, 2008; Behar et al., 2008; Carto et al., 2009; Crevecoeur et al., 2009; Gunz et al., 2009; Tishkoff et al., 2009; Marean, 2010). We use the frequency of paleoanthropological sites from across Africa as a crude proxy for changes in relative hominin population size for a given time interval. We expect that climate change and its more local impacts on floral and faunal communities will affect the nature, distribution, and abundance of human forager societies. However, environmental change, particularly increased aridity, likely had different effects on each of our four latitudinally-defined geographic regions. For example, drier intervals in tropical Africa may have made more areas accessible to hominin foragers through the fragmentation of dense forests and consequent creation of new or wider ecotones (e.g., Ambrose, 2001; Cornelissen, 2002). In contrast, some increase in aridity in parts of eastern Africa and the southern African interior could have promoted the expansion of grasslands, where much of the edible biomass is distributed among dispersed migratory game herds, potentially causing hominin foragers to experience resource stress, population dispersal or decline (see discussion in Marean, 1997). Marginal areas, such as deserts, may have been abandoned during periods of heightened aridity. Coastal zones may have been the least affected by increased aridity, although shallow gradient coastal margins would have shifted dramatically with lowered sea levels, exposing new coastal environments (Marean, 2010). We can predict relative increases and decreases in population density and site visibility from each of these outcomes. Specifically:

(a) *The southern African interior (and possibly the coast) was largely depopulated during arid intervals, particularly during the last 60 kyr, as a result of environmental degradation and shoreline shifts*. This hypothesis has been most clearly articulated in the work of Deacon and Thackeray (1984), Butzer (1988), and Klein (2009).

(b) *Hominin populations in the equatorial portions of the continent show relatively muted responses to climate change*. This hypothesis is consistent with Ambrose (1998), Marean and Assefa (2005), and Basell (2008). They suggest that hominin populations in East Africa and, to a lesser extent, tropical Africa may have been buffered from some of the extremes of climate change seen elsewhere as a result of locally steep altitudinal and rainfall gradients. As such, we predict muted demographic responses to environmental change compared with other regions. This hypothesis is also consistent with ecological studies indicating greater endemism among all vertebrate species in more tropical regions with high topographic relief (e.g., Sandel et al., 2011).

(c) *The nature and expanse of the Sahara strongly influenced the population history of northern Africa, with occupation of much of the interior of this region limited to periods of increased humidity when the 'green Sahara' was characterized by savanna and lake environments. As a corollary, 'out of Africa' hominin dispersals are similarly constrained to these humid intervals*. The impact of environmental change in the Sahara region on local human populations is an idea with a significant intellectual pedigree, but most recently synthesized by Osbourne et al. (2008) and Drake et al. (2011).

Methods

To test these hypotheses, we constructed a database from the published literature, synthesizing all relevant dated climatic and paleoanthropological data. The geographic locations of these datasets are shown in Figs. 1 and 2, with data synthesized in Tables 1 and 2. Note that throughout the paper, paleoclimate data archives are referenced by the numbers presented in Table 1.

Paleoclimate data collection

We collected and examined quantitative and semi-quantitative records of African paleoclimate for the 150–30 ka interval from the published literature from sites across the African continent and the surrounding regions of the Mediterranean, Near East and the adjacent ocean basins. The chosen terrestrial records are radiometrically dated, whereas the marine records are primarily dated through correlation with the marine oxygen isotope record. Data were compiled from published, tabulated information, or, when necessary, digitized from published graphs using DigitizeIt© (www.digitizeit.de). Changes in temperature and moisture availability are the primary indices of terrestrial paleoclimate variation, and we employ a number of different proxy measures of these variables in our analyses. These paleoclimate records from marine, nearshore, and terrestrial settings are summarized in Table 3, with syntheses relying strongly on sea surface temperatures (SSTs) for the marine records, and intervals of 'wet', 'dry', 'hot', or 'cold' relative to the average for a particular site.

African regions

As shown in Fig. 1, Africa and its surrounding area are divided into regions for comparisons among the marine and terrestrial data. Marine data archives are classified into one of four regions based on their geographic location: northern Atlantic and Mediterranean, southern Atlantic, Indian Ocean, and Southern Ocean (Fig. 1a). The

Please cite this article in press as: Blome, M.W., et al., The environmental context for the origins of modern human diversity: A synthesis of regional variability in African climate 150,000–30,000 years ago, Journal of Human Evolution (2012), doi:10.1016/j.jhevol.2012.01.011

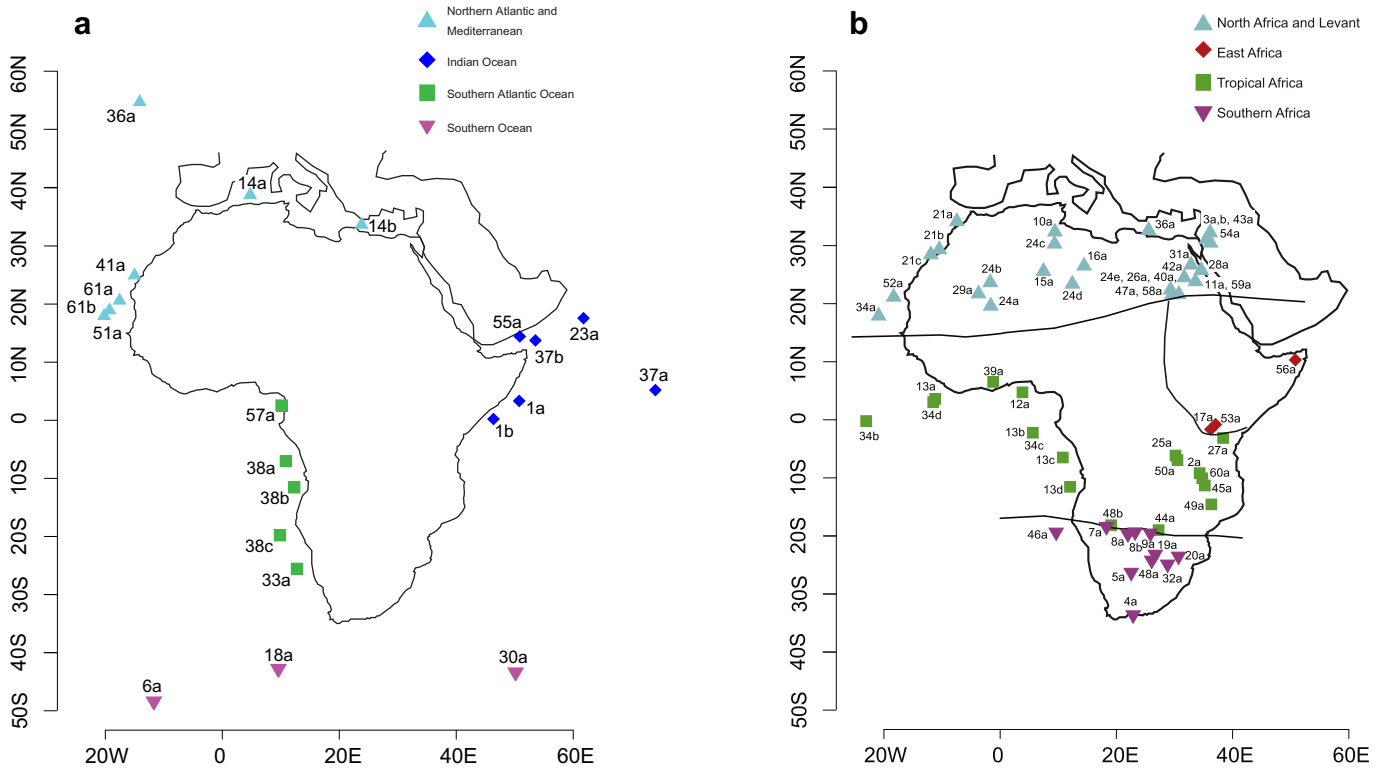

Figure 1. a) Regional distribution of marine climate sites. b) Regional distribution of continental climate sites.

terrestrial data were grouped into regions that show persistent climatic similarities through time, and that are distinct from bounding areas. Regions are divided as follows: North Africa and Levant, East Africa, tropical Africa, southern Africa (Fig. 1b). The North Africa region includes those areas north of ~15°N, East Africa extends northeast from the Eastern Rift Valley towards the Horn of Africa between the North Africa and tropical regions, the tropical region extends southward from ~15°N in western Africa and ~1°S in eastern Africa, with the southern boundary at ~19°S latitude, and southern Africa including areas south of ~19°S. The exact placement of the northern and southern boundaries for 'tropical Africa' is primarily defined by the location of sites displaying a 'megadrought' signal between 90 and 135 ka (see Scholz et al., 2007). The same terrestrial regions were used to analyze the paleoanthropological data and the data from marine cores housing paleoclimate archives of continental origin, such as wind-borne pollen records.

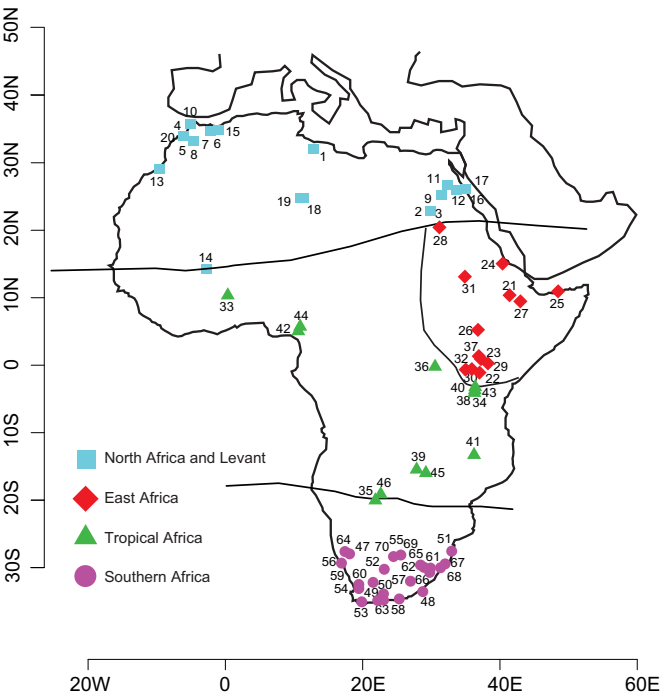

Figure 2. Regional distribution of paleoanthropological sites used in this synthesis.

Paleoclimate data analysis: regional analyses of temporal trends

Climate histories for the marine SSTs and continental data were summarized based on all data, including discrete and discontinuous datasets. We visually inspected the bivariate plots comparing changes in paleoclimate records and time, to assess the synchrony of aridity/humidity among the different regions of the continent with temperature in local and distant oceanic regions. The relation and timing of changes related to orbital forcing of subtropical summer insolation and high latitude variability and global glacial/interglacial phases was determined using principal components analysis (PCA) using R (http://www.r-project.org/).

Data used in the PCA were taken from each 'usable' dataset every 5 kyr over the period of the analysis, using multiple temperature and precipitation proxies from numerous locations. 'Usable datasets' did not include low-resolution datasets with binary-type information, and had to cover the entire time interval to be included in the analysis. These data were then transformed to satisfy the analytical assumptions of PCA. Specifically, data were normalized to a maximum value of one so that no large value was given more weight than others; rather the polarity of the trends (positive or negative) was highlighted. This normalization also eliminated the potential discrepancies associated with the differing units used in

Please cite this article in press as: Blome, M.W., et al., The environmental context for the origins of modern human diversity: A synthesis of regional variability in African climate 150,000–30,000 years ago, Journal of Human Evolution (2012), doi:10.1016/j.jhevol.2012.01.011

Table 1
Climate sites used in the synthesis. Those used for the PCA have S, T, or P under the heading "STP?" to designate the type of record: sea surface temperature (S), terrestrial temperature (T), or terrestrial precipitation (P).

Labels	Authors	Latitude	Longitude	Region	TerrSST	STP?
1a	Bard et al., 1997	3.18	50.43	Indian	SST	S
1b	Bard et al., 1997	0.02	46.03	Indian	SST	S
2a	Barker et al., 2003	−9.35	33.75	Tropical	Terr	
3a	Bar-Matthews et al., 2003	32.58	35.19	North	Terr	P
3b	Bar-Matthews et al., 2003	31.50	35.00	North	Terr	P
4a	Bar-Matthews et al., 2010	−34.21	22.09	South	Terr	
5a	Bateman et al., 2003	−27.00	22.00	South	Terr	
6a	Brathauer and Abelmann, 1999	−49.01	−12.70	South	SST	S
7a	Brook et al., 1996	−19.00	18.00	South	Terr	
8a	Burrough et al., 2007	−20.00	22.50	South	Terr	
8b	Burrough et al., 2007	−20.02	21.35	South	Terr	
9a	Burrough et al., 2009	−19.99	25.21	South	Terr	
10a	Causse et al., 2003	33.00	9.00	North	Terr	
11a	Crombie et al., 1997	24.00	32.30	North	Terr	
12a	Dupont and Weinelt, 1996	4.80	3.40	Tropical	Terr	T
13d	Dupont et al., 2000	−11.75	11.70	Tropical	Terr	T
13c	Dupont et al., 2000	−6.60	10.30	Tropical	Terr	T
13b	Dupont et al., 2000	−2.20	5.10	Tropical	Terr	T
13a	Dupont et al., 2000	3.75	−11.40	Tropical	Terr	T
14a	Emeis et al., 2003	38.99	4.02	North	SST	S
14b	Emeis et al., 2003	34.81	23.19	North	SST	S
15a	Fontes and Gasse, 1991	26.00	7.00	North	Terr	
16a	Gaven et al., 1981	27.00	14.00	North	Terr	
17a	Hillaire-Marcel et al., 1986	−2.00	36.00	East	Terr	
18a	Hodell et al., 2003	−42.92	8.90	South	SST	S
19a	Holmgren et al., 1995	−23.70	26.00	South	Terr	
20a	Holzkamper et al., 2009	−24.10	29.88	South	Terr	
21c	Hooghiemstra et al., 1992	29.05	−12.10	North	Terr	P
21b	Hooghiemstra et al., 1992	30.00	−10.65	North	Terr	
21a	Hooghiemstra et al., 1992	34.90	−7.80	North	Terr	P
22a	Laskar et al., 2004	15.00	N/A		Insol	INSOL
22b	Laskar et al., 2004	−15.00	N/A		Insol	INSOL
23a	Leuschner and Sirocko, 2000	17.50	61.50	Indian	SST	S
24a	Lezzine and Casanova, 1991	20.00	−2.00	North	Terr	
24e	Lezzine and Casanova, 1991	22.00	30.00	North	Terr	
24b	Lezzine and Casanova, 1991	24.00	−2.00	North	Terr	
24d	Lezzine and Casanova, 1991	24.00	12.00	North	Terr	
24c	Lezzine and Casanova, 1991	31.00	9.00	North	Terr	
25a	McGlue et al., 2008	−6.70	29.80	Tropical	Terr	
26a	McKenzie, 1993	23.00	29.00	North	Terr	
27a	Moernaut et al., 2010	−3.30	37.70	Tropical	Terr	
28a	Moeyersons et al., 2002	26.25	33.98	North	Terr	
29a	Morel et al., 1991	22.00	−4.00	North	Terr	
30a	Nürnberg and Groeneveld, 2006	−43.96	49.93	South	SST	S
31a	Osmond and Dabous, 2004	27.00	32.00	North	Terr	
32a	Partridge, 1999, tuned	−25.60	28.08	South	Terr	P
32b	Partridge, 1999, untuned	−25.60	28.08	South	Terr	P
33a	Pichevin et al., 2005	−25.81	12.13	Tropical	SST	S
34c	Pokras and Mix, 1985	−2.28	5.18	Tropical	Terr	P
34b	Pokras and Mix, 1985	−0.20	−23.15	Tropical	Terr	P
34d	Pokras and Mix, 1985	3.05	−11.82	Tropical	Terr	P
34a	Pokras and Mix, 1985	18.26	−21.10	North	Terr	P
35a	Raymo et al., 2004	55.00	−15.00	North	SST	S
36a	Rossignol-Strick, 1985	33.42	25.00	North	Terr	
37a	Rostek et al., 1997	5.07	73.88	Indian	SST	S
37b	Rostek et al., 1997	13.70	53.25	Indian	SST	S
38c	Schneider et al., 1995	−6.58	10.32	Tropical	SST	S
38b	Schneider et al., 1995	6.50	−1.40	Tropical	SST	S
38a	Schneider et al., 1995	−6.00	29.60	Tropical	SST	S
39a	Scholz et al., 2007	−20.10	9.18	Tropical	Terr	
39b	Scholz et al., 2007	−11.76	11.68	Tropical	Terr	
40a	Schwarcz et al., 1993	22.90	28.75	North	Terr	
41a	Sicre et al., 2000	25.00	−16.00	North	SST	S
42a	Smith et al., 2007	25.00	31.00	North	Terr	
43a	Sorin et al., 2010	31.30	35.30	North	Terr	P
44a	Stokes et al., 1998	−19.20	26.65	Tropical	Terr	
45a	Stone et al., 2011	−11.30	34.45	Tropical	Terr	P
46a	Stuut and Lamy, 2004	−20.00	9.26	South	Terr	P
47a	Szabo et al., 1995	22.00	29.00	North	Terr	
48a	Thomas and Shaw, 2003	−25.00	25.35	South	Terr	
48b	Thomas and Shaw, 2003	−18.80	18.40	Tropical	Terr	
49a	Thomas et al., 2009	−14.98	35.66	Tropical	Terr	

(*continued on next page*)

Please cite this article in press as: Blome, M.W., et al., The environmental context for the origins of modern human diversity: A synthesis of regional variability in African climate 150,000–30,000 years ago, Journal of Human Evolution (2012), doi:10.1016/j.jhevol.2012.01.011

Table 1 (*continued*)

Labels	Authors	Latitude	Longitude	Region	TerrSST	STP?
50a	Tierney et al., 2008	−6.70	29.83	Tropical	Terr	
51a	Tisserand et al., 2009	18.10	−21.15	North	SST	S
52a	Tjallingii et al., 2008	20.75	−18.57	North	Terr	
53a	Trauth et al., 2003	−0.90	36.33	East	Terr	P
54a	Vaks et al., 2007	31.60	35.10	North	Terr	
55a	Van Campo et al., 1982	14.40	50.50	Indian	SST	S
56a	Voight et al., 1990	10.50	49.90	East	Terr	
57a	Weldeab et al., 2007	2.50	9.40	Tropical	SST	S
58a	Wendorf et al., 1987	22.90	28.75	North	Terr	
59a	Wendorf et al., 1989	24.20	32.85	North	Terr	
60a	Woltering et al., 2011	−10.02	34.18	Tropical	Terr	
61b	Zhao et al., 1995	19.00	−20.17	North	SST	S
61a	Zhao et al., 1995	20.75	−18.58	North	SST	S

each dataset (e.g., count data may produce values from 0 to 1000, whereas percentage data may only range from 0 to 100).

We used PCA to examine all available continuous datasets, however, only 20 (primarily SST or offshore pollen records) covered the entire period from 150 to 30 ka. Therefore, to maximize the number and types of data included in the total analysis, four sub-intervals of time were selected for separate analyses: 150–100 ka, 140–30 ka, 115–30 ka, and 75–30 ka. These intervals were selected to sample periods of both high and low insolation variability and to maximize the number of datasets included in each discrete analysis. The continuity and length of the record determined which datasets were used for each time interval. More recent intervals are better represented among the published data, so the four sub-intervals included 32–40 datasets, respectively, in each analysis.

Paleoanthropological site data collection and analysis

We tabulated known, radiometrically-dated archaeological and hominin fossil sites from Africa with assemblages spanning 150–30 ka, summarized in Fig. 2 and Table 2, and used the density for evidence of hominin occupation of a region for a given temporal interval as a demographic measure with greater site density suggesting larger hominin populations. For more recent periods, others have used the frequency of radiocarbon-dated sites to estimate changes in population density (e.g., Gamble et al., 2005; Surovell et al., 2009). In seeking patterns among the frequency of radiometric dates, where the density of dates is high, a plausible argument can be made that the sheer volume of data removes concerns about error ranges and stratigraphic relations associated with the reported age estimates. This is what is done with most efforts that rely on very large databases ($n \approx 500$–2000) of radiocarbon age estimates (see discussion in Gamble et al., 2005). When the sample size is low, as it is here, these issues remain serious concerns, and we have opted instead to provide an age range that accounts for instrumental error or uncertainties as well as stratigraphic information, the latter particularly important as most of what is dated at paleoanthropological sites are not the artifacts or human fossils themselves but rather bounding strata or other materials that provide age minima or maxima.

Our data tabulation and presentation methods consist of six steps. (1) We provide one or more age ranges for each site based on the stratigraphic relations of the published radiometric age estimates (at one standard deviation) to the archaeological strata for a given site. In general, at open-air site complexes, individual sites with overlapping time ranges have been combined to make them more comparable with the more frequently reoccupied, and thus more archaeologically rich, caves and rockshelters. (2) The time span of 30–150 ka is divided into 10 kyr bins (31–40 ka…141–150 ka). Ten thousand years is our arbitrary maximum temporal resolution for the sites considered here. It is estimated on the basis of instrumental error and stratigraphic relations among dated deposits and paleoanthropologically relevant material. (3) A site is given equal probability for the 'true' age to occur within each of the 10 kyr bins in which its range falls. Thus, a site such as Enkapune ya Muto with an estimated age range of 33–55 ka would fall into the 31–40 ka, 41–50, and 51–60 ka bins. The advantage of this approach is that it requires the fewest analytical assumptions and accounts for the fact that we typically lack the basis to reliably assess the likelihood of site dating to a particular year within that range. The disadvantage is that dates with large error ranges that span numerous bins have the potential to mute variation within the total dataset. (4) For each region, we sum the total number of occurrences in each 10 kyr bin, and normalize this value to the total number of age bin occurrences in that region, expressed as a percentage. As a result, proportional change in one region is numerically independent of change in another region. (5) These data are then expressed as line diagrams to explore temporal changes in the frequency of sites relative to climate change for the each of the North, East, tropical, and southern African regions. (6) To offset the potentially confounding effect of locally increased moisture availability, we separate interior and 'coastal' sites for southern and northern Africa (coastal sites in our time range are largely lacking for East and tropical Africa), and consider the Nile Valley separately in this analysis as it represents a highly localized area of available water in otherwise often dry environments. Because the changing position of the South African shoreline is now well-understood, sites from this region are variably attributed to 'coastal' and 'interior' depending on contemporaneous coast location as per data from Van Andel (1989) and Fisher et al. (2010).

As emphasized by Bailey (2007), the temporal resolution of the dataset determines the scale of the questions to be asked, and a 10 kyr time span is too broad an interval to examine in detail the relation between environmental and human behavioral change. This can be seen particularly well in southern Africa, where a comprehensive program of single-grain optically stimulated luminescence dating has demonstrated that distinctive MSA archaeological entities and behavioral traditions such as those seen at Howiesons Poort and Still Bay sites in southern Africa appear, spread, and disappear within ~5 kyr (Jacobs et al., 2008a, b). This is less than the ~10 kyr resolution of our aggregate dataset, and in this particular case, site-specific paleoenvironmental reconstructions are still poorly defined and the relation between environmental and archaeological change is controversial (cf. Ambrose and Lorenz, 1990; McCall, 2007; Jacobs et al., 2008a; Chase, 2010). Rather than exploring the nature of environmental and behavioral

Please cite this article in press as: Blome, M.W., et al., The environmental context for the origins of modern human diversity: A synthesis of regional variability in African climate 150,000–30,000 years ago, Journal of Human Evolution (2012), doi:10.1016/j.jhevol.2012.01.011

Table 2
Paleoanthropological sites used in the synthesis. Uncalibrated radiocarbon age estimates have been calibrated using CalPal.

Site	Name	Age range	Region	Coast/inland	Latitude	Longitude	Reference
1	Ain Shakshuk	31–46	North	Inland	32.00	11.95	Barich et al., 2005
2	Bir Sahara East	70–110, 125–135	North	Inland	22.90	28.75	Wendorf et al., 1993
3	Bir Tarfawi	60–130	North	Inland	22.92	28.83	Wendorf et al., 1993
4	Dar-es-Soltan 1	31–145	North	Coast	33.97	−6.88	Barton et al., 2009
5	El Mnasra	<30–40	North	Coast	33.92	−6.95	Nespoulet et al., 2008
6	Grotte des Pigeons	20–113	North	Coast	34.81	−2.41	Bouzouggar et al., 2007
7	Ifri n'Ammar	38–183	North	Coast	34.78	−3.05	Richter et al., 2010
8	Jebel Irhoud	90–190	North	Coast	33.25	−5.50	Grün and Stringer, 1991; Smith et al., 2007
9	Kharga Oasis	89–126	North	Inland	25.30	30.47	Smith et al., 2007
10	Mugharet el 'Aliya	27–61	North	Coast	35.75	−5.93	Wrinn and Rink, 2003
11	Nazlet Khater 4	28–50	North	Nile Valley	26.78	31.38	Vermeersch, 2002
12	Nazlet Safaha	36–65	North	Nile Valley	26.1	32.57	Vermeersch, 2002
13	Oued Noun	25–53	North	Coast	29.10	−10.34	Weisrock et al., 2006
14	Ounjougou	25–69	North	Inland	14.4	−3.52	Robert et al., 2003; Rasse et al., 2004
15	Rhafas Cave	60–127	North	Coast	34.80	−1.88	Mercier et al., 2007
16	Sodmein Cave	25–137	North	Coast	26.24	33.97	Mercier et al., 1999; Moeyersons et al., 2002
17	Taramsa 1	50–80	North	Nile Valley	26.10	32.70	Vermeersch et al., 1998
18	Uan Afuda	61–100	North	Inland	24.87	10.50	Cremaschi et al., 1998; Cremaschi and Di Lernia, 1999; Di Lernia, 1999
19	Uan Tabu	51–71	North	Inland	24.86	10.11	Cremaschi et al., 1998; Cremaschi and Di Lernia, 1999
20	Zouhrah a El Harhoura	26–45	North	Coast	33.92	−6.92	Debénath et al., 1986
21	Aduma	80–120	East	N/A	10.42	40.52	Yellen et al., 2005
22	Enkapune ya Muto	33–55	East	N/A	−0.83	36.15	Ambrose, 1998
23	Kapedo Tuffs	123–135	East	N/A	1.07	36.08	Tryon et al., 2008
24	Massawa/Abdur	118–136	East	N/A	15.15	39.42	Walter et al., 2000
25	Midhishi 2	40–90	East	N/A	10.95	47.37	Brandt and Gresham, 1989
26	Omo Kibish (BNS)	103–198	East	N/A	5.41	35.90	Shea, 2008
27	Porc Epic	33–79	East	N/A	9.63	41.87	Clark et al., 1984; Assefa et al., 2008
28	Sai Island	30–160	East	N/A	20.57	30.25	Van Peer et al., 2003
29	Shurmai Rockshelter	20–46	East	N/A	0.50	37.20	Kuehn and Dickson, 1999
30	Simbi	50–200	East	N/A	−0.35	35.00	McBrearty, 1992
31	Singa	131–135	East	N/A	13.17	33.95	McDermott et al., 1996
32	Wasiriya Beds	33–100	East	N/A	−0.42	34.17	Tryon et al., 2010
33	Birimi	24–51	Tropical	N/A	10.54	−0.38	Quickert et al., 2003
34	Eyasi Beds	88–132	Tropical	N/A	−3.52	35.17	Domínguez-Rodrigo et al., 2008
35	Gi	33–65	Tropical	N/A	−19.62	21.02	Brooks et al., 1990
36	Katanda	60–120	Tropical	N/A	0.10	29.62	Brooks et al., 1995; Feathers and Migliorini, 2001
37	Matupi Cave	32–41	Tropical	N/A	1.50	36.00	Van Noten, 1977
38	Mumba	25–137	Tropical	N/A	−3.53	35.32	Mehlman, 1991
39	Mumbwa	32–46, 96–194	Tropical	N/A	−15.02	26.98	Barham, 2000
40	Nasera	23–57	Tropical	N/A	−2.74	35.36	Mehlman, 1991
41	Ngalue	42–105	Tropical	N/A	−12.85	35.18	Mercader et al., 2009
42	Njuinje	18–35	Tropical	N/A	5.25	9.73	Mercader and Martí, 2003
43	Olduvai Gorge Naisiusiu Beds	42–60	Tropical	N/A	−2.93	35.42	Manega, 1993; Skinner et al., 2003
44	Shum Laka	13–37	Tropical	N/A	5.85	10.07	Cornelissen, 2002
45	Twin Rivers	11–102	Tropical	N/A	−15.52	28.18	Barham, 2000
46	White Paintings	31–105	Tropical	N/A	−18.77	21.75	Robbins et al., 2000; Donahue et al., 2004
47	Apollo 11	30–83	South	Inland	−27.75	17.10	Miller et al., 1999
48	Blind River	122–127	South	Coast	−33.02	27.9	Wang et al., 2008
49	Blombos	60–140	South	Coast	−34.42	21.22	Henshilwood et al., 2002; Jacobs et al., 2006; Tribolo et al., 2006
50	Boomplaas	31–62	South	Inland	−33.38	22.18	Miller et al., 1999; Vogel, 2001
51	Border Cave	32–238	South	Inland	−27.02	31.99	Miller et al., 1999; Grün et al., 2003; Bird et al., 2003
52	Bundu Farm	129–370	South	Inland	−29.75	22.20	Kiberd, 2006
53	Die Kelders	50–80	South	Coast	−34.53	19.03	Feathers and Bush, 2000; Schwarcz and Rink, 2000
54	Diepkloof	46–75	South	Coast	−32.67	18.50	Tribolo et al., 2006; Jacobs et al., 2008a
55	Equus Cave	27–103	South	Inland	−27.62	24.63	Klein et al., 1991; Lee-Thorp and Beaumont, 1995
56	Florisbad	115–178	South	Inland	−28.77	16.07	Grün et al., 1996
57	Hofmeyr	33–39	South	Inland	−31.57	25.97	Grine et al., 2007
58	Klasies River	50–115	South	Coast	−34.10	24.40	Grün et al., 1990; Vogel, 2001; Feathers, 2002; Tribolo et al., 2005; Jacobs et al., 2008a
59	Klein Kliphuis	32–69	South	Inland	−32.07	18.51	Jacobs et al., 2008a
60	Lincoln Cave	118–298	South	Inland	−31.80	20.52	Reynolds et al., 2007
61	Melikane	33–82	South	Inland	−29.95	28.75	Vogel et al., 1986; Jacobs et al., 2008a
62	Ntloana Tsoana	55–73	South	Inland	−29.32	27.82	Jacobs et al., 2008a
63	Pinnacle Point	30–40, 90–130, 160–170	South	Coast	−34.21	22.09	Marean et al., 2010
64	Pockenbank	30–50 ka	South	Inland	−27.22	16.52	Vogelsang, 1998
65	Rose Cottage Cave	20–91	South	Inland	−29.22	27.47	Valladas et al., 2005; Jacobs et al., 2008a; Pienaar et al., 2008
66	Sehonghong	30–60	South	Inland	−29.77	28.78	Jacobs et al., 2008a
67	Sibudu	37–79	South	Inland	−29.00	31.00	Jacobs et al., 2008a, 2008b
68	Umhlatuzana Cave	32–75	South	Inland	−29.48	30.45	Lombard et al., 2010
69	Witkrans	33–106	South	Inland	−27.62	24.63	Butzer et al., 1978; Vogel and Partridge, 1984
70	Wonderwerk Cave	70–220	South	Inland	−27.85	23.56	Vogel, 2001; Beaumont and Vogel, 2006

Please cite this article in press as: Blome, M.W., et al., The environmental context for the origins of modern human diversity: A synthesis of regional variability in African climate 150,000–30,000 years ago, Journal of Human Evolution (2012), doi:10.1016/j.jhevol.2012.01.011

Table 3
Climate proxies and their interpretations.

Proxy	Interpretation	Selected reference
Oceanographic conditions		
Alkenones	Local SSTs: Uses the alkenone uncertainty index (Uk-37) devised by Prahl et al. (1988)	Bard et al., 1997
Mg/Ca	Local SSTs: Measured on planktonic foraminifera after Lea et al., 1999	Weldeab et al., 2007
$\delta^{18}O$	Global/Local SSTs: Measured on planktonic foraminifera after Wefer and Berger, 1991	Van Campo et al., 1982
$CaCO_3$	Indicator of increased primary production, often caused by local upwelling intensity	Leuschner and Sirocko, 2000
Continental precipitation variation		
Pollen	Arboreal pollen abundance increases with relative humidity	Hooghiemstra et al., 1992; Dupont et al., 2000
Groundwater carbonate	Groundwater carbonate abundance increases with relative humidity	Osmond and Dabous, 2004
Diatoms in offshore sites	Wind-borne diatom abundance increases with aridity-induced lake deflation	Pokras and Mix, 1985
Lake water level	Increases or decreases with changes in relative moisture availability; recorded seismically or by strandlines	Scholz et al., 2007; Burrough et al., 2009
Ostracodes	Species diagnostic of particular water conditions/depths	Cohen et al., 2007
Diatoms in continental lakes	Species diagnostic of particular water conditions/depths	Stone et al., 2011
Ratio (total aeolian dust/fluvial mud)	Yields a humidity index: Decreased ratio during times of increased humidity	Stuut and Lamy, 2004; Tjallingii et al., 2008
Dune growth	Active during period of aridity; stabilized with increased humidity	Stokes et al., 1998; Thomas and Shaw, 2003
$\delta^{18}O$	Paleo-rainfall amounts and seasonality	Holmgren et al., 1995
δD	Paleo-rainfall amounts and seasonality	Bar-Matthews et al., 2010
Continental temperature variation		
TEX_{86}	Records lake surface temperatures	Tierney et al., 2008

change, the scale of our dataset is more appropriate to larger scale questions about the demographic or biogeographic structure of the archaeological or paleontological record.

Population density or size is notoriously difficult to demonstrate from fossil or archaeological data (but see recent efforts for Late Pleistocene western Europe by Mellars and French, 2011). While a number of site-specific approaches have shown that human impacts on various animal taxa can be a good measure of population pressure (Klein, 1980; Stiner et al., 1999; Faith et al., 2011), these sorts of data are not available or reliable for many African sites. Although problematic, our use of site density as a measure of Pleistocene hominin demography for a given time interval remains the best measure available for our pan-African approach. We use bivariate plots to assess temporal changes in paleoanthropological site frequency for each of the four regions relative to the timing of inferred paleoclimate changes.

Interpretive frameworks for African paleoclimates

Modern African climates provide the basic interpretive framework for interpreting Pleistocene climate and environment. The climate of a given location describes the average annual as well as seasonal variation in temperature and precipitation over a long period of time. Climate dynamics refers to the physical mechanisms that create a particular climate in one location, and a different climate in another.

Oceanic currents and surface temperatures

There are four main surface ocean currents that encircle Africa: the Canary, Benguela, Agulhas, and the Antarctic Circumpolar Current (ACC) (Fig. 3). The strength and extent of these currents often dictates rainfall patterns along the coast by affecting mean air mass boundaries, and moisture availability and transport. The colder currents inhibit regional precipitation, whereas warm currents tend to promote increased rainfall in nearby areas. Global patterns of sea surface temperatures (SSTs) can have a significant effect on the precipitation patterns over the African continent. Two such patterns affecting rainfall in Africa are the El Niño Southern Oscillation (ENSO) and the Indian Ocean Dipole (IOD). 'Normal' ENSO years in the Indian Ocean are characterized by warmer waters in the eastern Indian Ocean (near Australia), colder SSTs in the western Indian Ocean, and 'normal' (limited) rainfall occurs over the Horn of Africa. During El Niño years, the SST patterns and associated rainfall patterns are reversed, bringing extreme drought to Australia and flooding to parts of East Africa. The IOD, once viewed as noise when analyzing ENSO, is increasingly being accepted as its own phenomenon (Marchant et al., 2007). The

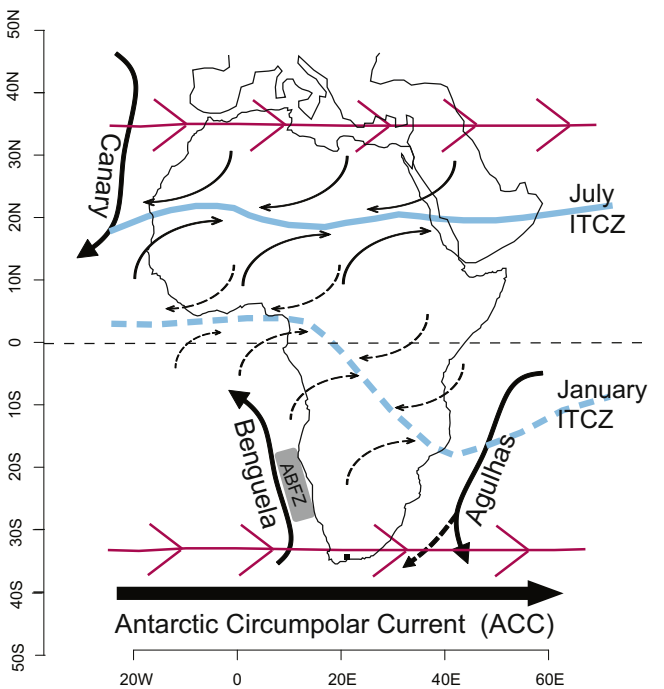

Figure 3. Idealized position of the Intertropical Convergence Zone (ITCZ) in January and July (blue lines), and the associated trade winds. Average position of mid-latitude Westerlies (red arrows). Major surface ocean currents and the Angola-Benguela Frontal Zone (ABFZ) are also labeled. (For interpretation of the references to colour in this figure legend, the reader is referred to the web version of this article.)

Please cite this article in press as: Blome, M.W., et al., The environmental context for the origins of modern human diversity: A synthesis of regional variability in African climate 150,000–30,000 years ago, Journal of Human Evolution (2012), doi:10.1016/j.jhevol.2012.01.011

dipole refers to SST variation across the Indian Ocean associated with the strength of the winter monsoon winds and a cold tongue in the Arabian Sea (Saji et al., 1999; Prasad and McClean, 2004). A positive IOD event produces a pattern similar to El Niño with colder waters near Australia and anomalously warm SSTs in the northwestern Indian Ocean, and the ENSO and IOD may modulate each other when they co-occur (Bowden and Semazzi, 2007; Yuan et al., 2008). Although ENSO and IOD may have far reaching atmospheric teleconnections, the IOD is defined strictly by temperature variation in the Indian Ocean whereas ENSO is defined by atmospheric pressure patterns over the Pacific Ocean. It is, however, these atmosphere-ocean teleconnections that may play a large role in local and regional SST to terrestrial precipitation relationships through time.

Air masses

African climate is affected primarily by tropical (continental and marine) and equatorial air masses. Precipitation patterns are driven by the mid-latitude Westerlies in the extreme northern and southern regions of Africa and the location of the Intertropical Convergence Zone, or ITCZ, in the middle portion (Fig. 3). The Westerlies are high altitude winds that blow from the west and define areas where cool dry air from the poles collides with warm, moist air from the tropics causing instability and convection (Rohli and Vega, 2008). These are 'frontal boundaries' and are often associated with rising moist air, cloud formation and precipitation. The position of the Westerlies, particularly around Antarctica has recently been shown to vary with global temperature (Toggweiler and Russell, 2008) with the Westerlies strengthening while contracting pole-ward during warm periods and weakening while expanding equator-ward during colder periods. If the location of the Westerlies is the dominant driver of African climate, then northern and southern Africa should be wet when the Westerlies are weak (equator-ward) because they then bring rainfall and weather systems to the region. However, when the Westerlies are strong, northern and southern Africa should be dry, without atmospheric circulation bringing moisture off the ocean.

The ITCZ approximates the zone of maximum insolation (solar energy) received by the atmosphere and the Earth's surface. Insolation duration and intensity is orbitally forced by eccentricity-modulated precession at low-latitudes with a periodicity of 19–23 kyr. The ITCZ moves between the Tropics of Cancer (June) and Capricorn (December), crossing the equator at the equinoxes. It is a 'convergence' zone because: (1) the sun's energy is converted to heat at the surface and in the atmosphere, and (2) air that is warmer than its surroundings will rise forming an area of surface low pressure. This draws in surface winds flowing equator-ward from the east (trade winds, Fig. 3) causing the trade winds from the Northern and Southern Hemispheres to converge at the ITCZ. Direct insolation effects on areas within the ITCZ include a 1 °C SST increase over the oceans leading to more evaporation, and on land a region of increased convection, and consequently rainfall (Liu et al., 2004).

Monsoons

Monsoon systems are "a seasonal reversal of wind caused by [large]-scale [atmospheric] pressure changes, often accompanied by seasonal changes in moisture" (Rohli and Vega, 2008: 416). The well-known South Asian monsoon, for example, brings torrential rainfall and flooding to the Indian continent. The West African monsoon and the East African monsoon are both caused by differential heating between the land and the neighboring ocean (e.g., enhanced land-ocean temperature contrasts) during the summer (Kutzbach and Liu, 1997). Terrestrial surfaces heat more quickly than the ocean surface as a result of the high specific heat capacity of water. When a coastal region warms, the land will heat more quickly than the neighboring ocean. Therefore, the air mass over the land will rise (low pressure), drawing moist air landward from the ocean. This convection in the presence of a moisture source produces rainfall. During an off-monsoon season, the land surface will also lose heat more quickly than the ocean, and the winds and pressures will reverse, with a high-pressure system situated over the land, stabilizing the air.

As discussed previously, the ITCZ follows the area of most intense insolation, which occurs when the sun is directly overhead (during the summer), and the position of the ITCZ drives the East and West African monsoons. However, because the monsoonal circulation system (associated with atmospheric pressure changes) is dependent on land-ocean temperature contrasts, an external perturbation (e.g., changes in land-surface albedo, variations in ocean circulation patterns and therefore temperature) in the system can cause monsoon rainfall to be weak or to not arrive at all. In addition, monsoons will be intensified when incoming insolation is high and vice versa.

Monsoons are dynamic systems in two ways: thermally and hydrologically, meaning monsoon systems respond to land/ocean temperature contrasts, and are also dependent on SSTs, evaporation from oceans, and water vapor transport to land (Kutzbach et al., 2008). The differential heating of land and ocean near and below the average location of the ITCZ can upset both oceanic and atmospheric dynamics, ultimately affecting the extent and position of tropical monsoons globally. As a consequence of its effect on monsoon systems, the average position of the ITCZ over time may also greatly affect the climate in regions on the extreme edge of the ITCZ range, as small shifts one way or another will have a greater impact there (Brown et al., 2007).

Major drivers of climate variability on millennial and longer time scales

Over the time period of interest in this synthesis, there are a number of important drivers of global and regional climate variability. These vary in scale, regional impact, and periodicity. Orbital (large) scale climate drivers include glacial-interglacial periods, greenhouse gas (GHG) concentrations, position of the Westerlies, and insolation intensity, the latter affecting the position of the ITCZ and monsoon strength. Orbital variations in insolation at both high- (obliquity) and low-latitudes (precession) are both potentially important drivers of the climate dynamics of the African continent. These variations affect ice volume at the poles, monsoon intensity, and global SSTs. Millennial scale climate drivers include changes in oceanic circulation patterns, which can change ice sheet stability triggering Heinrich and Dansgaard/Oeschger (D/O) events, which have local, regional and global effects.

The periodicity of orbital scale events is determined by the relative position of the Earth in its orbit around the sun at the equinox (precession), the angle of axial tilt relative to the plane of the ecliptic (obliquity), and the shape of the Earth's orbit (eccentricity). These have calculated periodicities of ~23 kyr, ~41 kyr and ~100 kyr, respectively. Additionally, each affects different regions of the globe more than others. Precession is a low-latitude (equatorial) forcing mechanism and is largely responsible for regulating the intensity of the monsoons (Kutzbach, 1981) with greater low-latitude insolation producing higher intensity monsoons (Rossignol-Strick, 1985; Kutzbach et al., 2008). Obliquity regulates high latitude insolation receipt and it, in combination with eccentricity, is responsible for the 100 kyr periodicity of glacial/interglacial cycles (Imbrie and Imbrie, 1980). Eccentricity also has an amplifying effect on the precession cycle, so much so

Please cite this article in press as: Blome, M.W., et al., The environmental context for the origins of modern human diversity: A synthesis of regional variability in African climate 150,000–30,000 years ago, Journal of Human Evolution (2012), doi:10.1016/j.jhevol.2012.01.011

that they are often combined when discussing low latitude forcing, 'eccentricity-modulated precession'. It is responsible for variations in tropical African monsoon intensity and timing (deMenocal and Rind, 1993; Trauth et al., 2009). Greenhouse gas concentrations, specifically CO_2, have been shown to vary in concert with global ice volume and thus glacial cycles, at a 100 kyr periodicity (Petit et al., 1999).

Millennial scale events, such as Heinrich and D/O events, are smaller in scale in both time and space, often lasting only a few thousand years or less. Heinrich events are times when numerous icebergs broke off from Arctic glaciers and melted, delivering significant quantities of cold, freshwater to the North Atlantic thereby altering global thermohaline circulation (Bond et al., 1992). D/O events are intervals of rapid warming followed by a gradual cooling (Dansgaard et al., 1993), whereas Heinrich events are characterized by rapid and sudden cooling in the Northern Hemisphere. Both of these events were originally thought to have only high latitude effects, but subsequent research has shown the existence of global teleconnections between presumed high latitude drivers and low latitude climate changes at these time scales, including in Africa (e.g., Tierney et al., 2008; Moernaut et al., 2010; Stager et al., 2011).

Paleoclimate results: sea surface temperatures and paleoceanographic conditions

Sea surface temperatures (SSTs) typically reflect changes in mean global temperature because they are global in extent, and water has a high heat capacity. The various measures of SST are summarized in Table 3. Fig. 4 summarizes various measures of sea surface temperatures for the northern Atlantic, Mediterranean, southern Atlantic, Indian Ocean, and Southern Ocean regions.

Northern Atlantic records

As shown in Fig. 4, Atlantic SSTs recorded off the NW coast of Africa (>35°N) from 150 to 30 ka are consistent with the North Atlantic-defined glacial/interglacial MIS pattern, with maximum temperatures around 125 ka and decreasing temperatures towards 50 ka. North Atlantic SSTs show a consistent saw-tooth glacial/interglacial pattern that mirrors the $\delta^{18}O$ record of ice volume recorded in the Greenland ice cores (GRIP and GISP2). At times of lower ice volume and warmer global temperatures, the North Atlantic reflects this change quickly with increased SSTs. This suggests that high latitude forcing affects the SSTs of the subtropical Atlantic Ocean off NW Africa.

Southern Atlantic records

The SST records from the equatorial and southern regions of the Atlantic Ocean (5°N to 25°S latitude) also display the characteristic North Atlantic saw-tooth pattern (Fig. 4). Between 50 and 45 ka, the records diverge as the most northerly record (7°S) and the most southerly record (26°S) inexplicably begin to increase in temperature.

Minor variations in each record may be explained by regional rather than global causes. These could include variations in dominant local wind patterns and/or upwelling activity. For example, a number of studies interpreted the circulation pattern of the Angola-Benguela Front (ABF – 4°N–20°S) through time (see Fig. 1) and all conclude that the trade wind belt over Angola has not shifted spatially over time with glacial/interglacial variation in climate. Instead of an increased alongshore flow of the Benguela current during glacial times, there was a shift to more offshore flow coincident with increased trade wind zonality and reduced

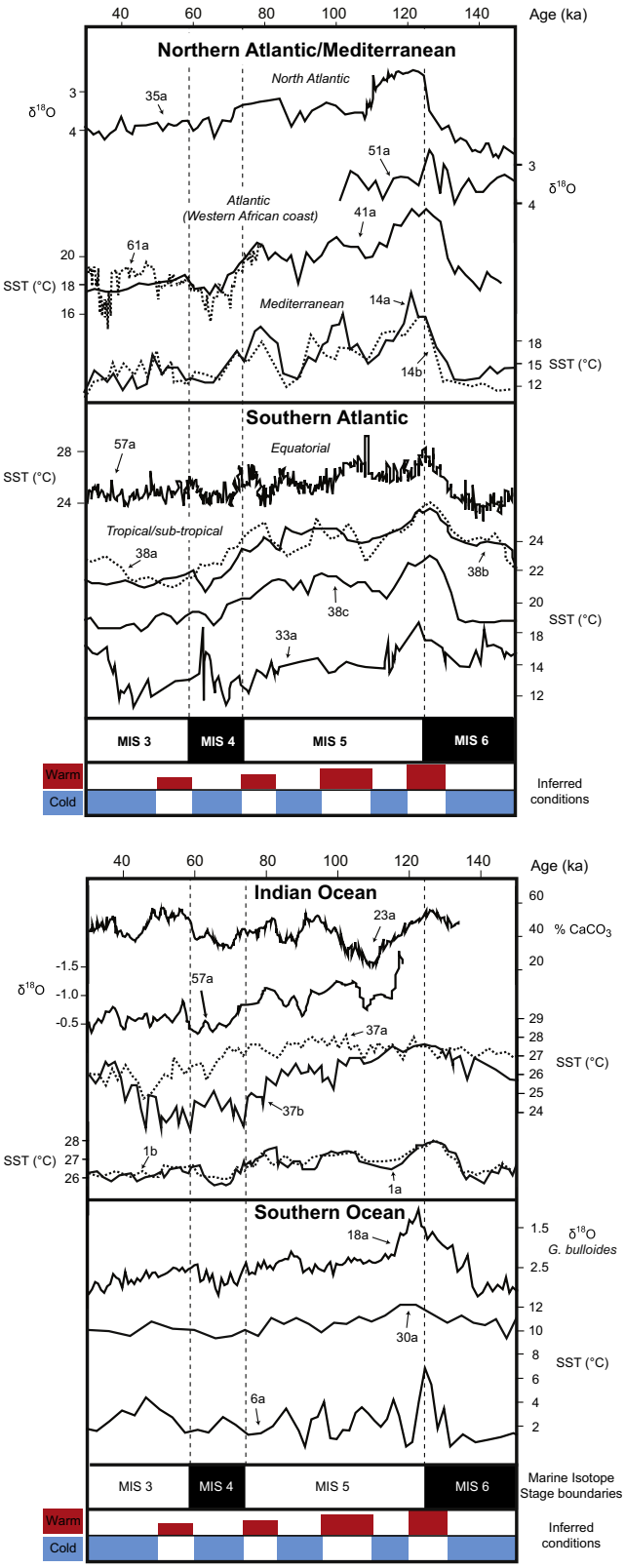

Figure 4. Sea surface temperature (SST) data by region. These data are ordered from north to south on the vertical axis within each region. Figs. 4–8: Site numbers are closely associated with their respective datasets. Marine Isotope Stages (MIS) 6–3 and the inferred regional climate conditions through time are noted at the bottom for all dataset figures. Additionally, peaks indicate periods of higher temperature or humidity, troughs indicate periods of lower temperature or humidity.

Please cite this article in press as: Blome, M.W., et al., The environmental context for the origins of modern human diversity: A synthesis of regional variability in African climate 150,000–30,000 years ago, Journal of Human Evolution (2012), doi:10.1016/j.jhevol.2012.01.011

monsoon intensity (see Table 1: 38a, b, c) (Schneider et al., 1995; Little et al., 1997). Other researchers using data from sites further south (33a) (e.g., Pichevin et al., 2005; Martinez-Méndez et al., 2010) found a negative correlation of SSTs and grain size. During periods of colder SSTs, the sediments being deposited were statistically coarser. As colder waters in this region may indicate upwelling activity and more energy is needed to move sediments of a larger size, it is reasonable to conclude that colder SSTs in the record signal periods of increased wind strength as well as upwelling activity. The different interpretations by Schneider et al. (1995) and Pichevin et al. (2005) of the dynamics in the southern Atlantic may be region-specific, with colder periods further north the result of increased trade wind zonality and further south resulting from stronger overall winds. There is also a 23 kyr periodicity observed in the SSTs off Angola, which Schneider et al. (1995) argue is produced by changes in low latitude insolation and monsoon intensity, and not by high latitude climate forcing, despite the apparent similarity to North Atlantic records.

These exceptions notwithstanding, the southern Atlantic SST curves are similar to the global marine $\delta^{18}O$ curve used to define the MIS boundaries.

Indian Ocean records

Like the Atlantic Ocean records, the time interval with the warmest SSTs in the Indian Ocean is 130–120 ka (Fig. 4). However, the similarity between the Atlantic and (Northern Hemisphere) Indian Oceans decreases through time, and with increased distance from the African coast. Closest to the African coast, the SST records from 3°N, 0°N, and 14°N (1a, 1b, 55a) are the most similar to the North Atlantic record, showing last interglacial peak temperatures (at ~125 ka) and the distinct saw-tooth pattern of temperature variation and decrease overall through time.

Some of the differences between the Atlantic Ocean and Indian Ocean records may again be attributed to changes in deep water upwelling patterns and variation in local to regional monsoonal winds, the latter correlated with Northern Hemisphere glacial/interglacial cycles and strengthened with insolation intensity. Pollen records suggest high frequencies of taxa from the Mediterranean steppe in the Arabian Sea during glacial periods, indicating stronger NE trade winds and increased regional aridity (Van Campo et al., 1982). Additionally, low $CaCO_3$ content in the Arabian Sea during colder periods reflect reduced upwelling due to decreased strength in the SW monsoon airflow (23a) (Leuschner and Sirocko, 2000). Similarly, SSTs determined from two cores off Oman and southwest of India (37a, b) contribute information about the timing of the NE and SW monsoons (Rostek et al., 1997). At these locations there is a correlation between increased productivity on precessional time scales and glacial periods, with concomitant decreases in productivity during interglacial periods. Like Van Campo et al. (1982) the authors interpret a stronger NE monsoon during glacial times as producing greater wind-induced surface mixing and therefore increased nutrient supply. However, the record off the coast of Oman is more complicated and does not show a precessional signal. The SST records from both sites indicate warmer temperatures during interglacials and interstadials and colder temperatures during glacials and stadials as expected. While the warmest period recorded in the sediments is at ~125 ka during the peak of the last interglacial, the coldest period occurs at ~45 ka, prior to the LGM. As discussed earlier, this may be the result of reduced upwelling during full glacial times, causing an apparent local increase in SST.

The three Indian Ocean SST records closest to the continent (55a, 1a, b) are similar to the global marine $\delta^{18}O$ curve used to define the MIS boundaries, although the 1a and 1b records show a muted response, likely due to their proximity to the equator. The remaining two records show more of a response to local wind and upwelling activity (23a, 37b). The one outlying record is from closer to the central Indian Ocean basin, and may be responding to something different altogether (37a).

Southern Ocean records

For the most part, SST records from the region that is the interface between the southern Atlantic Ocean and the Southern Ocean, which surrounds Antarctica, are extremely similar to the records from the rest of the Atlantic Ocean (Fig. 4). They have a characteristic saw-tooth pattern, with maximum SSTs between 120 ka and 130 ka, and gradually decrease in temperature towards 30 ka. However, the most southerly record (6a at 49°) lacks the saw-tooth pattern, with temperatures fluctuating around a midpoint of ~3 °C with no observable trend. It appears that this region is being affected more by the cold waters of the Antarctic Circumpolar Current (ACC) than the North Atlantic.

Sea surface temperature summary

The SSTs surrounding the African continent are generally consistent with the global marine isotope stage (MIS) record, although the causes for this may be different. Around the continent, the warmest SSTs occurred between 130 and 120 ka, during the peak of the last interglacial (MIS 5e). The Atlantic records display the characteristic saw-tooth pattern when not interfered with by regional monsoonal effects or local upwelling activity (e.g., Little et al., 1997; Weldeab et al., 2007; Martinez-Méndez et al., 2010) and generally decrease in temperature from ~125 ka to 30 ka. The Indian Ocean records are the least similar to the North Atlantic, with this region likely much more heavily influenced by the East African and Asian monsoons (Rostek et al., 1997; Leuschner and Sirocko, 2000).

Paleoclimate results: terrestrial and marine records of continental temperature and precipitation variability

SSTs are an important measure of global temperature and have an important impact on continental moisture availability, but the relationship between oceanic and continental records is complex. The continental records, although often providing less continuous data than the oceanic records, are more directly relevant for understanding the climatic and environmental context of Pleistocene human evolution. Areal coverage and the types of paleoclimate proxies and indicators available are more varied relative to those used to infer SSTs, summarized in Table 3. Figs. 5–8 summarize paleoclimate data by proxy type for each of the African sub-regions, showing the temporal relations of inferred regional wet/dry regimes relative to established MIS boundaries.

North Africa and the Levant (Fig. 5)

The types of paleoclimate indicators for North Africa (>18°N) are the most varied of the dataset, and provide the most abundant data. Unlike some of the other sub-regions, many of the datasets from North Africa have good chronological control because of multiple U/Th dated lacustrine (16a, 26a, 47a, 10a), spring-fed (40a, 42a), groundwater (31a), or speleothem carbonates (28a, 3a, b, 54a, 43a), all interpreted as reflecting more humid intervals. Additionally, there are numerous datasets with terrestrial climatic indicators collected from marine cores; e.g., pollen (21a–c), freshwater diatoms (34a) and siliciclastic grain size (52a).

$\delta^{18}O$ values in Soreq (3a) and Peqiin (3b) caves in the eastern Mediterranean and speleothem frequencies from a number of other

Please cite this article in press as: Blome, M.W., et al., The environmental context for the origins of modern human diversity: A synthesis of regional variability in African climate 150,000–30,000 years ago, Journal of Human Evolution (2012), doi:10.1016/j.jhevol.2012.01.011

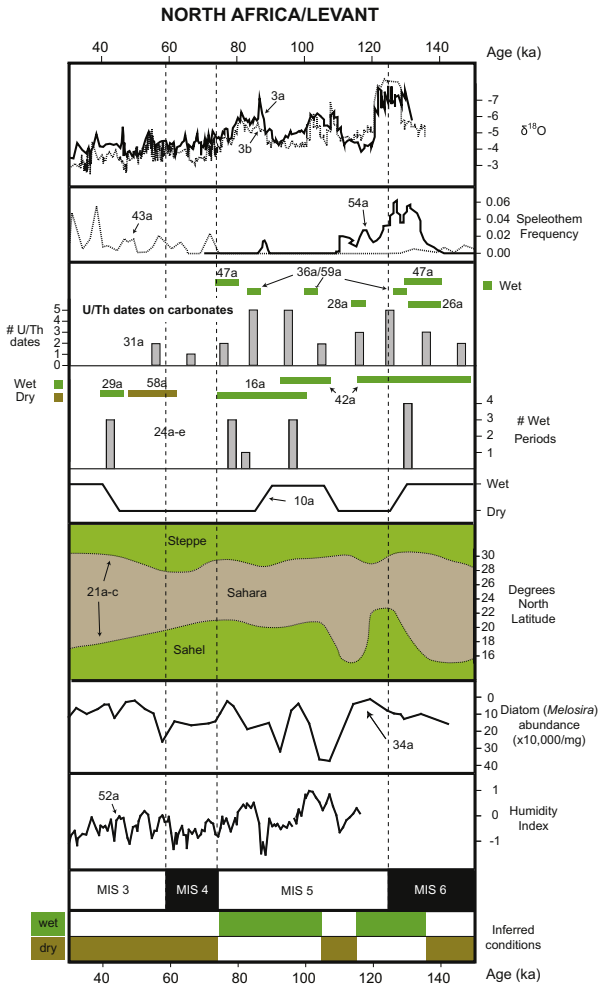

Figure 5. North Africa/Levant datasets. Records are arranged in the order they are discussed in the text and grouped by indicator type.

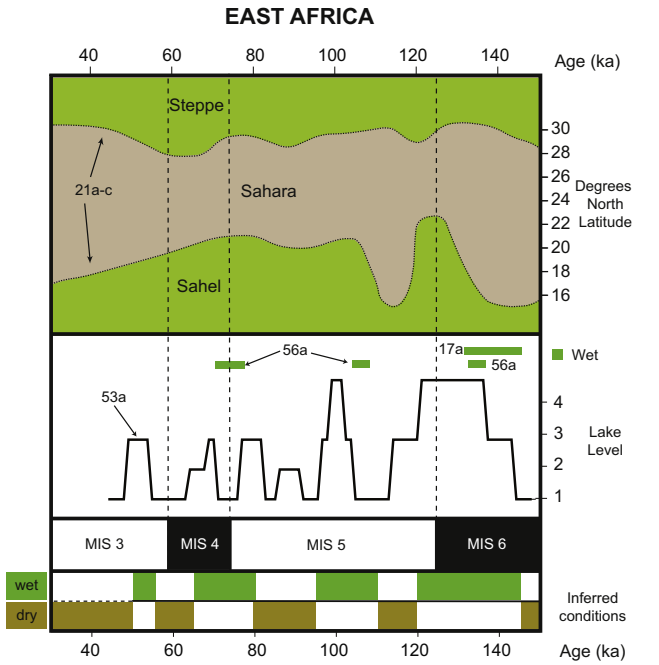

Figure 6. East African terrestrial datasets. Records are arranged in the order they are discussed in the text and grouped by indicator type.

caves in the Dead Sea region of Israel (43a, 54a) have been used to interpret paleo-rainfall and humidity. The Levantine $\delta^{18}O$ records are internally consistent with a considerable wet period extending from 135 ka to 120 ka, followed by a drier period from 120 ka to 90 ka. This is followed by a resurgence of humidity from 90 to 80 ka, after which these records show gradual aridification. In fact, the $\delta^{18}O$ records from Soreq and Peqiin caves record a pattern very similar to the North Atlantic and Mediterranean SST records, suggesting that the $\delta^{18}O$ values in the speleothems may be responding more to $\delta^{18}O$ values in the source water than to regional humidity (McDermott, 2004). Speleothem age frequencies are also used to infer periods of rapid speleothem growth and thus humidity (Vaks et al., 2007; Sorin et al., 2010). Speleothem frequencies from the Dead Sea region support the inference of humidity from 135 to 120 ka (54a), and record additional humid periods in the more recent record coincident with some seen throughout the rest of North Africa (43a).

Most of the records from carbonates in the Egyptian Sahara and across North Africa indicate wet conditions between 135 ka and 115 ka, similar to the Levantine records (24a–e, 31a, 42a). Like the records further east, there is then a short period of relative aridity followed by a return to humid conditions. Across North Africa this wet period lasted from 100 ka to 75 ka, with humid conditions beginning earlier and lasting longer than in the Levant. The majority of records from North Africa again display more arid conditions from 75 ka to ~45 ka when humid conditions return until 35 ka (24a–e, 30a, 16a, 10a), similar to the Dead Sea speleothems (44a).

Pollen records from three marine cores off the coast of Morocco (21a–c) allow for the reconstruction of the northern and southern boundaries of the NW Sahara. The north to south range of the cores allows for the demarcation of latitudinal differences in the pollen being swept to sea off the African continent and thus changes in the vegetation belts. Changes in the pollen regime from one site to the other allows for interpretation of the expansion and contraction of the NW Sahara through time. The extent of the Sahara fluctuates on glacial/interglacial cycles with an enlarged steppe-like transition zone north of the desert vegetation during glacial periods. Additionally, the northern boundary of the Sahara expanded further northward during glacial times. During interglacials this transition zone was narrow, with Mediterranean vegetation expanding towards the Sahara from the north and Sahelian (or tropical) woodland from the south. The pollen data from this region show a correlation with Northern Hemisphere ice volume.

Aeolian-derived freshwater diatoms of the genus *Melosira* (Pokras and Mix, 1985) from four sites off the coast of West Africa (34a–d) are indicators of extreme continental aridity. The most northerly record (34a) shows periods of aridity that closely follow times when the Saharan desert expands, and vice versa (Hooghiemstra et al., 1992). Generally, this record is similar to the northern records discussed above with a slight lag as this proxy records the extreme aridity that follows lake desiccation, deflation, and windblown transport. The more southerly diatom records (35b–d) reflect aridity in the tropical region and will be discussed further in that section.

A humidity index generated using the ratio of aeolian dust to fluvial mud (52a) has a comparatively fine scale resolution, so while following a similar long-term pattern as the Sahel/Sahara boundary observed from the offshore pollen record from sites 21a–c, it does not correspond well to the higher frequency freshwater diatom record (34a). In fact, for the period of time it covers (120–30 ka),

Please cite this article in press as: Blome, M.W., et al., The environmental context for the origins of modern human diversity: A synthesis of regional variability in African climate 150,000–30,000 years ago, Journal of Human Evolution (2012), doi:10.1016/j.jhevol.2012.01.011

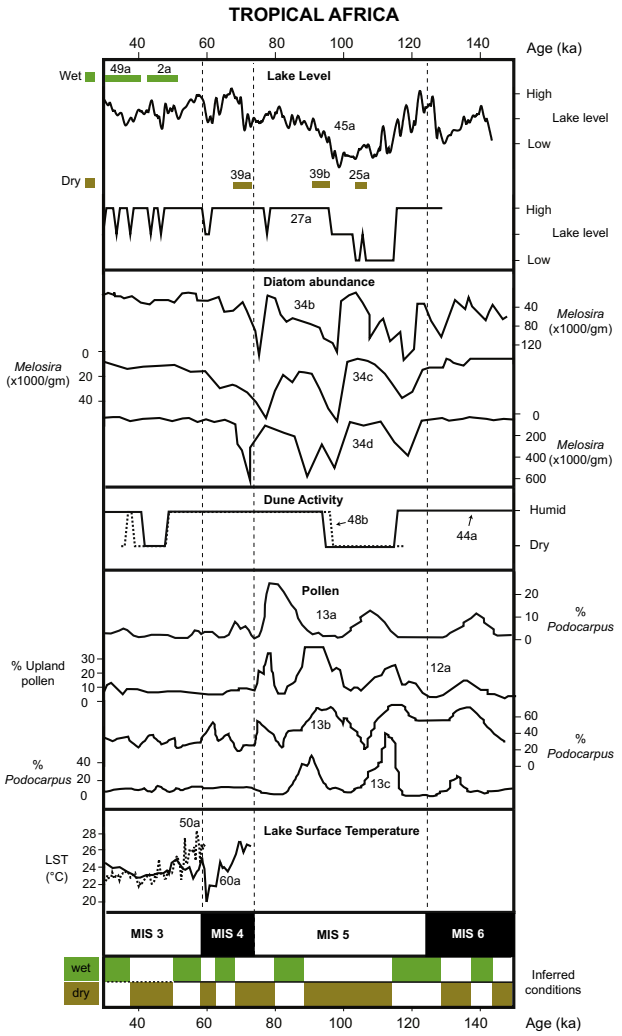

Figure 7. Terrestrial datasets from tropical Africa. Records are arranged in the order they are discussed in the text and grouped by indicator type.

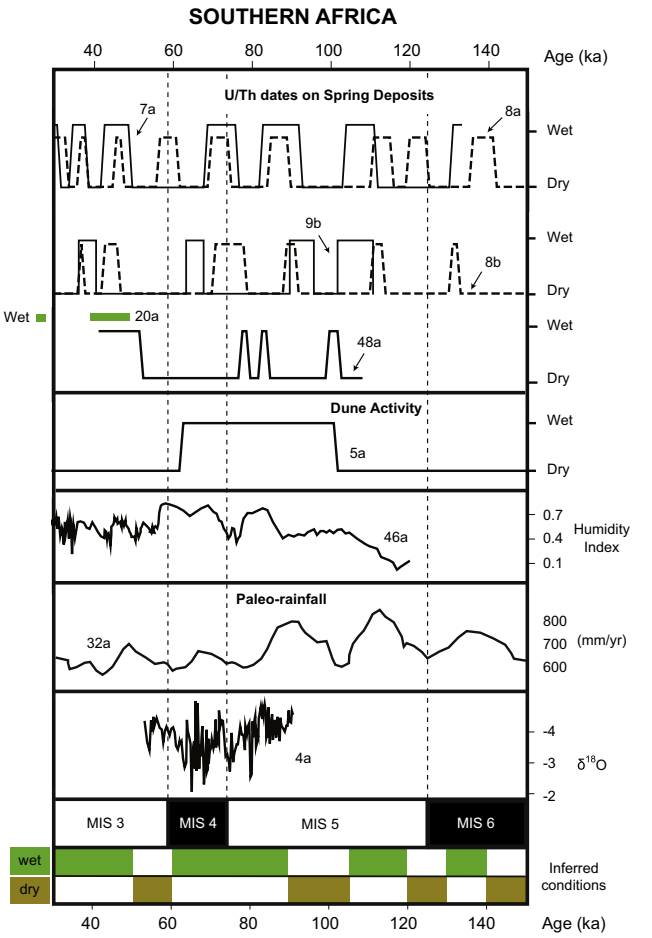

Figure 8. South African terrestrial datasets. Records are arranged in the order they are discussed in the text and grouped by indicator type.

the record is extremely similar to the oxygen isotope record from Peqiin Cave in Israel (3a). As mentioned earlier, the Israeli cave sites appear to strongly co-vary with changes in the SSTs of the Mediterranean and by extension, the Atlantic Ocean, suggesting that the underlying driver of this 'humidity index' may be marine SSTs, whether through atmospheric teleconnection, or a misinterpretation of the grain size indicator.

In summary, North Africa to the Levant experienced generally humid conditions beginning between 135 and 130 ka and lasting until 120–115 ka, and again from 100 to 95 ka until 75 ka. Additionally, a few records across the continent and Levant (44a, 24a–e, 10a, 30a) indicate a more recent wet period from 45 to 35 ka. These wet periods are dated by speleothem $\delta^{18}O$ measurements and frequencies, the deposition of lacustrine, spring-fed, groundwater and cave carbonates. Conversely, the region was drier between ~115–100 ka and from ~75–45 ka, based upon a paucity of dates for carbonate deposition during these periods and from pollen in offshore marine cores that illustrate the fluctuating limit of the Sahara. Additionally, the majority of Levantine cave records and the offshore diatom records are quite variable prior to 75 ka, at which point the climatic variability in NW Africa and the Levant dampens considerably through 30 ka. Overall the regional variations in climate do not appear to fluctuate in response to changing MIS.

East Africa

The records from this region (Fig. 6) are derived from a variety of indicators and were recovered from both terrestrial and marine localities. This region is small and in many respects it represents a paleoclimatic transitional zone between the North African records and the tropical records discussed next. On the continent, two discrete records of lake level highstands are interpreted from U/Th dating of lacustrine carbonates (17a, 56a), whereas a continuous record of lake level change was reconstructed using sediment characteristics and diatom assemblages (53a). The paleoclimatic interpretations of this region are relatively consistent with one another despite the variety of indicators used and time periods covered by the individual datasets.

The lake level records presented here are from the Ol Njorowa Gorge area (paleolake deposits close to modern Lake Naivasha) (53a), and Lake Magadi in Kenya, Lake Natron (17a) in Tanzania, and lakes in the Horn of Africa in Somalia (56a). These records show some similarities, with high lake levels indicating extremely wet periods occurring between ~145–120 ka, ~110–95 ka, and ~80–65 ka. The periods of increased humidity have been inferred to be times when the SW monsoon is most active, during interglacials and interstadials (Hillaire-Marcel et al., 1986; Voight et al., 1990). This interpretation is consistent with the offshore pollen record recovered (Van Campo et al., 1982) that demonstrates that interglacials were the most humid, likely due to the dominance of the SW monsoon over the NE monsoon that prevailed during glacial/stadial

periods. The NE monsoon brought Mediterranean pollen to the Arabian Sea, illustrating the dominant wind patterns at that time. These inferences are further supported by an upwelling record in the Arabian Sea (23a) that shows an increased abundance of $CaCO_3$ during interglacials, implying increased rates of primary production, and increased rates of aeolian deposition from the continent during glacial times, suggesting increased aridity. Increased productivity is an indication of increased upwelling, which brings nutrients to the surface, and it is expected when the SW monsoon is strongest. Likewise, decreased upwelling and aeolian deposition from the NE is expected when the NE monsoon is dominant. However the continuous record from Ol Njorowa Gorge demonstrates the importance of peaks in equatorial (local) insolation, rather than high latitude forcing (Trauth et al., 2003). Unlike insolation intensity further from the equator that is highly variable for a time and then dampens after 75 ka, the insolation at the equator maintains a constant variability in intensity throughout the period of interest (150–35 ka). This local forcing is evident in the constant, cyclic nature of this record (Trauth et al., 2003). Further, the records from East Africa share similar wet/dry interval patterns with the southern extent of the Saharan desert (21a–c). This suggests that the northern boundary of the region may be more transitional, whereas the East African records lack the characteristic 'megadrought' signal found at locations just to the south in the tropical region, suggesting that its southern boundary is more abrupt.

In summary, based on lake level and vegetation reconstructions and upwelling histories, we infer that the East African region was wet ~145–120 ka, ~110–95 ka, ~80–65 ka and 50–55 ka. These variations were likely caused by or related to the changing influences of the NE and SW monsoon regimes forced by changes in local insolation at the equator with increasing influence of high latitude/glacial forcing moving away from the equator.

Tropical Africa (Fig. 7)

The terrestrial data for tropical Africa are derived from a mix of offshore pollen and diatom records (12a, 13a–d, 34b–d), lacustrine records (48a, b, 45a, 27a) and aeolian dune sediments (2a, 44a, 49a). The northern part of the region contains both continuous and discrete records from a number of the East African Rift lakes, e.g., Tanganyika and Malawi, and meteorite/volcanic crater lakes, e.g., Bosumtwi (Ghana) and Challa (Tanzania). The southern area of the region extends to the northern Kalahari and yields a climate signal from dune migration.

The unifying climatic similarity of the records in this region is that they all show evidence of intense 'megadroughts' between 90 ka and 115 ka (Cohen et al., 2007; Scholz et al., 2007) that are not seen at locations both north and south of the region (53a and 7a, respectively; Fig. 7). At Lake Tanganyika, the maximum low-stand occurred at ~106 ka (25a) (McGlue et al., 2008). An earlier arid excursion is recorded at Lake Malawi (45a) and one offshore diatom record (34b) from 135 ka and 130 ka, but is not seen in the northern Kalahari records (44a), or the other two offshore diatom records (34c, d). Perhaps this was a very localized event that happened to be captured by one of three distant marine records. After 90 ka, the entire region gradually, though irregularly, becomes more humid until ~50 ka when the southern dune records are no longer synchronous with the northern lake records. Between 50 ka and 40 ka, the southern portion of the region (44a, 48b) becomes more arid while the northern lakes (45a, 27a) indicate greater or similar humidity (Fig. 7). The entire tropical region is wet between 35 ka and 30 ka. Off the coast of West Africa, three equatorial pollen records support the regional patterns of aridity and humidity primarily during MIS5, with a short time lag observed similar to the offshore diatom records (34b–d).

Compared to the dune records, some of the lake records provide climate data at a higher resolution over the entire period of interest (Stone et al., 2011) and during the more recent portion of that time period (Tierney et al., 2008; Woltering et al., 2011). Scholz et al. (2007) argued for high amplitude lake level variability at Lake Malawi prior to ~70 ka, with approximately 20 kyr periodicities, followed by lowered variability (but with overall high lake levels), consistent with a general pattern of insolation forcing (an eccentricity-modulated precessional pattern). A similar pattern appears to hold at Lake Tanganyika and perhaps Lake Bosumtwi. There is, for example, evidence at lakes Malawi and Bosumtwi for a short-lived arid event around 75 ka (39a, 45a). Additionally, at Lake Challa in the north there was a minor low-stand, inferred to have occurred at ~60 ka (27a), while at the same time, Lake Malawi LSTs dropped to their lowest temperature recorded between 65 and 55 ka (60a). Based on LSTs, diatoms, and sedimentology, Heinrich events 4, 5, and 6 have been recognized in lakes Tanganyika (Tierney et al., 2008), Malawi (Stone et al., 2011; Woltering et al., 2011), and Challa (Moernaut et al., 2010). Lake level and temperature data together indicate that this region may have been cold and dry for brief periods of time between 60 ka and 35 ka. The evidence for Heinrich events in the climate signal of tropical Africa suggests a relationship between the Northern Hemisphere climate and the equatorial interior of Africa.

Over the past 60 kyr, LST values for Lake Tanganyika suggest tropical African terrestrial precipitation is more closely linked to Indian Ocean SSTs, as opposed to local LSTs. Even during periods of colder local LST values, warmer Indian Ocean temperatures appear to provide sufficient moisture to induce rainfall in the region, whereas the location of the ITCZ (often considered the primary driver of tropical precipitation) appears to have primarily controlled wind direction at Lake Tanganyika (Tierney et al., 2008). Thus, Indian Ocean SSTs and the extent of the ITCZ need to be working in concert for extreme humid periods in tropical Africa. This apparent collaboration between Indian Ocean SSTs and the ITCZ/local insolation maxima between 60 ka and 30 ka adds to the mystery of the early Late Pleistocene African megadroughts. Between 115 ka and 90 ka, insolation variability was extreme and local Indian Ocean SSTs were relatively warm, suggesting that Lake Malawi (for example) should have been very dry, then very wet, as opposed to extremely dry for over 20 kyr. This suggested link between regional terrestrial precipitation and Indian Ocean SSTs also does not explain the widespread geographic extent of the extended megadrought period. The Indian Ocean records in this synthesis indicate a weakened SW monsoon with lower $CaCO_3$ and decreased upwelling off the coast of Oman (23a), suggesting a decreased contrast between land surface temperature and neighboring SSTs, but not substantially reduced SSTs; only 0.5–1 °C decrease, in the three records available (1a, b, 37b). Something must be different between the time of the megadrought event and the more recent record. Given these data, it is likely that the Indian Ocean SST effect is only evident in tropical Africa when the insolation swings are not as strong as they were prior to 70 ka.

The pollen data from off the west coast of tropical Africa are difficult to interpret over the entire time interval in terms of a regional signal because they are dominated by local pollen from mountainous refugia along the western coast of Africa, from Guinea to Angola (Dupont and Weinelt, 1996; Dupont et al., 2000). However, the patterns appear to indicate responses to North Atlantic SSTs with ubiquitous rainforest expansion during OIS substages 5a, 5c, and 5e, and dry woodland expansion during MIS substages 5b and 5d.

In summary, this region of tropical Africa extends from lakes Bosumtwi and Challa in the north to the northern Kalahari Desert in the south. A significant difference between it and the

Please cite this article in press as: Blome, M.W., et al., The environmental context for the origins of modern human diversity: A synthesis of regional variability in African climate 150,000–30,000 years ago, Journal of Human Evolution (2012), doi:10.1016/j.jhevol.2012.01.011

neighboring regions is the presence of a regional 'megadrought' signal from ~115–90 ka. Additionally, these records indicate a gradual, though at times erratic, trend toward a more humid climate from 90 ka to 35 ka. While not applicable over the entire period of interest, there appears to be a tenuous relationship between the tropical lakes and MIS, particularly after insolation variability dampens ~75 ka, at the beginning of MIS 4.

Southern Africa (Fig. 8)

Unlike the records of tropical Africa, the climate of southern Africa is much more punctuated with no clear trends of either increasing or decreasing humidity through time across the region. The Mababe Depression (Fig. 7, 44a at 19°S, 27°E) borders the region to the north and shows a punctuated megadrought-like signal from 110 to 95 ka. However, sites just to the west at Drotsky's Cave (8a at 20°S, 23°E) and to the south at Lobatse Caves (48a at 25°S, 25°E) demonstrate a clearly humid climate throughout this same time period. It is possible then that the southwest extent of the 'megadrought belt' lies between ~19°–25°S latitude, and ~23°–27°E longitude. The orientation of this border between the 'megadrought belt' and southern Africa may mirror the angled track of the ITCZ across the continent, suggesting that the extent of the ITCZ may be an important factor in the millennia-long megadrought events (see 'causal mechanisms').

The records that extend through the entire time period of interest do show a precessional signal (23 kyr cycle) of wet/dry periods (5a, 32a, 8a, b) (Brook et al., 1996; Partridge, 1999; Burrough et al., 2007) with humid periods coinciding with Southern Hemisphere insolation maxima. The record from Tswaing crater (32a), one of the two records that shows a variable humidity signal (not just a discrete signal of wet or not), does indicate a trend of decreasing variability from 90 to 35 ka as expected with eccentricity-modulated precession. However, the offshore humidity record (site 46a) does not correlate with the inferred rainfall record from the Tswaing Crater (cf. Fig. 8). The offshore record shows a slight trend towards increasing humidity from 115 to 35 ka, whereas Tswaing Crater shows a slight trend towards decreasing humidity over the same time interval. Although the tuning of the Tswaing Crater grain size record has been called into question in the past, the precessional cyclicity has been seen in the data using other proxies as well (Kristen et al., 2007). All records except the most southern dune record (5a at 27°S) depict a coherent, increasingly humid signal from ~60–45 ka. A possible explanation for this discrepancy is its relative proximity to both the eastern and southern coasts of the continent compared with the other dune records. Recent research suggests coastal or barrier dunes are primarily affected by distance to shore and thus sediment availability for dune migration, rather than the classic interpretation that dunes migrate during arid times and are stable during humid times (Carr et al., 2006, 2007; Bateman et al., 2011). Despite this site's relative proximity to the coasts, compared with the other dune sites discussed in this synthesis, it is hardly a 'coastal dune' location. In addition, it is bordered to the west and east by mountain barriers to coastal influence and thus OSL dates from this site should be responding to an aridity signal unlike true 'coastal' dunes. Thus the reason for this discrepancy must be a more local effect.

The isotope record from Pinnacle Point on the tip of South Africa displays trends coherent with the Southern Ocean SST records that follow a North Atlantic SST pattern (4a) (Bar-Matthews et al., 2010). During MIS 4 (glacial), the speleothem carbonates are isotopically enriched (higher $\delta^{18}O$). This is expected because during ice ages, oxygen isotopes in ocean water will be preferentially heavier than during interglacial periods (lighter isotopes of oxygen locked in polar and mountain ice), causing the rain-water, and thus cave-water to begin its hydrologic journey more enriched during glacial periods.

In summary, the northern boundary of this region exhibits a modified/punctuated 'megadrought' signal, whereas the rest of the region does not. There is a clear eccentricity-modulated precessional cyclicity to the wet/dry climate of southern Africa, although no clear trend toward increasing or decreasing humidity through the time interval of interest. In addition, there appears to be no clear regional climatic relationship to the MIS boundaries.

Regional coherence of temporal trends in African climate change

The evidence presented above indicates that SSTs often co-vary with climate changes predicted by $\delta^{18}O$-derived MIS boundaries, with terrestrial data often out of phase although varying by subregion. Principal components analysis (PCA) provides a more formal means of comparing aggregate data from both marine and terrestrial sources. On a PCA plot, datasets with similar patterns of variability will plot together. The PCA results are presented in Figs. 9–11. For the purposes of clarifying regional trends, the data are presented with their site number plotted on the PC ordination plot for each time period, and the PC axis values are mapped spatially by data type, identified by a single letter prefix for SSTs (S), terrestrial temperature (T), or precipitation (P). In addition to circum-Africa datasets, maximum summer insolation values at 15°N and 15°S were also included in each analysis, as well as a typical North Atlantic SST dataset (35a) (Raymo et al., 2004), to determine the correlation of the individual African paleoclimate datasets to possible regional/global influences on local paleoclimate records. We present here the results of comparisons for 140–30 ka, 115–30 ka and 75–30 ka, as patterns (or lack thereof) in the data are clearest for these time intervals. The analysis for the 150–100 ka interval is presented as online SOM. In all analyses, the first principal component (PC1) is statistically significant, and is interpreted as the response to variability due to North Atlantic SST forcing, whereas the second principal component (PC2) (with differing degrees of significance) is interpreted as the response to insolation variability.

140–30 ka (Fig. 9, Table 4)

This time period was chosen because it maximizes the number of datasets used (32) over the greatest percentage of the time period of interest (92%). Over this interval, only the first two principal components were statistically significant: PC1 (SST) explains 42% of the variance and PC2 (insolation variability) explains 16% of variance. Most of the SST records cluster together and are particularly constrained along the PC1 axis with values ranging from −1.07 to −0.79 (Fig. 9). One SST record falls somewhat outside the tightly constrained PC1 range, 34a (26°S), and another SST record, 6a (49°S, nearly in the Southern Ocean), differs significantly from the other SST records. This may be a reflection of the circum-Antarctica SST trends as opposed to circum-Africa SSTs (Fig. 9).

The terrestrial records (both precipitation and temperature) plot away from the 'SST cluster' along the PC1 axis, and most have similar trends to the maximum Northern Hemisphere summer insolation (N. Insol). Notable exceptions to this are four precipitation records: two off the northwest coast of Africa (21c, 34a), one in sub-tropical East Africa (45a), and another in the Levant (43a). The lake level record from Lake Malawi (45a) surprisingly shows almost no correlation with PC2 axis, perhaps indicating another factor contributing strongly to PC2 in this interval. In contrast to the $\delta^{18}O$ records at Peqiin and Soreq caves (3a, b), which again vary in concert with the SST records, the climatic trends observed in the

Please cite this article in press as: Blome, M.W., et al., The environmental context for the origins of modern human diversity: A synthesis of regional variability in African climate 150,000–30,000 years ago, Journal of Human Evolution (2012), doi:10.1016/j.jhevol.2012.01.011

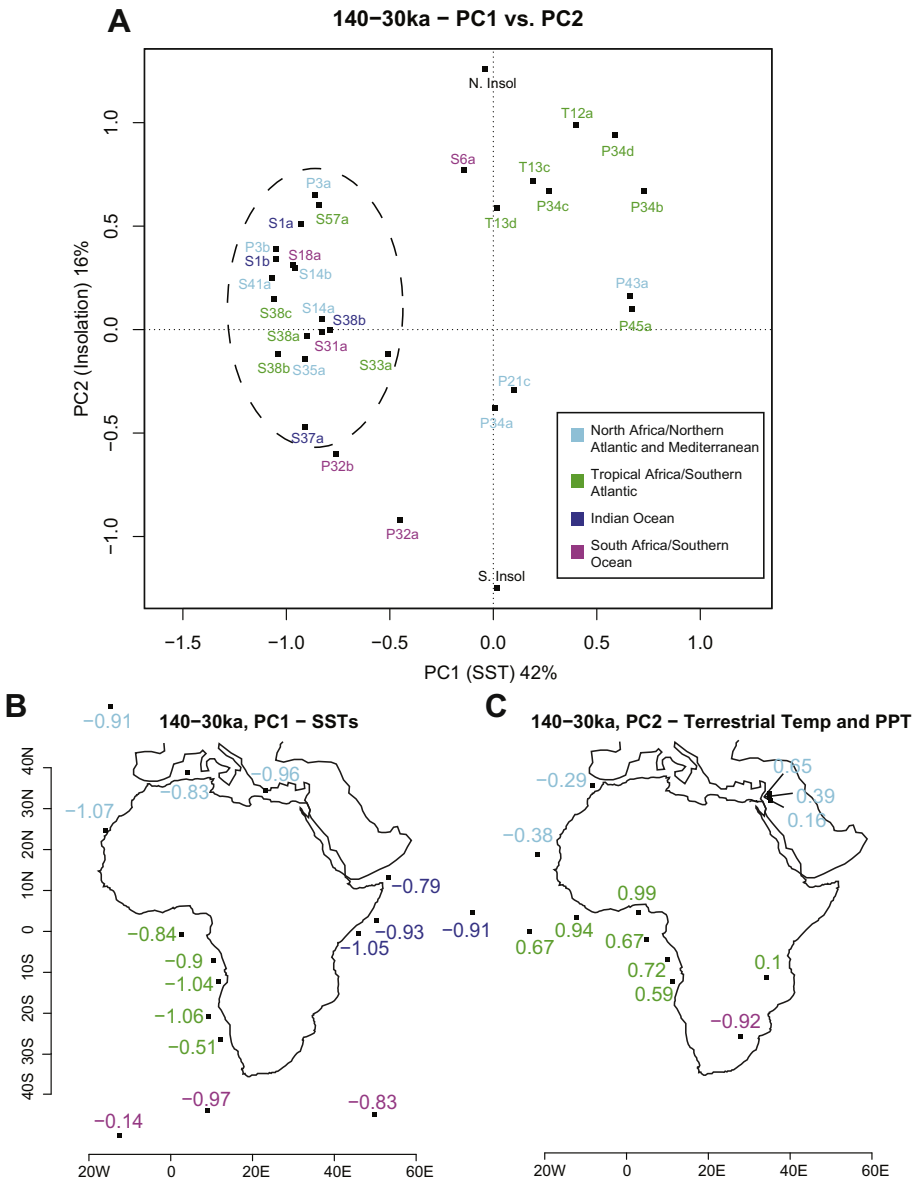

Figure 9. Principal component (PC) analysis of all available continuous data over the 140–30 ka time interval. Regional color key applicable to entire figure. A) Ordination plot. Dashed oval indicates "SST Cluster" discussed in text. B) Spatial distribution of PC1 scores from circum-Africa SST datasets. C) Spatial distribution of PC2 scores from terrestrial precipitation and temperature datasets.

record of speleothem growth frequency in the Levant (43a) are surprisingly similar to those over this period at Lake Malawi (45a), and yet they differ greatly from the other records in the North African region (see Fig. 9: 34a, 21c). Offshore records of tropical African climate are strongly correlated with 15°N insolation, and both the tuned and un-tuned records of the Pretoria Salt Pan in southern Africa (32a, b) are more similar to the maximum southern summer insolation, and again show some relationship to the climatic trends of SST records (Fig. 9).

115–30 ka (Fig. 10, Table 5)

This interval was chosen to increase the number of datasets used (38) over a significant percentage of the time period of interest (71%). This period also covered an interval of decreasing insolation variability in the latter part of this interval. In spite of this, there are still very clear, significant patterns in the climatic trends of SSTs (PC1, 44% of variance) and northern versus southern maximum summer insolation (PC2, 15% of variance). There is a very tight cluster of PC1 values for the majority of SST records (−0.99 to −0.69). The southern Atlantic site (33a) at 26°S latitude, which for the 140–30 ka interval analysis was significantly offset from the remaining SST cluster, is more closely linked to this cluster for the 115–30 ka analysis (Fig. 10). In contrast, two SST records vary considerably from the other SST records (Fig. 10): one again from the Southern Ocean (6a at 49°S), the other in an upwelling zone off the Arabian Peninsula (23a at 18°N). As observed in the previous time intervals, the Levantine cave records plot within the SST cluster (3a, b), as does another precipitation record, (52a) the offshore grain-size humidity index. This confirms the similarity through time of these two records noted earlier.

The majority of terrestrial precipitation and temperature records plot away from the SST group along the PC1 axis and there is a very coherent grouping along the PC2 axis as well with values

Please cite this article in press as: Blome, M.W., et al., The environmental context for the origins of modern human diversity: A synthesis of regional variability in African climate 150,000–30,000 years ago, Journal of Human Evolution (2012), doi:10.1016/j.jhevol.2012.01.011

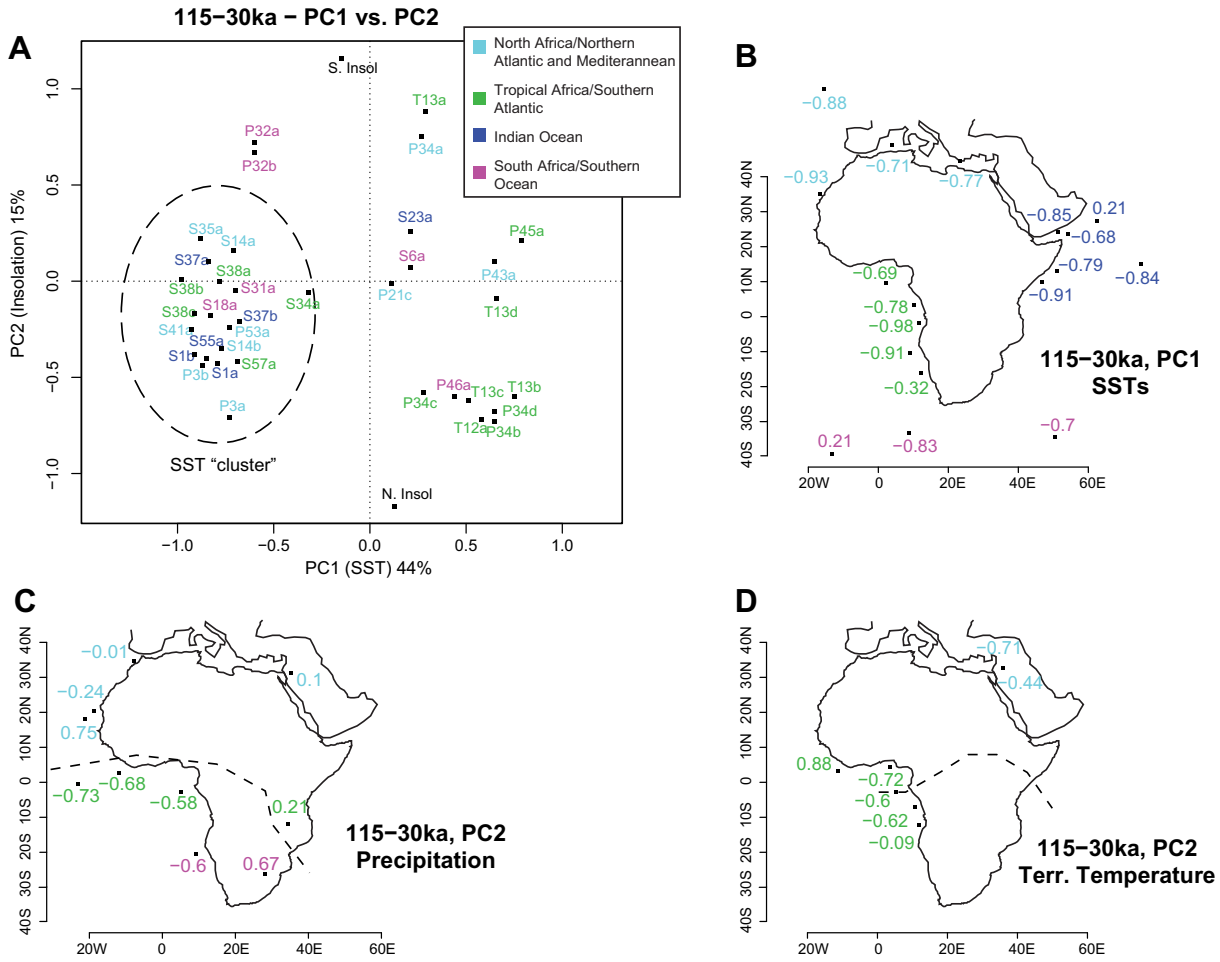

Figure 10. Principal component (PC) analysis of all available continuous data over the 115–30 ka time interval. Regional color key applicable to entire figure. A) Ordination plot - note sea surface temperature (SST) 'cluster' labeled. B) Spatial distribution of PC1 scores on SST datasets. C) Spatial distribution of PC2 scores from terrestrial precipitation, and D) temperature datasets. Dashed line represents interpreted location of a division in climate trends over this time period.

ranging from −0.72 to −0.57, still trending over time similar to 15°N maximum summer insolation. Exceptions for this time period once again include the Tswaing crater records (32a, b), plotting half way between the SST grouping and the 15°S maximum summer insolation pattern. However, both the tuned and un-tuned grain size records plot similarly, reaffirming that the tuning quality of the records is unlikely to explain the pattern seen in the dataset (e.g., Kristen et al., 2007). Instead, the Tswaing crater data suggests that insolation plays a much smaller role in the response of this record over the 115–30 ka interval than for 140–30 ka. The Lake Malawi (45a) and Levantine speleothem frequency (43a) records once again plot towards the origin of the PC2 axis, and the terrestrial temperature record that is furthest south (13d) at 12°S plots near the middle of PC2 (Fig. 10). Off the coast of northwest Africa, both a precipitation record at 18°N (34a) and temperature record at 4°N (13a) appear to be anti-correlated with trends in both types of records just to the south (Fig. 10). Perhaps ~4°N is an important climatic boundary over this time period.

75–30 ka (Fig. 11, Table 6)

This interval was chosen to investigate possible spatial patterns during a period of dampened insolation variability. This interval also had the highest number of usable datasets (40). For this interval, only one axis was significant (PC1), which explains 39% of the variance, and Northern and Southern Hemisphere insolation no longer shows significant loadings relative to the entire dataset (Fig. 11a). Although the majority of SST records versus terrestrial records are still strongly contrasted along the PC1 axis (with no strong relationship to latitude), they are considerably more scattered than the previous time periods analyzed. The tropical terrestrial precipitation records continue to have values similar to that of 15°N maximum summer insolation (Fig. 11b), or 15°S for the Tswaing Crater (33a, 33b), whereas the terrestrial temperature records show little to no spatial correlation pattern in PC1 values (Fig. 11c). As anticipated, there is a decreased effect of insolation maxima on terrestrial records during this interval of dampened eccentricity-modulated precession.

The PCA results support a generally clear separation between SST data and those from terrestrial sources, the latter often associated with maximum insolation. This separation is only apparent during periods of lower insolation variability (e.g., 75–30 ka). These results suggest that different climate mechanisms are affecting the marine and terrestrial environments in Africa during much of the 150–30 ka period.

An evaluation of causal mechanisms

Throughout the discussion of the SST records, there was a recurring theme: all records seem to follow global MIS boundaries, except where they do not. In other words, circum-Africa SSTs record both the global temperature variability, as well as

Please cite this article in press as: Blome, M.W., et al., The environmental context for the origins of modern human diversity: A synthesis of regional variability in African climate 150,000–30,000 years ago, Journal of Human Evolution (2012), doi:10.1016/j.jhevol.2012.01.011

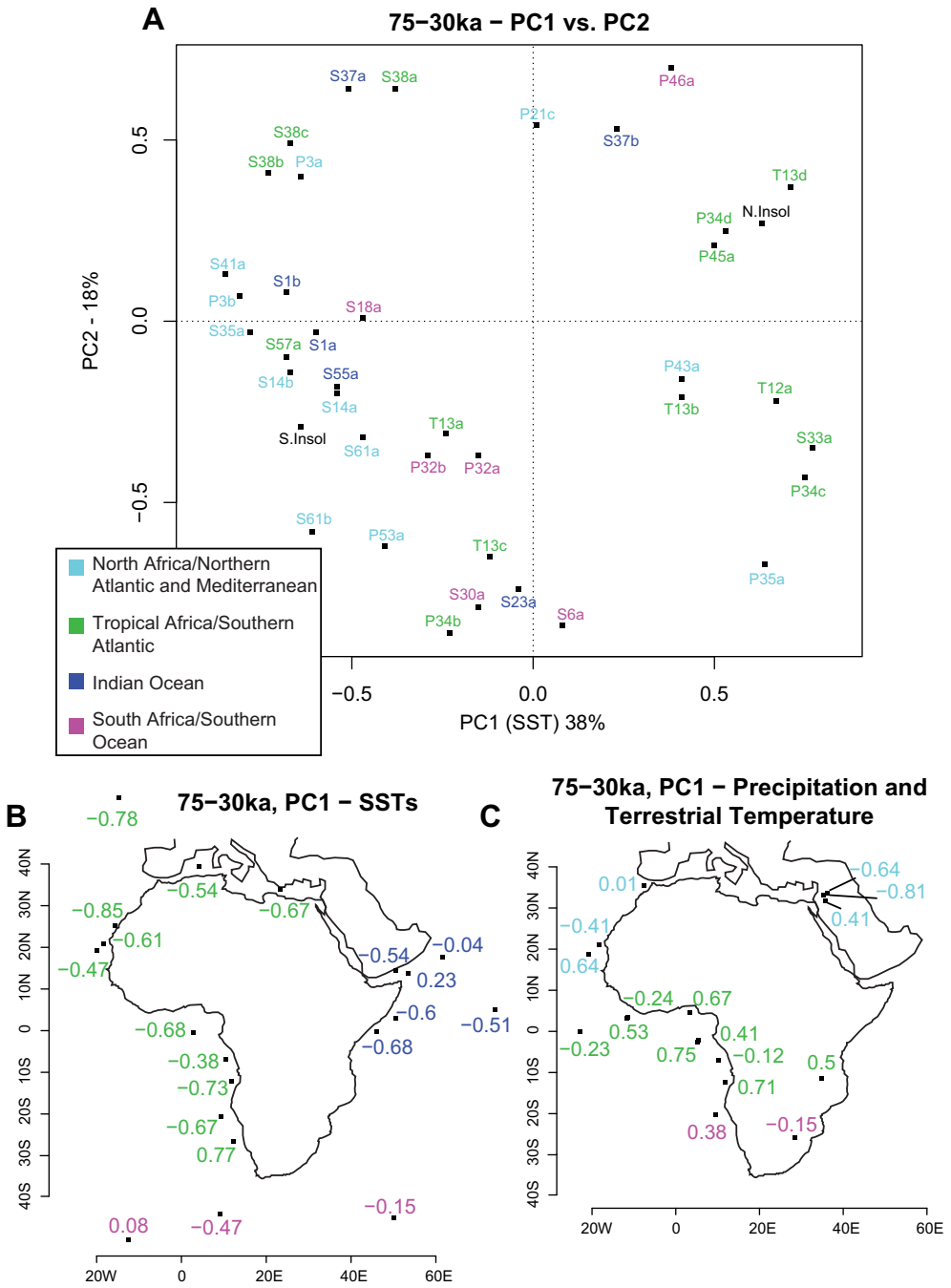

Figure 11. Principal component (PC) analysis for time interval 75–30 ka. Regional color key applicable to entire figure. A) Ordination plot, only PC1 is significant. Notice how the variation due to insolation appears to be more muted during this time interval whereas the SST variability still shows a coherent trend along the PC1 axis, the only significant axis. B) Spatial distribution of PC1 scores from circum-Africa SST datasets. C) Spatial distribution of PC1 scores from terrestrial precipitation and temperature datasets.

perturbations in that overall signal by local or regional effects such as changing wind zonality and/or upwelling activity. As illustrated in the previous section, terrestrial temperature and precipitation across Africa do not seem to be responding to North Atlantic SST forcing (MIS boundaries, PC1 on Figs. 9–11). This does not imply that SST and other marine data have no useful information for continental climate variability. Rather, those perturbations in the global marine temperature signal may be the key to discrete periods of continental climate variability. In this section, we examine two potential drivers of local or regional climate variability: the changing position of the Westerlies and the ITCZ through time. We consider how these regional variations would be represented in the paleo-record, and whether we see evidence for changes in the location of either the Westerlies or the ITCZ between 150 ka and 30 ka.

Position of the Westerlies

Strengthening or weakening of the Westerlies may help explain moisture variation in the northern and southern extremes of Africa. This strengthening was modeled by Toggweiler and Russell (2008) to occur when there is a significant contrast between temperatures at the equator and at the poles, similar to the modern climate. When the Westerlies are strong, they are pulled closer to the poles

Table 4
Principal components (PC) axes 1 and 2 values by site for the 140-30 ka interval. 32 datasets included.

Site	PC1	PC2	STP	Latitude	Longitude
S1a	−0.93	0.51	S	3.18	50.43
S1b	−1.05	0.34	S	0.02	46.03
P3b	−1.05	0.39	P	31.50	35.00
P3a	−0.86	0.65	P	32.58	35.19
S6a	−0.14	0.77	S	−49.01	−12.70
T13c	0.19	0.72	T	−6.60	10.30
T13d	0.02	0.59	T	−11.75	11.70
T12a	0.4	0.99	T	4.80	3.40
S14a	−0.83	0.05	S	38.99	4.02
S14b	−0.96	0.3	S	34.81	23.19
S18a	−0.97	0.31	S	−42.92	8.90
P21c	0.1	−0.29	P	34.90	−7.80
P22a	−0.04	1.26	P	15.00	68.00
P22b	0.02	−1.25	P	−15.00	68.00
S31a	−0.83	−0.01	S	−43.96	49.93
P33a	−0.45	−0.92	P	−25.60	28.08
P33b	−0.76	−0.6	P	−25.60	28.08
S34a	−0.51	−0.12	S	−25.81	12.13
P35b	0.73	0.67	P	−0.20	−23.15
P35a	0.01	−0.38	P	18.40	−21.10
P35c	0.27	0.67	P	−2.28	5.18
P35d	0.59	0.94	P	3.05	−11.82
S36a	−0.91	−0.14	S	55.00	−15.00
S38b	−0.79	0	S	13.70	53.25
S38a	−0.91	−0.47	S	5.07	73.88
S39a	−0.9	−0.03	S	−6.58	10.32
S39b	−1.04	−0.12	S	−11.76	11.68
S39c	−1.06	0.15	S	−20.10	9.18
S42a	−1.07	0.25	S	25.00	−16.00
P44a	0.66	0.16	P	31.30	35.30
P46a	0.67	0.1	P	−11.30	34.45
S59a	−0.84	0.6	S	−0.35	2.50

Table 5
Principal components (PC) axes 1 and 2 values by site for the 115-30 ka interval. 38 datasets included.

Site	PC1	PC2	STP	Latitude	Longitude
S1a	−0.79	−0.43	S	3.18	50.43
S1b	−0.91	−0.38	S	0.02	46.03
P3b	−0.87	−0.44	P	31.50	35.00
P3a	−0.73	−0.71	P	32.58	35.19
S6a	0.21	0.07	S	−49.01	−12.70
T13c	0.51	−0.62	T	−6.60	10.30
T13d	0.66	−0.09	T	−11.75	11.70
T12a	0.58	−0.72	T	4.80	3.40
T13b	0.75	−0.6	T	−2.20	5.10
T13a	0.29	0.88	T	3.75	−11.40
S14a	−0.71	0.16	S	38.99	4.02
S14b	−0.77	−0.35	S	34.81	23.19
S18a	−0.83	−0.18	S	−42.92	8.90
P21c	0.11	−0.01	P	34.90	−7.80
P22a	0.13	−1.17	P	15.00	68.00
P22b	−0.15	1.16	P	−15.00	68.00
S23a	0.21	0.26	S	17.50	61.50
S31a	−0.7	−0.05	S	−43.96	49.93
P33a	−0.6	0.72	P	−25.60	28.08
P33b	−0.6	0.67	P	−25.60	28.08
S34a	−0.32	−0.06	S	−25.81	12.13
P35b	0.65	−0.73	P	−0.20	−23.15
P35a	0.27	0.75	P	18.40	−21.10
P35c	0.28	−0.58	P	−2.28	5.18
P35d	0.65	−0.68	P	3.05	−11.82
S36a	−0.88	0.22	S	55.00	−15.00
S38b	−0.68	−0.21	S	13.70	53.25
S38a	−0.84	0.1	S	5.07	73.88
S39a	−0.78	0.000	S	−6.58	10.32
S39b	−0.98	0.010	S	−11.76	11.68
S39c	−0.91	−0.170	S	−20.10	9.18
S42a	−0.93	−0.3	S	25.00	−16.00
P44a	0.65	0.10	P	31.30	35.30
P46a	0.79	0.21	P	−11.30	34.45
P47a	0.44	−0.6	P	−20.00	9.26
P53a	−0.73	−0.24	P	20.75	−18.57
S57a	−0.85	−0.4	S	14.40	50.50
S59a	−0.69	−0.42	S	−0.35	2.50

and divert the rain elsewhere. Alternatively, during glacial or stadial periods there is less of a temperature contrast between the equator and poles, the Westerlies are weaker, and they are positioned closer to the equator, bringing precipitation to both extreme regions of Africa (Fig. 12a). This interpretation is consistent with recent research on the southern African coast where colder periods (such as MIS4) were also wetter (Chase, 2010). Grain size analysis of ocean sediment from a marine core taken from just south of the South African shore (36°19.2′S; 19°28.2′E) suggests a northward movement of the Antarctic Circumpolar Current (ACC) during glacial periods as well (Martinez-Méndez et al., 2008), perhaps following the equator-ward movement of the Westerlies.

Multiple indicators can be examined to infer the paleo-location of the Westerlies. In the Southern Hemisphere, when the Westerlies are strong and pulled tighter around the poles they leave a gap between the tip of Africa and their circulation pattern. When this happens, warm water from the Indian Ocean (the Agulhas Current) is able to round the tip of Africa making the SSTs off of the western tip of South Africa warm. Colder SSTs in the same region would therefore indicate weakened Westerlies that cross the southern tip of Africa and prevent Indian Ocean leakage into the South Atlantic. If the location of the Westerlies is the dominant driver of African climate, then North and South Africa should be wet when the Westerlies are weak (equator-ward), and the SSTs in the Benguela current should be cold. However, when the Westerlies are strong, northern and southern Africa should be dry, and the SSTs in the Benguela current will be warm (Fig. 12b). From 130 to 115 ka, the SSTs in the Benguela region are warm and many paleo-precipitation records in the north and south indicate dry conditions (strengthened, pole-shifted Westerlies). However, Egyptian records (37a, 48a, 32a) indicate very wet conditions for this time. In contrast, from 50 to 35 ka when SSTs are cold, northern and southern Africa are wet, again with the exception of the Egyptian records, which are dry (weak, equator shifted Westerlies).

These data suggest the strength and position of the Westerlies likely had a significant impact on regional precipitation patterns throughout the 150–30 ka interval. However, they also demonstrate that eastern North Africa and the Levant are out of phase with the rest of the northern and southern portions of the continent. For the earlier period (130–115 ka), perhaps the pole-ward shift of the Westerlies allowed the SE trade winds to bring moisture from a different source to eastern North Africa (e.g., the Indian Ocean), meanwhile NW Africa remained dry in response to colder North Atlantic SSTs. For the later period (50–35 ka), perhaps the moisture-laden Westerly winds were rained-out crossing the expansive, dry Sahara prior to reaching Egypt and the Levant.

Influence of ITCZ location

Changes in the average ITCZ position over extended time periods may explain long-term moisture variation between ~20°N and 15°S over the 150–30 ka time interval. As shown in our PCA, precipitation across tropical Africa fluctuated similarly with changes in tropical insolation, particularly over periods of maximum NH insolation variability and intensity.

Monsoons are dynamic systems in two ways: thermal and hydrologic, meaning monsoon systems respond to land/ocean temperature contrasts, and are also dependent on SSTs, evaporation from oceans, and water vapor transport to land (Kutzbach et al.,

Please cite this article in press as: Blome, M.W., et al., The environmental context for the origins of modern human diversity: A synthesis of regional variability in African climate 150,000–30,000 years ago, Journal of Human Evolution (2012), doi:10.1016/j.jhevol.2012.01.011

Table 6
Principal components (PC) axes 1 and 2 values by site for the 75-30 ka interval. 40 datasets included.

Site	PC1	PC2	STP	Latitude	Longitude
S1a	−0.6	−0.03	S	3.18	50.43
S1b	−0.68	0.08	S	0.02	46.03
P3b	−0.81	0.07	P	31.50	35.00
P3a	−0.64	0.4	P	32.58	35.19
S6a	0.08	−0.84	S	−49.01	−12.70
T13c	−0.12	−0.65	T	−6.60	10.30
T13d	0.71	0.37	T	−11.75	11.70
T12a	0.67	−0.22	T	4.80	3.40
T13b	0.41	−0.21	T	−2.20	5.10
T13a	−0.24	−0.31	T	3.75	−11.40
S14a	−0.54	−0.2	S	38.99	4.02
S14b	−0.67	−0.14	S	34.81	23.19
S18a	−0.47	0.01	S	−42.92	8.90
P21c	0.01	0.54	P	34.90	−7.80
P22a	0.63	0.27	P	15.00	68.00
P22b	−0.64	−0.29	P	−15.00	68.00
S23a	−0.04	−0.74	S	17.50	61.50
S31a	−0.15	−0.79	S	−43.96	49.93
P33a	−0.15	−0.37	P	−25.60	28.08
P33b	−0.29	−0.37	P	−25.60	28.08
S34a	0.77	−0.35	S	−25.81	12.13
P35b	−0.23	−0.86	P	−0.20	−23.15
P35a	0.64	−0.67	P	18.40	−21.10
P35c	0.75	−0.43	P	−2.28	5.18
P35d	0.53	0.25	P	3.05	−11.82
S36a	−0.78	−0.03	S	55.00	−15.00
S38b	0.23	0.53	S	13.70	53.25
S38a	−0.51	0.64	S	5.07	73.88
S39a	−0.38	0.64	S	−6.58	10.32
S39b	−0.73	0.41	S	−11.76	11.68
S39c	−0.67	0.49	S	−20.10	9.18
S42a	−0.85	0.13	S	25.00	−16.00
P44a	0.41	−0.16	P	31.30	35.30
P46a	0.5	0.21	P	−11.30	34.45
P47a	0.38	0.7	P	−20.00	9.26
P53a	−0.41	−0.62	P	20.75	−18.57
S57a	−0.54	−0.18	S	14.40	50.50
S59a	−0.68	−0.1	S	−0.35	2.50
S63a	−0.47	−0.32	S	19.00	−20.17
S63b	−0.61	−0.58	S	20.75	−18.58

2008). The differential heating of land and ocean near and below the average location of the ITCZ can upset both oceanic and atmospheric dynamics, ultimately affecting the extent and position of tropical monsoons globally. As a consequence of its effect on monsoon systems, the average position of the ITCZ over time may also greatly affect the climate in regions on the extreme edge of the ITCZ range, as small shifts one way or another will have a greater impact there (Brown et al., 2007). For example, during periods of extreme insolation variability, when Asian monsoonal circulation is intensified, the average position of the ITCZ may in fact be further north over those time periods, and consequently areas at the edge of the southern range of the ITCZ may not receive much rainfall at all.

This idea can be tested by comparing the hydrologic record of Lake Malawi (currently at the edge of the southern range of the ITCZ) with Northern Hemisphere tropical insolation. If the Asian monsoon has such an extreme effect on the southern extent of the ITCZ, in years when the Asian monsoon is strong, and the ITCZ is further north, Lake Malawi (and other areas in the extreme southern tropics of Africa) will be drier (Fig. 13a). The reverse is also true. The tropical region will likely be wet during times when the Asian monsoon (and Northern Hemisphere insolation) is weak. It has been observed in climate models that the stronger Asian monsoons occur during times of Northern Hemisphere insolation maxima (or ice volume minima, e.g., interglacials) and vice versa (Clemens et al., 2008). This idea appears to be valid in the tropical region until ~75 ka when the variability, or the range of extreme values, in insolation declines (Fig. 13b). This is exactly what is seen in the PCA of terrestrial precipitation patterns. The majority of the tropical datasets vary in concert with tropical insolation (PC2), until the 75–30 ka analysis. From 75 ka to 30 ka, insolation variability is weakening and there is no clear relationship between insolation and precipitation (Fig. 13c). This weakening may allow other factors to become relatively more significant at this time, and may help explain why some lakes outside the 'megadrought belt' stabilize at low levels after 70 ka, whereas lakes Malawi, Tanganyika and Bosumtwi all stabilize at high levels after this time.

Synthesis: African climate from 150 to 30 ka

African paleoclimates from 150 to 30 ka are spatially and temporally complex, with variation in the outcome of multiple related processes. We summarize these here before considering their implications for human evolution, determining the degree to which our hypotheses are supported or rejected.

Hypothesis 1. Pleistocene African climate change is coincident with North Atlantic glacial/interglacial periods.

Fig. 14 demonstrates that although SSTs do tend to vary with glacial/interglacial cycles and MIS boundaries, this pattern does not hold for much of the African continent over the 150–30 ka interval. There do appear to be instances after 75 ka in three of the four regions (North, tropical, and southern Africa) when terrestrial precipitation and temperature change is coincident with MIS boundaries (cf. Fig. 14, MIS 4 interval).

Hypothesis 2. Pleistocene African climate change is coincident with Northern and Southern Hemisphere insolation cycles.

Our PCA results (Figs. 9–11) support this hypothesis, showing that precipitation across tropical Africa fluctuated similarly with changes in tropical insolation. However, more detailed comparison of continuous datasets indicate that this hypothesis is supported only for ~150–75 ka, a period of high Northern Hemisphere insolation variability and intensity, and is not well supported for the ~75–30 ka interval of dampened insolation variability and intensity (see also SOM).

Hypothesis 3. Pleistocene African climate change is the result of the complex interaction of a number of factors, including atmospheric dynamics.

Our results support this hypothesis (Figs. 12 and 13). The position of the Westerlies and the ITCZ through time appear to have affected terrestrial climate variability at discrete times, and also may be the underlying cause of region/site specific temperature excursions in circum-Africa SSTs between 150 and 30 ka.

Hypothesis 4. Climate change is asynchronous across Africa.

As shown in Fig. 14, there is strong support for this hypothesis for terrestrial climates. This suggests that continental-scale examinations of climate, environment, and human evolution must account for these temporal offsets between regions, with inter-regional differences in the timing of shifts to humid or arid conditions often on the order of 10 kyr.

Paleoanthropological implications

The results of our regional comparisons of paleoanthropological site density and inferred climate for each of the four sub-regions are summarized in Fig. 15. The results are used to test each of our three hypotheses linking climate change to Pleistocene African hominin demography, followed by suggestions for further testing at similar and finer analytical scales. Overall, there is a general increase in the relative frequency of sites over time in

Please cite this article in press as: Blome, M.W., et al., The environmental context for the origins of modern human diversity: A synthesis of regional variability in African climate 150,000–30,000 years ago, Journal of Human Evolution (2012), doi:10.1016/j.jhevol.2012.01.011

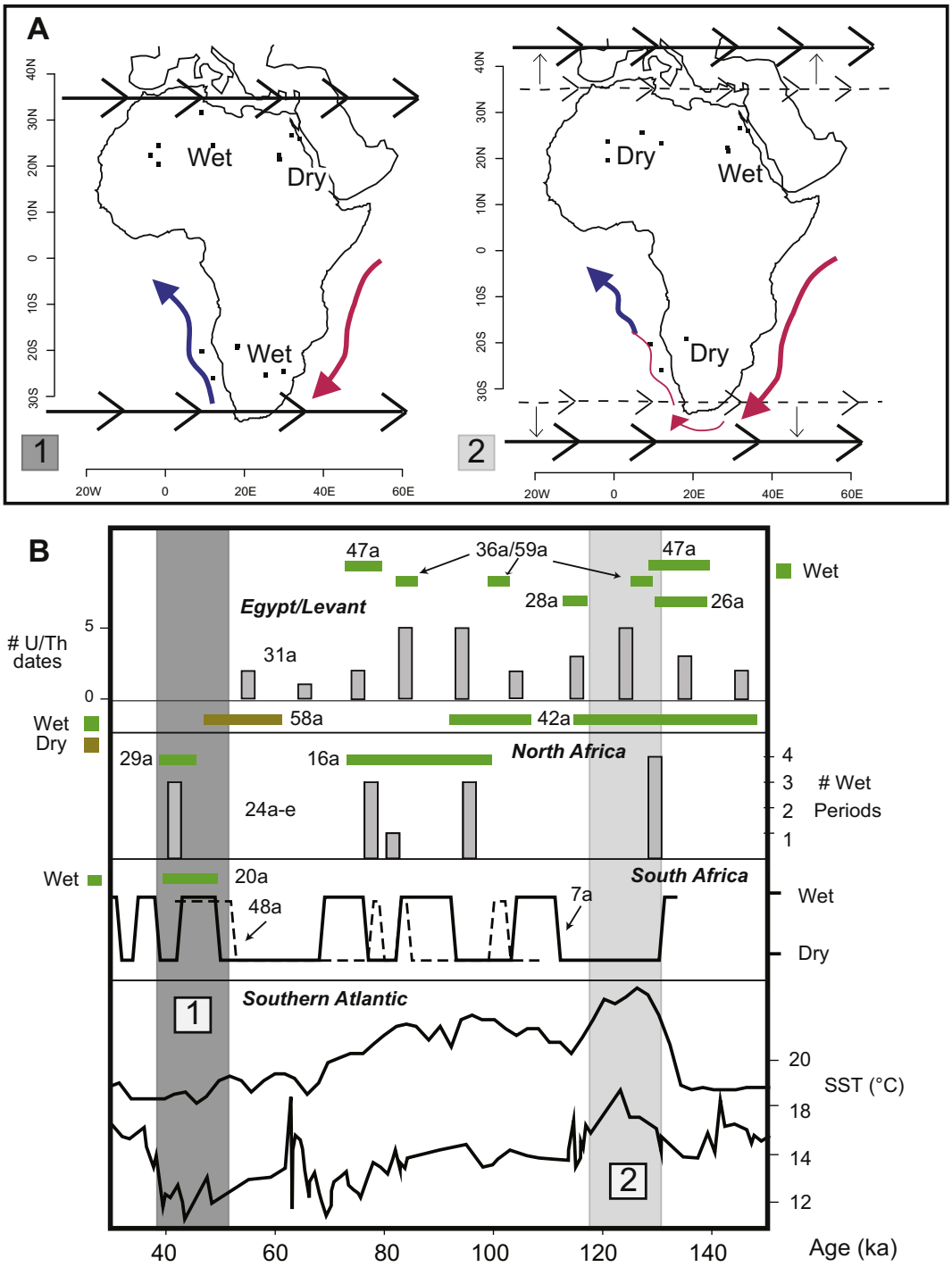

Figure 12. A) Diagram illustrating the possible consequences of the Westerlies shifting over time. Situation 1 places the Westerlies more equator-ward bringing precipitation to North and South Africa, and cutting off Agulhas current 'leakage' around the tip of the continent. Situation 2 shows the Westerlies more pole-ward, with the opposite effect. B) Paleo-data showing that the two scenarios are observed in the record for North and South Africa. Also illustrates how the records from Egypt may be responding to another dynamic mechanism as they are out of phase with either situation over the 150–30 ka period.

most regions (Fig. 15). This pattern is consistent with the taphonomic bias modeled by Surovell et al. (2009), in which younger sites are more likely to be found and thus skew inferences of demographic change from these data. As the models of Surovell et al. (2009) extend only to ~40 ka, the extent to which our dataset spanning ~150–30 ka is affected by taphonomic bias is unknown. Examining differences between or within regions for particular time intervals partially offsets this, as there is no evidence at the moment to suggest that the taphonomic bias against site recovery affects one region or area more than another for any given time interval.

Hypothesis 5a. The southern African interior (and possibly the coast) was largely depopulated during arid intervals, particularly within the last 60 kyr.

This hypothesis predicts strong evidence for a decrease in site abundance in the 60–30 ka interval. For inland sites, there is no evidence for a decline in site numbers <60 ka and thus no support

Please cite this article in press as: Blome, M.W., et al., The environmental context for the origins of modern human diversity: A synthesis of regional variability in African climate 150,000–30,000 years ago, Journal of Human Evolution (2012), doi:10.1016/j.jhevol.2012.01.011

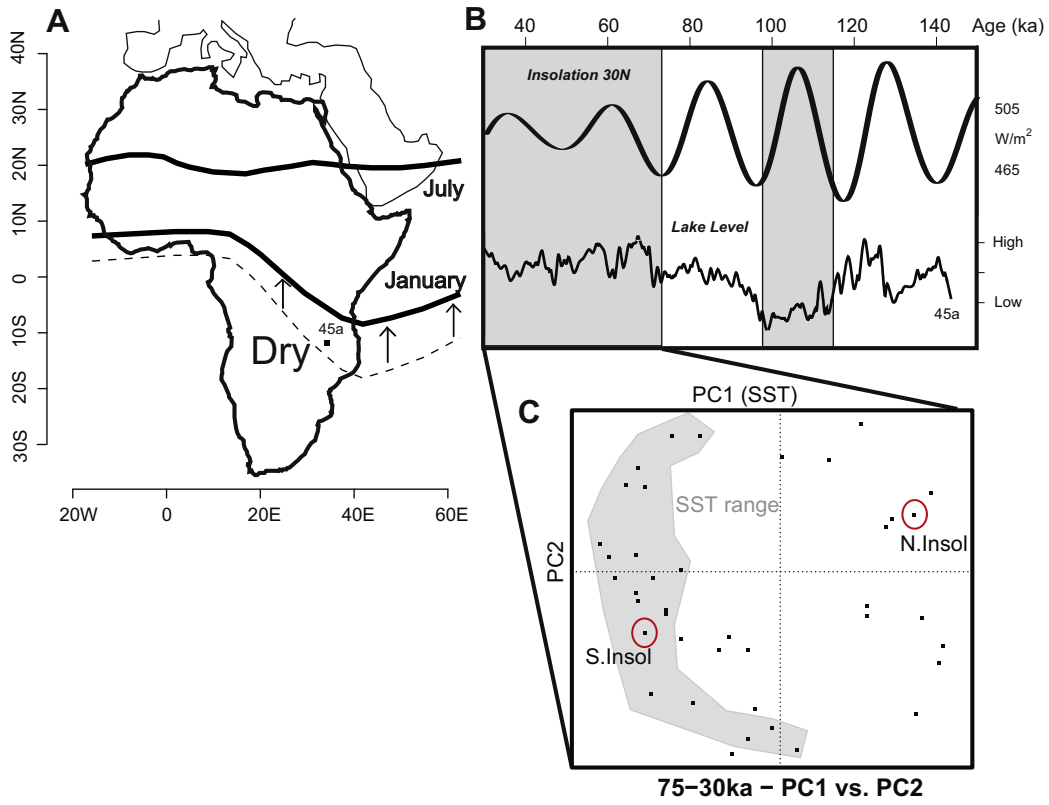

Figure 13. A) Diagram showing possible northward movement of the Intertropical Convergence Zone (ITCZ) during periods of strong Northern Hemisphere insolation. B) Paleo-data supporting the hypothesis from 98 to 117 ka with extremely strong Northern Hemisphere insolation during the peak of the 'megadrought', as well as a gradual wettening and subsequent decrease in variability at Lake Malawi (45a) as Northern Hemisphere insolation weakens and becomes less variable (70–30 ka). C) Principal component (PC) analysis plot from 75 to 30 ka supports this observation, showing the decreased control insolation has on climate variability during this interval.

for the hypothesis, with inland site numbers showing a slight increase during this interval (Fig. 15), nor is there support for inland population decline during prior arid intervals. In particular, our data actually suggest relatively humid conditions at coastal and near-coastal sites during MIS 4 (~72–60 ka), as also reported by Chase (2010). This is in contrast with earlier models that suggest that Still Bay and Howiesons Poort industries appear during arid or more open conditions previously inferred for MIS 4 in southern Africa (e.g., Ambrose and Lorenz, 1990; McCall, 2007), demonstrating the complex relation between marine isotope stages and terrestrial African climates.

The number of coastal sites in southern Africa does show a decline from ~75–65 ka, followed by a sharp decline consistent with the hypothesis of population decline or regional abandonment (Fig. 15). However, the decline in coastal site numbers is likely due to the seaward movement of the coast during arid/glacial intervals and the loss of these habitation sites and associated rich coastal plain resources during subsequent sea level rise, e.g., during MIS 3 (see Van Andel, 1989; Fisher et al., 2010). Our data provide no support for population declines in southern Africa that cannot be explained as a function of sea level fluctuation.

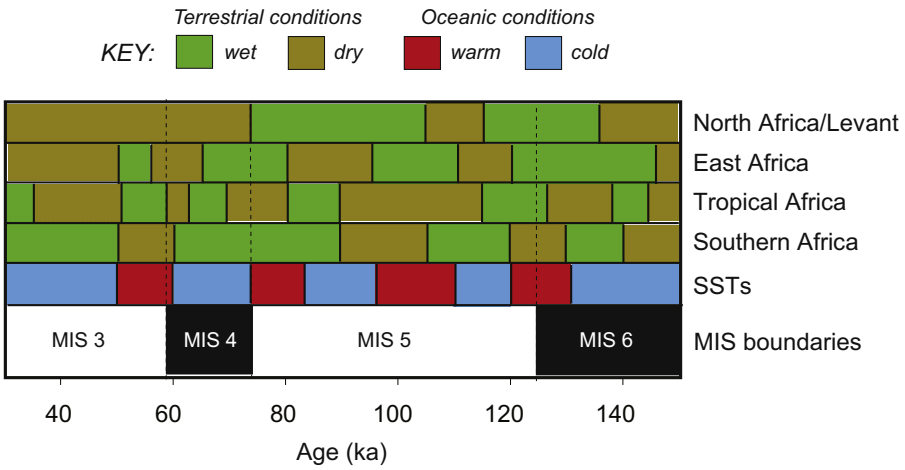

Figure 14. Summary of the circum-Africa climate data from 150 to 30 ka including sea surface temperatures (SSTs) and each region from north to south on the continent. The terrestrial data across the continent do not vary in concert with the Marine Isotope Stages, whereas the SSTs appear to be following this more global signal.

Please cite this article in press as: Blome, M.W., et al., The environmental context for the origins of modern human diversity: A synthesis of regional variability in African climate 150,000–30,000 years ago, Journal of Human Evolution (2012), doi:10.1016/j.jhevol.2012.01.011

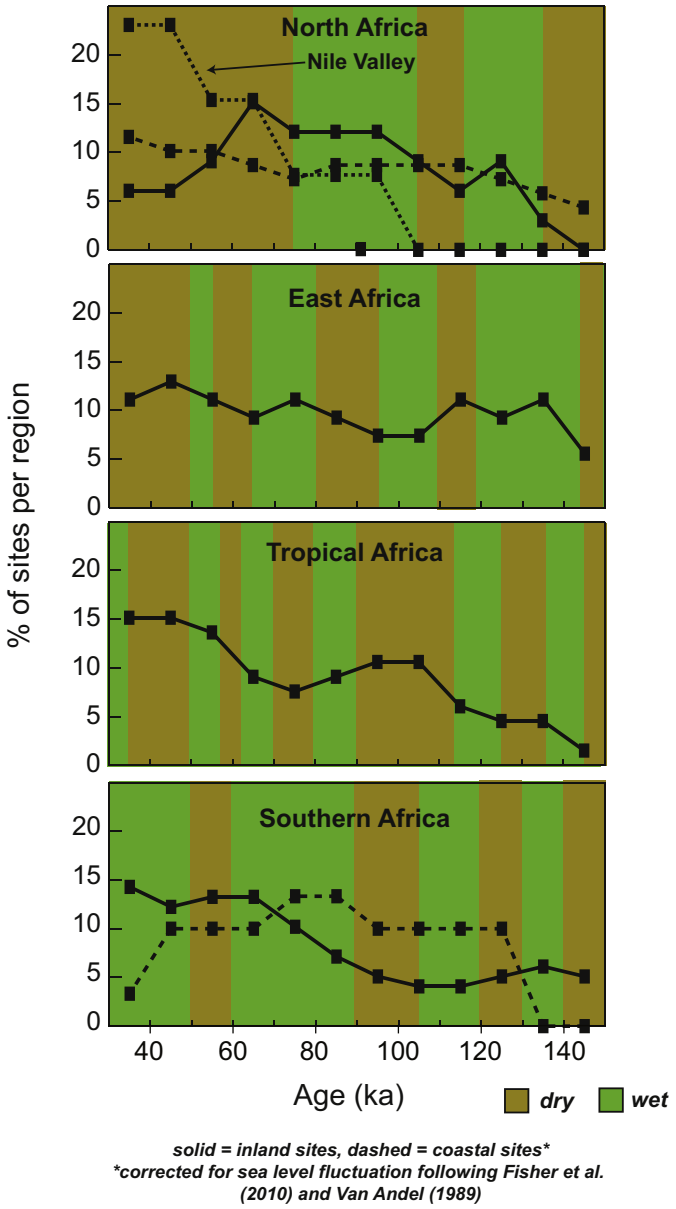

Figure 15. Line graphs summarizing the relative density of archaeological sites in 10 kyr bins for the North, East, tropical, and southern African regions. Data from Table 2. Juxtaposed with the archaeological data are the regional climate histories for a first-order summary of climate-demography interaction from 150 to 30 ka. See text for further discussion.

Hypothesis 5b. Hominin populations in the tropical and eastern portions of the continent show relatively muted responses to climate change.

This hypothesis predicts little change in hominin site abundances relative to changes in relative humidity. The data summarized in Fig. 15 support this hypothesis. Despite extreme changes in climate, fluctuations in relative site density in East Africa and tropical Africa are relatively minor. Comparisons between the two regions indicate that East and tropical Africa show inversely related abundances throughout much of the time span considered here, particularly between ~130–60 ka. During much of this interval, when relative site frequency increases in the tropical region, it decreases in East Africa. As noted above, site proportions are calculated independently for each region, such that change in one need not cause a change in the other. Relative site abundances in tropical Africa increase during one period of aridity (~115–90 ka), and in East Africa decline during the comparable interval of humidity (~110–95 ka). As such, the data suggest that the mid-latitudinal portions of the continent may be linked in interesting ways in terms of population and environmental histories during parts of the Late Pleistocene. Neither the patterning in inversely related site abundance between regions nor climatic change within regions holds after ~65 ka.

The scale of our analysis does not permit direct identification of the reasons for little change in the hominin demographic signal for East and tropical Africa. The consequences of absolute changes in long-term water availability may be less dramatic for these regions compared with North or South Africa. For example, following Ambrose (1998), Mercader et al. (2000), Marean and Assefa (2005), and Basell (2008), the periods of increased aridity in these regions may be offset by relatively steep gradients in altitudinal relief and rainfall that may have allowed localized movement to higher, cooler, and wetter altitudes, as well as the expansion of forest populations when the canopy was more open and fragmented.

Although increased aridity is often associated with a decrease in habitat suitability for hominin populations (cf. North Africa discussed below), the opposite may hold true for heavily forested regions such as those found in much of the tropical African region. Tropical rainforests are difficult environments for human foragers, and forest fragmentation increases ecotone extent, potentially making the region more attractive to hominin populations (cf. Ambrose, 2001; Cornelissen, 2002). Our meso-scale results shown in Fig. 15 provide some support for this, with increased site abundances in tropical Africa during shifts to aridity, particularly during the ~115–90 ka interval. This pattern is also supported at the smaller scale of individual archaeological sites. The sites of Katanda (36), dated to 120–60 ka, and Matupi Cave (37), dated to 32–41 ka are both found in what are today ecotones on the margins of heavily forested regions of the Democratic Republic of the Congo. Several lines of evidence suggest that Pleistocene hominin occupation of these sites favored drier intervals when more open grassland habitats occurred in their vicinities. Site Kt9 at Katanda preserves fossils of zebra (*Equus* cf. *E. burchelli*) and wildebeest (*Connochaetes taurinus*), indicative of open savanna grasslands and not found in the area today (Brooks et al., 1995). At Matupi Cave, grass (*Gramineae*) pollen and spores, isotopic analyses of speleothem, and a fossil fauna that includes ostrich (*Struthio camelus*) and warthog (*Phacochoerus aethiopicus*) all suggest a cooler, drier, and more open habitat than at present (Van Noten, 1977; Van Neer, 1989; Brook et al., 1990). These data suggest Stone Age occupation of forest ecotones during drier, more open conditions and emphasize that arid (and conversely humid) intervals may have had different impacts on human populations in each of the four African subregions.

Another consequence of forest fragmentation is the creation of a mosaic of local refugia that were intermittently connected as a result of environmental change. Genetic evidence provides some support that these processes may have led to the accumulation of biological differences in various animal populations, in particular multiple species of bovid (Lorenzen et al., 2010). Among humans, mtDNA, Y-chromosome, and non-coding regions of the human nuclear genome suggest that the ancestors of central African forest ('pygmy') hunter-gatherers and ancestors of Bantu-speaking agricultural populations in tropical Africa likely diverged ca. 71 (50–106) ka (Batini et al., 2007, 2011; Quintana-Murci et al., 2008; Patin et al., 2009), with mtDNA evidence suggesting that asymmetric gene flow from pygmy maternal lineages to eventual farming populations was reinitiated sometime after 40 ka and followed by multiple gene flow events involving other African

Please cite this article in press as: Blome, M.W., et al., The environmental context for the origins of modern human diversity: A synthesis of regional variability in African climate 150,000–30,000 years ago, Journal of Human Evolution (2012), doi:10.1016/j.jhevol.2012.01.011

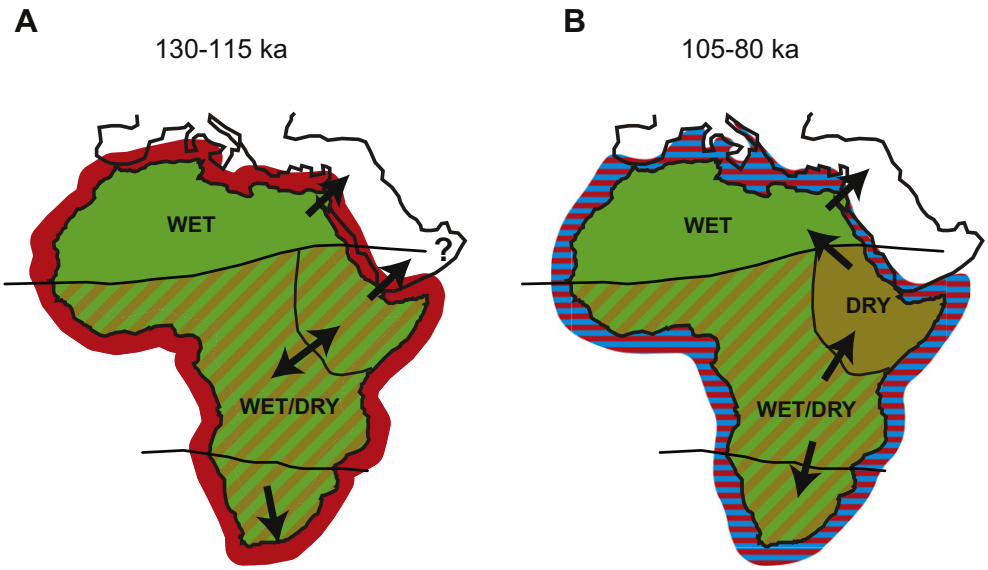

Figure 16. Synthesis of variability in African terrestrial and oceanic conditions during A) 130–115 ka, and B) 105–80 ka (see Fig. 14), with arrows indicating possible hominin population movements based on demographic changes among regions.

populations during the terminal Pleistocene and Holocene. The work of Tishkoff et al. (2009) implies similar complex relationships between the ancestors of various present-day forest hunter-gatherer groups and those of surrounding populations. Offshore terrestrial temperature (12a, 13a–d) and precipitation/aridification records (34b–d) suggest a significant cold period just prior to the suggested divergence interval. Regional precipitation records indicate a significant dry spell just before or concurrent with the beginning of the 73–60 ka divergence interval and a return to humid conditions <60 ka (Fig. 15). These results are consistent with models suggesting that forest fragmentation during arid conditions are periods when population fragmentation, isolation, and differentiation are most likely (e.g., Cowling et al., 2008). The archaeological data for this region are sparse and as yet lack the sort of chronological control to offer support for this model (Cornelissen, 2002; Mercader and Martí, 2003), but these results do suggest the power of integrating genetic, demographic, and meso-scale environmental data.

Hypothesis 5c. The nature and expanse of the Sahara strongly influenced the population history of northern Africa, with occupation of much of the interior of this region limited to periods of increased humidity when the 'green Sahara' was characterized by savanna environments. As a corollary, 'out of Africa' hominin dispersals are similarly constrained to these humid intervals.

This hypothesis predicts that hominin site density should co-vary with climate change, with decreased site abundance during periods of increased aridity. This hypothesis is variably supported according to site location along the coast or in the interior (Fig. 15). Coastal sites show a very gradual increase in numbers over time, with little evidence for any linkage between hominin demography and climate change. The absence of a noticeable recent decline in coastal site numbers is likely due to the relatively steep gradient of the northwest African Mediterranean coast relative to that in South Africa; sea level change had a minimal impact on site-to-shore distance in northwest Africa.

Sites in the interior of northern Africa reveal a more complex pattern. Because the Nile River provides a narrow zone of available water in otherwise often dry environments, the Nile Valley sites of Nazlet Khater 4, Nazlet Safaha, and Taramsa 1 are plotted separately on Fig. 15. Among our dataset, radiometrically dated sites from the Nile Valley are first documented at ~100 ka, with a progressive increase through time. This increase may simply reflect taphonomic bias, and further interpretation is hampered by a particularly small sample size.

The remaining sites from the interior of North Africa show a very different pattern, with multiple periods marked by substantial increases or decreases in relative site abundance. Site numbers show a sharp increase ~130–120 ka, reach their maximum ~100–70 ka, and show a sharp decline <70 ka (Fig. 15). The periods of site increase or maximum density broadly coincide with humid intervals in northern Africa, whereas the rapid decline in site density in the interior from ~70–30 ka starts shortly after the return to arid conditions (Fig. 15). These findings support the 'green Sahara' hypothesis of Drake et al. (2011), which suggest the repeated reoccupation of the Sahara by animal communities (including humans) during humid intervals. These data suggest that much of the occupation of the northern African interior by Aterian MSA hominin populations was largely limited to humid intervals when savanna environments may have dominated the region. This is supported by the limited available faunal data from undated Aterian sites from the Sahara, including equids (*Equus* sp.) and alcelaphine bovids (*Alcelaphus buselaphus*, reported as *Bubalis boselaphus*) from the Aterian type-site of Bir-el-Ater in Algeria (Morel, 1974), and more strikingly, cut-marked hippopotamus (*Hippopotamus amphibius*) remains from Adrar Bous, in the Aïr Mountains of Niger (Gifford-Gonzalez and Parham, 2008).

Hominin dispersals to Eurasia via northern Africa have also been linked to humid intervals (Osbourne et al., 2008; Drake et al., 2011). From ~30–75 ka, North Africa experienced arid climate regimes. The Sahara expanded 65–50 ka and the demographic data imply abandonment of the interior of North Africa during this time (Fig. 15), suggesting that dispersals from North Africa occurred prior to 75 ka. This finding is at odds with hypotheses that posit a dispersal timing of ca. 60 ka (Mellars, 2006), or a dispersal origin in the South African Howiesons Poort industry at 65–60 ka (Marean, 2010), although a ca. 65–60 ka dispersal could well have occurred from East Africa over the Bab el-Mendeb, as humid conditions dominated the latter region between 80 and 65 ka. The timing of the humid intervals in North Africa

Please cite this article in press as: Blome, M.W., et al., The environmental context for the origins of modern human diversity: A synthesis of regional variability in African climate 150,000–30,000 years ago, Journal of Human Evolution (2012), doi:10.1016/j.jhevol.2012.01.011

(~135–115 ka and ~105–75 ka) corresponds with those in the Levant (54a) (Vaks et al., 2007), providing multiple opportunities for one or more earlier hominin dispersals out of Africa via the Sahara, or an early exodus from East Africa to Arabia over the Bab el Mendeb (e.g., Rose et al., 2011). This pattern does not rule out possible migrations from this region during either the earlier or the later interval through the Nile Valley. However, during the ~105–75 ka humid interval in North Africa, East Africa (where the sources of the Nile occur) was largely under an arid climate regime, except for a narrow window ~80 ka when both northern and eastern Africa were experiencing humid climates (Fig. 15), placing a more restricted temporal window on dispersal via the Nile Valley. We note that although only one out of Africa event is recorded in the modern human genome (e.g., Prugnolle et al., 2005), this fact is not inconsistent with earlier multiple migration and extinction events using any of these routes, with only a single lineage surviving to the present.

Conclusions

In this paper. we synthesized African paleoclimate from 150 ka to 30 ka using diverse datasets at a regional scale, testing for coherence with North Atlantic glacial/interglacial phases, Northern and Southern Hemisphere insolation cycles, and the atmospheric dynamics responsible for the observed regional climates. We have examined the temporal and spatial components of paleoenvironmental change across the continent, in order to further investigate the relationship between the varying regional climates and the evidence of human occupation in those regions.

Between 150 and 30 ka, the SSTs from the northern Atlantic and the Mediterranean Sea are consistent with the North Atlantic glacial/interglacial SST pattern observed further north, as are the SSTs recorded in the southern Atlantic. This suggests the importance of high latitude forcing for all Atlantic SSTs off the western coast of Africa. Southern Ocean records close to the African continent also show a strong coherence with North Atlantic SSTs, suggesting that the influence of the North Atlantic extends all the way down the African coast until the Antarctic Circumpolar Current takes over dominance around 49°S latitude. The Indian Ocean records are the least similar to the North Atlantic, suggesting that this region is much more heavily influenced by the East African and Asian monsoons over this time interval. However, it is likely that glacial boundary conditions and insolation intensity together modulate the strength of the monsoons on either side of the continent. This is evident from the 'SST clusters' observed in the PCA, which includes all regional SSTs. There is a very tight 'cluster' during periods of high insolation variability and strength, and a diffuse, scattered relationship between 75 and 35 ka when insolation variability and strength is low.

North Africa experienced humid conditions beginning between 135 and 130 ka and lasting until 120–115 ka, and again from 100 to 95 ka until 75 ka. Many North African records are also quite variable prior to 75 ka, after which time the climatic variability in the region dampens considerably through 30 ka, suggesting a link between insolation strength and variability and North African climate. There is also evidence suggesting that North African precipitation is affected by the expansion and contraction of the Westerlies, diverting moisture towards the continent when they are weak (equator-ward), and away when they are strong (pole-ward). This is particularly evident between 100 ka and 70 ka.

The East African region was wet ~145–120 ka, ~110–195 ka, ~80–65 ka, and 55–50 ka. These variations were likely caused by or related to the changing influences of the NE and SW monsoon regimes, forced by changes in local insolation at the equator with increasing influence of high latitude/glacial forcing moving away from the equator.

The regional climate from 150 to 30 ka in tropical Africa differs from its neighboring regions primarily due to the presence of a region-wide series of 'megadroughts' from ~115–90 ka. Based on the spatial distribution of sites displaying a megadrought signal, it is likely that the southwest extent of the 'megadrought belt' lies between ~19°S and 25°S latitude, and ~23°E and 27°E longitude. The northern boundary lies at approximately 18°N from the Atlantic Ocean in the west to ~37°E longitude where the northern boundary shifts to 3°S latitude. The cause of these megadroughts may lie in a northward shift of the ITCZ, resulting from extremely strong Northern Hemisphere insolation and thus intensification of the Asian monsoon. Although there is evidence of insolation-driven control of regional precipitation in tropical Africa (specifically prior to 70 ka), the more recent record (60–30 ka) suggests that Indian Ocean SSTs also control precipitation in tropical Africa; i.e., the oceanic teleconnections to tropical Africa precipitation patterns are more evident when not swamped by a strong insolation signal. This SST-regional precipitation relationship is also observed in modern data.

The climate in the Southern African region differs from north to south. The northern boundary of this region exhibits a modified/punctuated 'megadrought' signal, whereas the rest of the region does not. There is a clear eccentricity-modulated precessional cyclicity to the wet/dry climate of southern Africa, although no clear trend toward increasing or decreasing humidity through the time interval of interest. As in North Africa, there is evidence that regional precipitation in South Africa is affected by the expansion and contraction of the Westerlies between 100 and 70 ka.

Four sub-intervals of time were further analyzed for temporal trends in the data using a PCA: 150–100 ka, 140–30 ka, 115–30 ka, and 75–30 ka. The analyses suggest that North Atlantic SSTs are a consistent determinant of variability through the entire time interval. This is evident especially in the earlier three sub-intervals when the majority of SST records surrounding the continent plot in a tight 'cluster' particularly along the main axis of variability. However, even in the latter sub-interval the majority of SST datasets are loosely correlated with one another and none are anti-correlated. It is evident that variability in terrestrial climate from 150 to 30 ka is strongly correlated with the local hemisphere insolation maxima, except during periods of time when insolation variability and intensity is negligible (e.g., 75–30 ka), at which times other factors, such as regional SSTs can become dominant drivers of climate variability at 1–10 kyr time scales.

This climate synthesis provides a framework to test hypotheses regarding regional climate influences on the demographic structure of African hominins from ~150–30 ka. A dataset of 64 sites demonstrates multiple temporal changes in the frequency of sites relative to climate change for the each of the North, East, tropical, and southern African regions. Southern African sites do not show any decline in relative frequency that is not explicable by changes in sea level, which is inconsistent with hypotheses that suggest periodic depopulation of that region within the last 60 kyr.

The degree of temporal change in site density in East and tropical Africa is low compared with North and southern Africa, and consistent with hypotheses that steep altitudinal gradients or other local changes in environment may have buffered populations in these regions from the extremes of climate change. East and tropical Africa also show inversely related abundances throughout much of the time span considered here, particularly between ~130–60 ka. This suggests that the history of early populations of *H. sapiens* in the generally wetter mid-latitudinal portions of the continent may be linked in different ways than at the more arid north and south ends of the continent. During arid intervals

Please cite this article in press as: Blome, M.W., et al., The environmental context for the origins of modern human diversity: A synthesis of regional variability in African climate 150,000–30,000 years ago, Journal of Human Evolution (2012), doi:10.1016/j.jhevol.2012.01.011

between ~120–80 ka, relative site abundances in tropical Africa increase, whereas those of eastern Africa decrease, perhaps tracking the local effects of forest fragmentation and grassland expansion. Processes of forest fragmentation and grassland expansion may also explain population isolation and contact suggested by genetic data from the region, which indicate a complex intertwining of climate and human population movement between these two interior continental regions.

Site densities in the interior of northern Africa record changes that appear to track climatic changes, with relative increases during humid intervals and declines with shifts to aridity, consistent with hypotheses linking human occupation of the Sahara to wetter conditions when the region supported a number of lakes and savanna habitats. Fig. 16 summarizes contrasting paleoenvironmental syntheses for two humid time intervals during which hominin populations may have dispersed out of Africa through either northern Africa (Osbourne et al., 2008; Drake et al., 2011) or via the Horn of Africa (Armitage et al., 2011). Fig. 16 serves to further emphasize synchronous climate variability across Africa for a given time interval, as well as the complex relation between changes in terrestrial and oceanic conditions.

Our comparisons are constrained by the ~10 kyr resolution of our dataset, but our results demonstrate the following: (1) There is often a poor fit between the timing and nature of environmental change on continental Africa and oceanic records; (2) the timing of relative changes in moisture availability varied with latitude, such that different climate regimes characterized different regions of Africa at any given time; and (3) coarse measures of Pleistocene hominin demographic change can be used to test hypotheses that relate human population history to climate change. We look forward to exploring new avenues of research into demography/climate change connections in Africa at the local to regional scale as the density of the archaeological record improves, measures of population diversification are refined, and age estimates for archaeological and fossil sites as well as intervals of genetic changes are increasingly resolved.

Acknowledgments

Many thanks to the NSF Integrative Graduate Education and Research Traineeship (IGERT) program and the Foreign Language and Area Studies (FLAS) fellowship program for providing financial support during the research and writing of this manuscript. In addition, many thanks to colleagues who provided comments, advice, and support throughout the process, especially Michael McGlue, Christine Gans, Jessica Conroy, Sarah Ivory, Mark Warren, Daniel Peppe, and Tyler Faith. Sarah Pilliard and Ryan Higgins assisted with some of the archaeological data collection. The initial data collection coincided with the development of the Smithsonian Human Origins Data Base, part of an NSF-HOMINID grant to Potts and co-PIs (BCS - 0218511). This grant also funded a conference on the importance of climate change in human evolution, which sparked this collaborative effort. Tryon was supported by the Human Origins Program at the Smithsonian Institution's National Museum of Natural History (NMNH) and Cohen by a Senior Fellowship and the Paleobiology Department of the NMNH and NSF EAR-0602350 during the early phases of this project, and both would like to particularly acknowledge the support of Rick Potts and Kay Behrensmeyer.

Appendix A. Supplementary information

Supplementary data related to this article can be found online at doi:10.1016/j.jhevol.2012.01.011.

References

Ambrose, S.H., 1998. Late Pleistocene human population bottlenecks, volcanic winter and differentiation of modern humans. J. Hum. Evol. 34, 623–651.

Ambrose, S.H., 2001. Middle and Later Stone Age settlement patterns in the Central Rift Valley, Kenya: comparisons and contrasts. In: Conard, N.J. (Ed.), Settlement Dynamics in the Middle Paleolithic and Middle Stone Age. Kerns-Verlag, Tübingen, pp. 21–44.

Ambrose, S.H., 2003. Population bottleneck. In: Robinson, R. (Ed.), 2003. Genetics, vol. 3. MacMillan Reference, USA, New York, pp. 167–171.

Ambrose, S.H., Lorenz, K.G., 1990. Social and ecological models for the Middle Stone Age in southern Africa. In: Mellars, P. (Ed.), The Emergence of Modern Humans: An Archaeological Perspective. Edinburgh University Press, Edinburgh, pp. 3–33.

Armitage, S.J., Jasim, S.A., Marks, A.E., Parker, A.G., Usik, V.I., Uerpmann, H.P., 2011. The southern route "Out of Africa": evidence for an early expansion of modern humans into Arabia. Science 331, 453–456.

Assefa, Z., Lam, Y.M., Mienis, H.K., 2008. Symbolic use of terrestrial gastropod opercula during the Middle Stone Age at Porc-Epic Cave, Ethiopia. Curr. Anthropol. 49, 746–756.

Bailey, G., 2007. Time perspectives, palimpsests and the archaeology of time. J. Anthropol. Archaeol. 26, 198–223.

Bard, E., Rostek, F., Sonzogoni, C., 1997. Interhemispheric synchrony of the last deglaciation inferred from alkenone paleothermometry. Nature 385, 707–710.

Barham, L.H., 2000. The Middle Stone Age of Zambia, South Central Africa. Western Academic and Specialist Press Limited, Bristol.

Barham, L.H., Mitchell, P., 2008. The First Africans: African Archaeology from the Earliest Tool Makers to Most Recent Foragers. Cambridge University Press, Cambridge.

Barich, B.E., Garcea, E.A.A., Giraudi, C., 2005. Between the Mediterranean and the Sahara: geoarchaeological reconnaissance in the Jebel Gharbi, Libya. Antiquity 80, 567–582.

Barker, P., Williamson, D., Gasse, F., Gibert, E., 2003. Climatic and volcanic forcing revealed in a 50,000-year diatom record from Lake Massoko, Tanzania. Quatern. Res. 60, 368–376.

Bar-Matthews, M., Ayalon, A., Gilmour, M., Matthews, A., Hawkesworth, C.J., 2003. Sea-land oxygen isotopic relationships from planktonic foraminifera and speleothems in the Eastern Mediterranean region and their implications for paleo-rainfall during interglacial intervals. Geochim. Cosmochim. Acta 67, 3181–3199.

Bar-Matthews, M., Marean, C.W., Jacobs, Z., Karkanas, P., Fisher, E.C., Herries, A.I.R., Brown, K., Williams, H.M., Bernatchez, J., Ayalon, A., Nilssen, P.J., 2010. A high resolution and continuous isotopic speleothem record of paleoclimate and paleoenvironment from 90–53 ka from Pinnacle Point on the south coast of South Africa. Quatern. Sci. Rev. 29, 2131–2145.

Barraclough, T.G., Nee, S., 2001. Phylogenetics and speciation. Trends Ecol. Evol. 16, 391–399.

Barton, R.N.E., Bouzouggar, A., Collcutt, S.N., Schwenninger, J.-L., Clark-Balzan, L., 2009. OSL dating of the Aterian levels at Dar es-Soltan I (Rabat, Morocco) and implications for the dispersal of modern *Homo sapiens*. Quatern. Sci. Rev. 28, 1914–1931.

Basell, L.S., 2008. Middle Stone Age (MSA) site distributions in eastern Africa and their relationship to Quaternary environmental change, refugia and the evolution of *Homo sapiens*. Quatern. Sci. Rev. 27, 2484–2498.

Bateman, M.D., Carr, A.S., Dunajko, A.C., Holmes, P.J., Roberts, D.L., McLaren, S.J., Bryant, R.G., Marker, M.E., Murray-Wallace, C.V., 2011. The evolution of coastal barrier systems: a case study of the Middle-Late Pleistocene wilderness barriers, South Africa. Quatern. Sci. Rev. 30, 63–81.

Bateman, M.D., Thomas, D.S.G., Singhvi, A.K., 2003. Extending the aridity record of the southwest Kalahari: current problems and future perspectives. Quatern. Int. 111, 37–49.

Batini, C., Coia, V., Battaggia, C., Rocha, J., Pilkington, M.M., Spedini, G., Comas, D., Destro-Bisol, G., Calafell, F., 2007. Phylogeography of the human mitochondrial L1c haplogroup: genetic signatures of the prehistory of Central Africa. Mol. Phylogenet. Evol. 43, 635–644.

Batini, C., Lopes, J., Behar, D.M., Calafell, F., Jorde, L.B., van der Veen, L., Quintana-Murci, L., Spedini, G., Destro-Bisol, G., Comas, D., 2011. Insights into the demographic history of African Pygmies from complete mitochondrial genomes. Mol. Biol. Evol. 28, 1099–1110.

Beaumont, P.B., Vogel, J.C., 2006. On a timescale for the past million years of human history in central South Africa. S. Afr. J. Sci. 102, 217–228.

Behar, D.M., Villems, R., Soodyall, H., Blue-Smith, J., Pereira, L., Metspalu, E., Scozzari, R., Makkan, H., Tzur, S., Comas, D., Bertranpetit, J., Quintana-Murci, L., Tyler-Smith, C., Wells, R.S., Rosset, S., 2008. The dawn of human matrilineal diversity. Am. J. Hum. Genet. 82, 1130–1140.

Binford, L.R., 2001. Constructing Frames of Reference: An Analytical Method for Archaeological Theory Building Using Ethnographic and Environmental Data Sets. University of California Press, Berkeley.

Bird, M.I., Fifield, L.K., Santos, G.M., Beaumont, P.B., Zhou, Y., di Tada, M.L., Hausladen, P.A., 2003. Radiocarbon dating from 40 to 60 ka BP at Border Cave, South Africa. Quatern. Sci. Rev. 22, 943–947.

Bond, G., Heinrich, H., Broecker, W., Labeyrie, L., Mcmanus, J., Andrews, J., Huon, S., Jantschik, R., Clasen, S., Simet, C., Tedesco, K., Klas, M., Bonani, G., Ivy, S., 1992. Evidence for massive discharges of icebergs into the North-Atlantic Ocean during the last glacial period. Nature 360, 245–249.

Bouzouggar, A., Barton, N., Vanhaeren, M., d'Errico, F., Collcutt, S., Higham, T., Hodge, E., Parfitt, S., Rhodes, E., Schwenninger, J.-L., Stringer, C., Turner, E., Ward, S., Moutmir, A., Stambouli, A., 2007. 82,000-year-old shell beads from North Africa and implications for the origins of modern human behavior. Proc. Natl. Acad. Sci. 104, 9964–9969.

Bowden, J.H., Semazzi, F.H.M., 2007. Empirical analysis of intraseasonal climate variability over the Greater Horn of Africa. J. Clim. 20, 5715–5731.

Brandt, S.A., Gresham, T.H., 1989. L'âge de la pierre en Somalie. L'Anthropologie 94, 459–482.

Brathauer, U., Abelmann, A., 1999. Late Quaternary variations in sea surface temperatures and their relationship to orbital forcing recorded in the Southern Ocean (Atlantic sector). Paleoceanography 14, 135–148.

Bräuer, G., 2008. The origin of modern anatomy: by speciation or intraspecific evolution. Evol. Anthropol. 17, 22–37.

Brook, G.A., Burney, D.A., Cowart, J.B., 1990. Paleoenvironmental data for Ituri, Zaire, from sediments in Matupi Cave, Mt. Hoyo. In: Boaz, N.T. (Ed.), Evolution of Environments and Hominidae in the African Western Rift Valley. Virginia Museum of Natural History Memoir 1, pp. 49–70. Martinsville.

Brook, G.A., Cowart, J.B., Marais, E., 1996. Wet and dry periods in the southern African summer rainfall zone during the last 300 kyr from speleothem, tufa and sand dune age data. Palaeoecol. Afr. Surround. Isl. Antarct. 24, 147–158.

Brooks, A.S., Hare, P.E., Kokis, J.E., Miller, G.H., Ernst, R.D., Wendorf, F., 1990. Dating Pleistocene archaeological sites by protein diagenesis in ostrich eggshell. Science 248, 60–64.

Brooks, A.S., Helgren, D.M., Cramer, J.M., Franklin, A., Hornyak, W., Keating, J.M., Klein, R.G., Rink, W.J., Schwarcz, H.P., Smith, J.N.L., Stewart, K., Todd, N.E., Verniers, J., Yellen, J.E., 1995. Dating and context of three Middle Stone Age sites with bone points in the upper Semliki Valley, Zaire. Science 268, 548–553.

Brown, E.T., Johnson, T.C., Scholz, C.A., Cohen, A.S., King, J.W., 2007. Abrupt change in tropical African climate linked to the bipolar seesaw over the past 55,000 years. Geophys. Res. Lett. 34, L20702. doi:10.1029/2007GL031240.

Burrough, S.L., Thomas, D.S.G., Shaw, P.A., Bailey, R.M., 2007. Multiphase Quaternary highstands at Lake Ngami, Kalahari, northern Botswana. Palaeogeogr. Palaeoclimatol. Palaeoecol. 253, 280–299.

Burrough, S.L., Thomas, D.S.G., Singarayer, J.S., 2009. Late Quaternary hydrological dynamics in the Middle Kalahari: forcing and feedbacks. Earth-Sci. Rev. 96, 313–326.

Butzer, K.W., 1988. A 'marginality' model to explain major spatial and temporal gaps in the Old and New World Pleistocene settlement records. Geoarchaeology 3, 193–203.

Butzer, K.W., Beaumont, P.B., Vogel, J.C., 1978. Lithostratigraphy of Border Cave, Kwazulu, South-Africa: a Middle Stone-Age sequence beginning c. 195,000 b.p. J. Archaeol. Sci. 5, 317–341.

Carr, A.S., Bateman, M.D., Holmes, P.J., 2007. Developing a 150 ka luminescence chronology for the barrier dunes of the southern Cape, South Africa. Quatern. Geochronol. 2, 110–116.

Carr, A.S., Thomas, D.S.G., Bateman, M.D., 2006. Climatic and sea level controls on Late Quaternary eolian activity on the Agulhas Plain, South Africa. Quatern. Res. 65, 252–263.

Carto, S.L., Weaver, A.J., Hetherington, R., Lam, Y., Wiebe, E.C., 2009. Out of Africa and into an ice age: on the role of global climate change in the late Pleistocene migration of early modern humans out of Africa. J. Hum. Evol. 56, 139–151.

Causse, C., Ghaleb, B., Chkir, N., Zouari, K., Ouezodou, H.B., Mamou, A., 2003. Humidity changes in southern Tunisia during the late Pleistocene inferred from U-Th dating of mollusc shells. Appl. Geochem. 18, 1691–1703.

Chase, B.M., 2010. South African palaeoenvironments during marine oxygen isotope stage 4: a context for the Howiesons Poort and Still Bay industries. J. Archaeol. Sci. 37, 1359–1366.

Clark, J.D., Beyene, Y., Wolde Gabriel, G., Hart, W.K., Renne, P., Gilbert, H., Defleur, A., Suwa, G., Katoh, S., Ludwig, K.R., Boisserie, J.-R., Asfaw, B., White, T.D., 2003. Stratigraphic, chronological and behavioural contexts of Pleistocene *Homo sapiens* from Middle Awash, Ethiopia. Nature 423, 747–752.

Clark, J.D., Williams, K.D., Michels, J.W., Marean, C.A., 1984. A Middle Stone Age occupation site at Porc Epic Cave, Dire Dawa (east-central Ethiopia). Afr. Archaeol. Rev. 2, 37–72.

Clemens, S.C., Prell, W.L., Sun, Y., Liu, Z., Chen, G., 2008. Southern Hemisphere forcing of Pliocene $\delta^{18}O$ and the evolution of Indo-Asian monsoons. Paleoceanography 23, 1–15.

Cohen, A.S., Stone, J.R., Beuning, K.R.M., Park, L.E., Reinthal, P.N., Dettman, D., Scholz, C.A., Johnson, T.C., King, J.W., Talbot, M.R., Brown, E.T., Ivory, S.J., 2007. Ecological consequences of early Late Pleistocene megadroughts in tropical Africa. Proc. Natl. Acad. Sci. 104, 16422–16427.

Cornelissen, E., 2002. Human responses to changing environments in central Africa between 40,000 and 12,000 B.P. J. World Prehist. 16, 197–235.

Cowling, S.A., Cox, P.M., Jones, C.D., Maslin, M.A., Peros, M., Spall, S.A., 2008. Simulated glacial and interglacial vegetation across Africa: implications for species phylogenies and trans-African migration of plants and animals. Glob. Change Biol. 14, 827–840.

Cremaschi, M., Di Lernia, S., 1999. Wadi Teshuinat: Palaeoenvironment and Prehistory in South-Western Fezzan (Libyan Sahara). Edizioni All'Insegna del Giglio, Firenze.

Cremaschi, M., Di Lernia, S., Garcea, E.A.A., 1998. Some insights on the Aterian in the Libyan Sahara: chronology, environment, and archaeology. Afr. Archaeol. Rev. 15, 261–286.

Crevecoeur, I., Rougier, H., Grine, F., Froment, A., 2009. Modern human cranial diversity in the Late Pleistocene of Africa and Eurasia: evidence from Nazlet Khater, Peştera cu Oase, and Hofmeyr. Am. J. Phys. Anthropol. 140, 347–358.

Crombie, M.K., Arvidson, R.E., Sturchio, N.C., El Alfy, Z., Abu Zeid, K., 1997. Age and isotopic constraints on Pleistocene pluvial episodes in the Western Desert. Egypt. Palaeogeogr. Palaeoclimatol. Palaeoecol. 130, 337–355.

Crowley, T.J., Hyde, W.T., 2008. Transient nature of late Pleistocene climate variability. Nature 456, 226–230.

Dansgaard, W., Johnsen, S.J., Clausen, H.B., Dahljensen, D., Gundestrup, N.S., Hammer, C.U., Hvidberg, C.S., Steffensen, J.P., Sveinbjornsdottir, A.E., Jouzel, J., Bond, G., 1993. Evidence for general instability of past climate from a 250-kyr ice-core record. Nature 364, 218–220.

Deacon, H.J., Thackeray, J.F., 1984. Late Pleistocene environmental changes and implications for the archaeological record in southern Africa. In: Vogel, J.C. (Ed.), Late Cainozoic Palaeoclimates of the Southern Hemisphere. A.A. Balkema, Rotterdam, pp. 375–390.

Debénath, A., Raynal, J.-P., Roche, J., Texier, J.-P., Ferembach, D., 1986. Stratigraphie, habitat, typologie et devenir de l'Atérien Marocain: données récentes. L'Anthropologie 90, 233–246.

deMenocal, P.B., 2004. African climate change and faunal evolution during the Pliocene-Pleistocene. Earth Planet. Sci. Lett. 220, 3–24.

deMenocal, P.B., Rind, D., 1993. Sensitivity of Asian and African climate to variations in seasonal insolation, glacial ice cover, sea surface temperature, and Asian orography. J. Geophys. Res. 98, 7265–7287.

deMenocal, P.B., Ruddiman, W.F., Pokras, E.M., 1993. Influences of high- and low-latitude processes on African terrestrial climate: Pleistocene eolian records from equatorial Atlantic Ocean Drilling Program Site 663. Paleoceanography 8, 209–242.

Di Lernia, S., 1999. The Uan Afuda Cave: Hunter-gatherer Societies of Central Sahara. In: Arid Zone Archaeology, Monographs 1. Edizioni All'Insegna del Giglio, Firenze. 223–237.

Domínguez-Rodrigo, M., Mabulla, A., Luque, L., Thompson, J.W., Rink, J., Bushozi, P., Díez-Martin, F., Alcala, L., 2008. A new archaic *Homo sapiens* fossil from Lake Eyasi, Tanzania. J. Hum. Evol. 54, 899–903.

Donahue, R.E., Murphy, M.L., Robbins, L.H., 2004. Lithic microwear analysis of Middle Stone Age artifacts from white paintings rock shelter, Botswana. J. Field Archaeol. 29, 155–163.

Drake, N.A., Blench, R.M., Armitage, S.J., Bristow, C.S., White, K.H., 2011. Ancient watercourses and biogeography of the Sahara explain the peopling of the desert. Proc. Natl. Acad. Sci. 108, 458–462.

Drake, N.A., El-Hawat, A.S., Turner, P., Armitage, S.J., Salem, M.J., White, K.H., McLaren, S., 2008. Palaeohydrology of the Fazzan Basin and surrounding regions: the last 7 million years. Paleogeogr. Paleoclimatol. Paleoecol. 263, 131–145.

Dupont, L.M., Jahns, S., Marret, F., Ning, S., 2000. Vegetation change in equatorial West Africa: time slices for the last 150 ka. Palaeogeogr. Palaeoclimatol. Palaeoecol. 155, 95–122.

Dupont, L., Weinelt, M., 1996. Vegetation history of the Savanna corridor between the Guniean and the Congolian rain forest during the last 150,000 years. Veg. Hist. Archaeobot. 5, 273–292.

Emeis, K.C., Schulz, H., Struck, U., Rossignol-Strick, M., Erelnkeuser, H., Howell, M.W., Kroon, D., Mackensen, A., Ishizuka, S., Oba, T., Sakamoto, T., Koizumi, I., 2003. Eastern Mediterranean surface water temperatures and $\delta^{18}O$ composition during deposition of sapropels in the late Quaternary. Paleoceanography 18, 1005. doi:10.1029/2000PA000617.

Eswaran, V., Harpending, H., Rogers, A.R., 2005. Genomics refutes an exclusively African origin of humans. J. Hum. Evol. 49, 1–18.

Excoffier, L., 2002. Human demographic history: refining the recent African origin model. Curr. Opin. Genet. Dev. 12, 675–682.

Faith, J.T., Choiniere, J.N., Tryon, C.A., Peppe, D.J., Fox, D.L., 2011. Taxonomic status and paleoecology of *Rusingoryx atopocranion* (Mammalia, Artiodactyla), an extinct Pleistocene bovid from Rusinga Island, Kenya. Quatern. Res. 75, 697–707.

Feathers, J.K., 2002. Luminescence dating in less than ideal conditions: case studies from Klasies River main site and Duinefontein, South Africa. J. Archaeol. Sci. 29, 177–194.

Feathers, J.K., Bush, D.A., 2000. Luminescence dating of Middle Stone Age deposits at Die Kelders. J. Hum. Evol. 38, 91–119.

Feathers, J.K., Migliorini, E., 2001. Luminescence dating at Katanda: a reassessment. Quatern. Sci. Rev. 20, 961–966.

Fisher, E.C., Bar-Matthews, M., Jerardino, A., Marean, C.W., 2010. Middle and Late Pleistocene paleoscape modeling along the southern coast of South Africa. Quatern. Sci. Rev. 29, 1382–1398.

Fontes, J.C., Gasse, F., 1991. Palhydaf (paleohydrology in Africa) program: objectives, methods, major results. Palaeogeogr. Palaeoclimatol. Palaeoecol. 84, 191–215.

Forster, P., 2004. Ice Ages and the mitochondrial DNA chronology of human dispersals: a review. Phil. Trans. R. Soc. B 359, 255–264.

Gamble, C., Davies, W., Pettitt, P., Hazelwood, L., Richards, M., 2005. The archaeological and genetic foundations of the European population during the late glacial: implications for 'agricultural thinking'. Cambridge Archaeol. J. 15, 193–223.

Garrigan, D., Hammer, M.F., 2006. Reconstructing human origins in the genomic era. Nat. Rev. Genet. 7, 669–680.

Garrigan, D., Kingan, S.B., Pilkington, M.M., Wilder, J.A., Cox, M.P., Soodyall, H., Strassmann, B., Destro-Bisol, G., de Knijff, P., Novelletto, A., Friedlaender, J., Hammer, M.F., 2007. Inferring human population sizes, divergence times and

rates of gene flow from mitochondrial, X and Y chromosome resequencing data. Genetics 177, 2195–2207.
Gaven, C., Hillaire-Marcel, C., Petit-Maire, N., 1981. A Pleistocene lacustrine episode in southeastern Libya. Nature 290, 131–133.
Gifford-Gonzalez, D., Parham, J.F., 2008. Fauna from Adrar Bous and surrounding areas. In: Gifford-Gonzalez, D. (Ed.), Adrar Bous: Archaeology of a Central Saharan Granitic Ring Complex in Niger. Royal Museum for Central Africa Studies in Human Sciences, vol. 170, pp. 313–353. Tervuren.
Gonder, M.K., Mortensen, H.M., Reed, F.A., de Sousa, A., Tishkoff, S.A., 2007. Whole mtDNA genome sequence analysis of ancient African lineages. Mol. Biol. Evol. 24, 757–768.
Grine, F.E., Bailey, R.M., Harvarti, K., Nathan, R.P., Morris, A.G., Henderson, G.M., Ribot, I., Pike, A.W.G., 2007. Late Pleistocene human skull from Hofmeyr, South Africa, and modern human origins. Science 315, 226–229.
Grün, R., Beaumont, P.B., Tobias, P.V., Eggins, S., 2003. On the age of Border Cave 5 human mandible. J. Hum. Evol. 45, 155–167.
Grün, R., Brink, J.S., Spooner, N.A., Taylor, L., Stringer, C.B., Franciscus, R.G., Murray, A.S., 1996. Direct dating of Florisbad hominid. Nature 382, 500–501.
Grün, R., Shackleton, N.J., Deacon, H.J., 1990. Electron-spin-resonance dating of tooth enamel from Klasies River Mouth Cave. Curr. Anthropol. 31, 427–432.
Grün, R., Stringer, C., 1991. Electron spin resonance dating and the evolution of modern humans. Archaeometry 33, 153–199.
Gunz, P., Bookstein, F.L., Mitteroecker, P., Stadlmayr, A., Seidler, H., Weber, G.W., 2009. Early modern human diversity suggests subdivided population structure and a complex out-of-Africa scenario. Proc. Natl. Acad. Sci. 106, 6094–6098.
Hammer, M.F., Woerner, A.E., Mendez, F.L., Watkins, J.C., Wall, J.D., 2011. Genetic evidence for archaic admixture in Africa. Proc. Natl. Acad. Sci. 108, 15123–15128.
Harding, R.M., McVean, G., 2004. A structured ancestral population for the evolution of modern humans. Curr. Opin. Genet. Dev. 14, 667–674.
Harvati, K., Stringer, C., Grün, R., Aubert, M., Allsworth-Jones, P., Folorunso, C.A., 2011. The Later Stone Age calvaria from Iwo Eleru, Nigeria: morphology and chronology. Plos One 6, e24024.
Henshilwood, C., d'Errico, F., Yates, R., Jacobs, Z., Tribolo, C., Duller, G.A.T., Mercier, N., Sealy, J., Valladas, H., Watts, I., Wintle, A., 2002. Emergence of modern human behaviour: Middle Stone Age engravings from South Africa. Science 295, 1278–1280.
Henshilwood, C.S., Marean, C.W., 2003. The origin of modern human behavior: a review and critique of models and test implications. Curr. Anthropol. 44, 627–651.
Hillaire-Marcel, C., Carro, O., Casanova, J., 1986. ^{14}C and Th/U dating of Pleistocene and Holocene stromatolites from East Africa paleolakes. Quatern. Res. 25, 312–329.
Hodell, D.A., Venz, K.A., Charles, C.D., Ninnemann, U.S., 2003. Pleistocene vertical carbon isotope and carbonate gradients in the South Atlantic sector of the Southern Ocean. Geochem. Geophy. Geosy. 4, 1–19.
Holmgren, K., Karlen, W., Shaw, P., 1995. Paleoclimatic significance of the stable isotope composition and petrology of a Late Pleistocene stalagmite from Botswana. Quatern. Res. 43, 320–328.
Holzkamper, S., Holmgren, K., Lee-Thorp, J., Talma, S., Mangini, A., Partridge, T., 2009. Late Pleistocene stalagmite growth in Wolkberg Cave, South Africa. Earth Planet. Sci. Lett. 282, 212–221.
Hooghiemstra, H., Stalling, H., Agwu, C.O.C., Dupont, L., 1992. Vegetational and climatic changes at the northern fringe of the Sahara 250,000–5000 years BP: evidence from 4 marine pollen records located between Portugal and the Canary Islands. Rev. Palaeobot. Palyno. 74, 1–52.
Howell, F.C., 1999. Paleo-demes, species clades, and extinctions in the Pleistocene hominin record. J. Anthropol. Res. 55, 191–243.
Imbrie, J., Imbrie, J.Z., 1980. Modeling the climatic response to orbital variations. Science 207, 943–953.
Ingman, M., Kaessmann, H., Pääbo, S., Gyllensten, U., 2000. Mitochondrial genome variation and the origin of modern humans. Nature 408, 708–713.
Jacobs, Z., Duller, G.A.T., Wintle, A.G., Henshilwood, C.S., 2006. Extending the chronology of deposits at Blombos Cave, South Africa, back to 140 ka using optical dating of single and multiple grains of quartz. J. Hum. Evol. 51, 255–273.
Jacobs, Z., Roberts, R.G., Galbraith, R.F., Deacon, H.J., Grün, R., Mackay, A., Mitchell, P., Vogelsang, R., Wadley, L., 2008a. Ages for the Middle Stone Age of southern Africa: implications for human behavior and dispersal. Science 322, 733–735.
Jacobs, Z., Wintle, A.G., Duller, G.A.T., Roberts, R.G., Wadley, L., 2008b. New ages for the post-Howiesons Poort, late and final Middle Stone Age at Sibudu, South Africa. J. Archaeol. Sci. 35, 1790–1807.
Kelly, R.L., 1995. The Foraging Spectrum. Smithsonian Institution Press, Washington.
Kiberd, P., 2006. Bundu farm: a report on archaeological and palaeoenvironmental assemblages from a pan site in Bushmanland, Northern Cape, South Africa. S. Afr. Archaeol. Bull. 61, 189–201.
Kingston, J.D., 2007. Shifting adaptive landscapes: progress and challenges in reconstructing early hominid environments. Yearb. Phys. Anthropol. 50, 20–58.
Klein, R.G., 1980. Environmental and ecological implications of large mammals from Upper Pleistocene and Holocene sites in southern Africa. Ann. S. Afr. Mus. 81, 223–283.
Klein, R.G., 2009. The Human Career, third ed. University of Chicago Press, Chicago.
Klein, R.G., Cruz-Uribe, K., Beaumont, P.B., 1991. Environmental, ecological, and paleoanthropological implications of the Late Pleistocene mammalian fauna from Equus Cave, Northern Cape Province, South Africa. Quatern. Res. 36, 94–119.
Kristen, I., Fuhrmann, A., Thorpe, J., Röhl, U., Wilkes, H., Oberhänsli, H., 2007. Hydrological changes in southern Africa over the last 200 ka as recorded in lake sediments from the Tswaing impact crater. S. Afr. J. Geol. 110, 311–326.
Kuehn, D.D., Dickson, B.D., 1999. Stratigraphy and noncultural site formation at the Shurmai Rockshelter (GnJm1) in the Mukugodo Hills of north-central Kenya. Geoarchaeology 14, 63–85.
Kuhn, S.L., Stiner, M.C., 2001. The antiquity of hunter-gatherers. In: Panter-Brick, C., Layton, R.H., Rowley-Conwy, P. (Eds.), Hunter-Gathgrers: An Interdisciplinary Perspective. Cambridge University Press, Cambridge, pp. 99–142.
Kutzbach, J.E., 1981. Monsoon climate of the Early Holocene: climate experiment with the Earth's orbital parameters for 9000 years ago. Science 214, 59–61.
Kutzbach, J.E., Liu, Z., 1997. Response of the African monsoon to orbital forcing and ocean feedbacks in the Middle Holocene. Science 278, 440–443.
Kutzbach, J.E., Liu, X., Liu, Z., 2008. Simulation of the evolutionary response of global summer monsoons to orbital forcing over the past 280,000 years. Clim. Dynam. 30, 567–579.
Lahr, M.M., Foley, R., 1998. Towards a theory of modern human origins: geography, demography, and diversity in recent human evolution. Yearb. Phys. Anthropol. 41, 137–176.
Laskar, J., Robutel, P., Joutel, F., Gastineau, M., Correia, A.C.M., Levrard, B., 2004. A long-term numerical solution for the insolation quantities of the Earth. Astron. Astrophys. 428, 261–265.
Lea, D.W., Mashiotta, T.A., Spero, H.J., 1999. Controls on magnesium and strontium uptake in planktonic foraminifera determined by live culturing. Geochim. Cosmochim. Acta 63, 2369–2379.
Lee-Thorp, J.A., Beaumont, P.B., 1995. Vegetation and seasonality shifts during the late Quaternary deduced from ^{13}C/^{12}C ratios of grazers at Equus Cave, South Africa. Quatern. Res. 43, 426–432.
Leuschner, D.C., Sirocko, F., 2000. The low-latitude monsoon climate during Dansgaard-Oeschger cycles and Heinrich events. Quatern. Sci. Rev. 19, 243–254.
Lezzine, A., Casanova, J., 1991. Correlated oceanic and continental records demonstrate past climate and hydrology of North Africa (0–140 ka). Geology 19, 307–310.
Little, M.G., Schneider, R.R., Kroon, D., Price, B., Bickert, T., Wefer, G., 1997. Rapid palaeoceanographic changes in the Benguela Upwelling System for the last 160,000 years as indicated by abundances of planktonic foraminifera. Palaeogeogr. Palaeoclimatol. Palaeoecol. 130, 135–161.
Liu, Z., Harrison, S.P., Kutzbach, J., Otto-Bliesner, B., 2004. Global monsoons in the mid-Holocene and oceanic feedback. Clim. Dynam. 22, 157–182.
Lombard, M., Wadley, L., Jacobs, Z., Mohapi, M., Roberts, R.G., 2010. Still Bay and serrated points from Umhlatuzana Rock Shelter, Kwazulu-Natal, South Africa. J. Archaeol. Sci. 37, 1773–1784.
Lorenzen, E.D., Masembe, C., Actander, P., Siegismund, H.R., 2010. A long-standing Pleistocene refugium in southern Africa and a mosaic of refugia in East Africa: insights from mtDNA and the common eland antelope. J. Biogeogr. 37, 571–581.
Manega, P.C., 1993. Geochronology, geochemistry and isotopic study of the Plio-Pleistocene hominid sites and the Ngorongoro Volcanic Highlands in northernTanzania. Ph.D. Dissertation, University of Colorado.
Marchant, R., Mumbi, C., Behera, S., Yamagata, T., 2007. The Indian Ocean dipole – the unsung driver of climatic variability in East Africa. Afr. J. Ecol. 45, 4–16.
Marean, C.W., 1997. Hunter-gatherer foraging strategies in tropical grasslands: model-building and testing in the East African Middle and Later Stone Age. J. Anthropol. Archaeol. 16, 189–225.
Marean, C.W., 2010. Pinnacle point cave 13B (Western Cape Province, South Africa) in context: the Cape Floral kingdom, shellfish, and modern human origins. J. Hum. Evol. 59, 425–443.
Marean, C.W., Assefa, Z., 2005. The Middle and Upper Pleistocene African record for the biological and behavioral origins of modern humans. In: Stahl, A.B. (Ed.), African Archaeology. Blackwell Publishing, Malden, pp. 93–129.
Marean, C.W., Bar-Matthews, M., Bernatchez, J., Fisher, E., Goldberg, P., Herries, A.I.R., Jacobs, Z., Jerardino, A., Karkanas, P., Minichillo, T., Nilssen, P.J., Thompson, E., Watts, I., Williams, H.M., 2007. Early human use of marine resources and pigment in South Africa during the Middle Pleistocene. Nature 449, 905–908.
Marean, C.W., Bar-Matthews, M., Fisher, E., Goldberg, P., Herries, A., Karkanas, P., Nilssen, P.J., Thompson, E., 2010. The stratigraphy of the Middle Stone Age sediments at Pinnacle Point Cave 13B (Mossel Bay, Western Cape Province, South Africa). J. Hum. Evol. 59, 234–255.
Marlowe, F.W., 2005. Hunter-gatherers and human evolution. Evol. Anthopol. 14, 54–67.
Martinez-Méndez, G., Zahn, R., Hall, I.R., Frank, J.C., Peeters, L.D., Cacho, I., Negre, C., 2010. Contrasting multiproxy reconstructions of surface ocean hydrography in the Agulhas Corridor and implications for the Agulhas Leakage during the last 345,000 years. Paleoceanography 25, PA4227. doi:10.1029/2009PA001879.
Martinez-Méndez, G., Zahn, R., Hall, I.R., Pena, L.D., Cacho, I., 2008. 345,000-year-long multi-proxy records off South Africa document variable contributions of Northern versus Southern Component Water to the Deep South Atlantic. Earth Planet. Sci. Lett. 267, 309–321.
Mayr, E., 2001. What Evolution Is. Basic Books, New York.
McBrearty, S., 1992. Sangoan technology and habitat at Simbi, Kenya. Nyame Akuma 38, 29–33.
McBrearty, S., Brooks, A., 2000. The revolution that wasn't: a new interpretation of the origin of modern human behavior. J. Hum. Evol. 39, 453–563.

Please cite this article in press as: Blome, M.W., et al., The environmental context for the origins of modern human diversity: A synthesis of regional variability in African climate 150,000–30,000 years ago, Journal of Human Evolution (2012), doi:10.1016/j.jhevol.2012.01.011

McCall, G.S., 2007. Behavioral ecological models of lithic technological change during the later Middle Stone Age of South Africa. J. Archaeol. Sci. 34, 1738–1751.

McDermott, F., 2004. Palaeo-climate reconstruction from stable isotope variations in speleothems: a review. Quatern. Sci. Rev. 23, 901–918.

McDermott, F., Stringer, C., Grün, R., Williams, C.T., Din, V.K., Hawkesworth, C.J., 1996. New Late-Pleistocene uranium-thorium and ESR dates for the Singa hominid (Sudan). J. Hum. Evol. 31, 507–516.

McDougall, I., Brown, F.H., Fleagle, J.G., 2005. Stratigraphic placement and age of modern humans from Kibish, Ethiopia. Nature 433, 733–736.

McGlue, M.M., Lezzar, K.E., Cohen, A.S., Russell, J.M., Tiercelin, J.J., Felton, A.A., Mbede, E., Nkotagu, H.H., 2008. Seismic records of late Pleistocene aridity in Lake Tanganyika, tropical East Africa. J. Paleolimnol. 40, 635–653.

McKenzie, J.A., 1993. Pluvial conditions in the eastern Sahara following the penultimate deglaciation: implications for changes in atmospheric circulation patterns with global warming. Palaeogeogr. Palaeoclimatol. Palaeoecol. 103, 95–105.

Mehlman, M.J., 1991. Context for the emergence of modern man in eastern Africa: some new Tanzanian evidence. In: Clark, J.D. (Ed.), Cultural Beginnings: Approaches to Understanding Early Hominid Life-Ways in the African Savanna. Dr. Rudolph Habelt GMBH, Bonn, pp. 177–196.

Mellars, P., 2006. Why did modern human populations disperse from Africa ca. 60,000 years ago? A new model. Proc. Natl. Acad. Sci. 103, 9381–9386.

Mellars, P., French, J.C., 2011. Tenfold population increase in Western Europe at the Neanderthal-to-modern human transition. Science 333, 623–627.

Mercader, J., Asmerom, Y., Bennett, T., Raja, M., Skinner, A., 2009. Initial excavation and dating of Ngalue Cave: a Middle Stone Age site along the Niassa Rift, Mozambique. J. Hum. Evol. 57, 63–74.

Mercader, J., Martí, R., 2003. The Middle Stone Age occupation of Atlantic Central Africa: new evidence from equatorial Guinea and Cameroon. In: Mercader, J. (Ed.), Under the Canopy: The Archaeology of Tropical Rain Forests. Rutgers University Press, London, pp. 64–92.

Mercader, J., Runge, F., Vrydaghs, L., Doutrelepont, H., Ewango, C.E.N., Juan-Tresseras, J., 2000. Phytoliths from archaeological sites in the tropical forest of Ituri, Democratic Republic of Congo. Quatern. Res. 54, 102–112.

Mercier, N., Valladas, H., Froget, L., Joron, J.-L., Vermeersch, P.M., Van Peer, P., Moeyersons, J., 1999. Thermoluminescence dating of a Middle Paleolithic occupation at Sodmein Cave, Red Sea Mountains (Egypt). J. Archaeol. Sci. 26, 1339–1345.

Mercier, N., Wengler, L., Valladas, H., Joron, J.-L., Froget, L., Reyss, J.-L., 2007. The Rhafas Cave (Morocco): chronology of the Mousterian and Aterian archaeological occupations and their implications for Quaternary geochronology based on luminescence (TL/OSL) age determinations. Quatern. Geochronol. 2, 309–313.

Miller, G.H., Beaumont, P.B., Deacon, H.J., Brooks, A.S., Hare, P.E., Jull, A.J.T., 1999. Earliest modern humans in southern Africa dated by isoleucine epimerization in ostrich eggshell. Quatern. Sci. Rev. 18, 1537–1548.

Moernaut, J., Verschuren, D., Charlet, F., Kristen, I., Fagot, M., De Batist, M., 2010. The seismic-stratigraphic record of lake-level fluctuations in Lake Challa: hydrological stability and change in equatorial East Africa over the last 140 kyr. Earth Planet. Sci. Lett. 290, 223–241.

Moeyersons, J., Vermeersch, P.M., Van Peer, P., 2002. Dry cave deposits and their paleoenvironmental significance during the last 115 ka, Sodmein Cave, Red Sea Mountains. Egypt. Quatern. Sci. Rev. 21, 837–851.

Morel, J., 1974. La station eponyme de l'Oued Djebbana a Bir-el-Ater (Est Algérien): contribution a la connaissance de son industrie et de sa fauna. L'Anthropologie 78, 53–80.

Morel, A., Tillet, Th., Poupeau, G., 1991. Le bassin de Taoudenni. In: Tillet, G. (Ed.), Paleoenvironments and Prehistoric Populations of the Sahara in the Upper Pleistocene. Abstracts Colloque de Solignac, PICG 252.

Nespoulet, R., El Hajraoui, M.A., Amani, F., Ben Ncer, A., Debénath, A., El Idrissi, A., Lacombe, J.-P., Michel, P., Oujaa, A., Stoetzel, E., 2008. Paleolithic and Neolithic occupations in the Témara region (Rabat, Morocco): recent data on hominin contexts and behavior. Afr. Archaeol. Rev. 25, 21–39.

Nicholson, S.E., Flohn, H., 1980. African environmental and climatic changes and the general atmospheric circulation in Late Pleistocene and Holocene. Clim. Change 2, 313–348.

Nürnberg, D., Groeneveld, J., 2006. Pleistocene variability of the subtropical convergence at East Tasman Plateau: evidence from (ODP Site 1172A). Geochem. Geophys. Geosy. 7, Q04P11.

Osbourne, A.H., Vance, D., Rohling, E.J., Barton, N., Rogerson, M., Fello, N., 2008. A humid corridor across the Sahara for the migration of early modern humans out of Africa 120,000 years ago. Proc. Natl. Acad. Sci. 105, 16444–16447.

Osmond, J.K., Dabous, A.A., 2004. Timing and intensity of groundwater movement during Egyptian Sahara pluvial periods by U-series analysis of secondary U in ores and carbonates. Quatern. Res. 61, 85–94.

Partridge, T.C., 1999. Tswaing: Investigations into the Origin, Age and Palaeoenvironments of the Pretoria Saltpan. In: S. Africa Memoir 85. Council for Geoscience.

Patin, E., Laval, G., Barreiro, L.B., Salas, A., Semino, O., Santachiara-Benerecetti, S., Kidd, K.K., Kidd, J.R., van der Veen, L., Hombert, J.M., Gessain, A., Froment, A., Bahuchet, S., Heyer, E., Quintana-Murci, L., 2009. Inferring the demographic history of African farmers and Pygmy hunter-gatherers using a multilocus resequencing data set. Plos Genet. 5, 1–7.

Pearson, O.M., 2008. Statistical and biological definitions of 'anatomically modern' humans: suggestions for a unified approach to modern morphology. Evol. Anthopol. 17, 38–48.

Petit, J.R., Jouzel, J., Raynaud, D., Barkov, N.I., Barnola, J.M., Basile, I., Bender, M., Chappellaz, J., Davis, M., Delaygue, G., Delmotte, M., Kotlyakov, V.M., Legrand, M., Lipenkov, V.Y., Lorius, C., Pepin, L., Ritz, C., Saltzman, E., Stievenard, M., 1999. Climate and atmospheric history of the past 420,000 years from the Vostok ice core, Antarctica. Nature 399, 429–436.

Pichevin, L., Cremer, M., Giraudeau, J., Bertrand, P., 2005. A 190 kyr record of lithogenic grain-size on the Namibian slope: forging a tight link between past wind-strength and coastal upwelling dynamics. Mar. Geol. 218, 81–96.

Pienaar, M., Woodborne, S., Wadley, L., 2008. Optically stimulated luminescence dating at Rose Cottage Cave. S. Afr. J. Sci. 104, 65–70.

Pokras, E.M., Mix, A.C., 1985. Eolian evidence for spatial variability of late Quaternary climates in tropical Africa. Quatern. Res. 24, 137–149.

Potts, R., 1998. Environmental hypotheses of hominin evolution. Yearb. Phys. Anthropol. 41, 93–136.

Potts, R., Behrensmeyer, A.K., Ditchfield, P., 1999. Paleolandscape variation and Early Pleistocene hominid activities: Members 1 and 7, Olorgesailie Formation, Kenya. J. Hum. Evol. 37, 747–788.

Powell, A., Shennan, S., Thomas, M.G., 2009. Late Pleistocene demography and the appearance of modern human behavior. Science 324, 1298–1301.

Prahl, F.G., Muehlhausen, L.A., Zahnle, D.L., 1988. Further evaluation of long-chain alkenones as indicators of paleoceanographic conditions. Geochim. Cosmochim. Acta 52, 2303–2310.

Prasad, T.G., McClean, J.L., 2004. Mechanisms for anomalous warming in the western Indian Ocean during dipole mode events. J. Geophys. Res. Oceans 109, CO2019. doi:10.1029/2003JC001872.

Prugnolle, F., Manica, A., Balloux, F., 2005. Geography predicts neutral genetic diversity of human populations. Curr. Biol. 15, 159–160.

Quickert, N.A., Godfrey-Smtih, D.I., Casey, J.L., 2003. Optical and thermoluminescence dating of Middle Stone Age and Kintampo bearing sediments at Birimi, a multi-component archaeological site in Ghana. Quatern. Sci. Rev. 22, 1291–1297.

Quintana-Murci, L., Quach, H., Harmant, C., Luca, F., Massonnet, B., Patin, E., Sica, L., Mouguiama-Daouda, P., Comas, D., Tzur, S., Balanovsky, O., Kidd, K.K., Kidd, J.R., van der Veen, L., Hombert, J.M., Gessain, A., Verdu, P., Froment, A., Bahuchet, S., Heyer, E., Dausset, J., Salas, A., Behar, D.M., 2008. Maternal traces of deep common ancestry and asymmetric gene flow between Pygmy hunter-gathereres and Bantu-speaking farmers. Proc. Natl. Acad. Sci. 105, 1596–1601.

Rasse, M., Soriano, S., Tribolo, C., Stokes, S., Huysecom, E., 2004. La séquence Pléistocène supérieur d'Ounjougou (Pays dogon, Mali, Afrique de l'Ouest): évolution géomorphologique, enregisterements sédimentaires et changements culturels. Quaternaire 15, 329–341.

Raymo, M.E., Oppo, D.W., Flower, B.P., Hodell, D.A., McManus, J.F., Venz, K.A., Kleiven, K.F., McIntyre, K., 2004. Stability of North Atlantic water masses in face of pronounced climate variability during the Pleistocene. Paleoceanography 19, PA2008. doi:10.1029/2003PA000921.

Reed, F.A., Tishkoff, S.A., 2006. African human diversity, origins and migrations. Curr. Opin. Genet. Dev. 16, 597–605.

Reynolds, S.C., Clarke, R.J., Kuman, K.A., 2007. The view from the Lincoln Cave: mid- to late Pleistocene fossil deposits from Sterkfontein hominid site, South Africa. J. Hum. Evol. 53, 260–271.

Richter, D., Moser, J., Nami, M., Eiwanger, J., Mikdad, A., 2010. New chronometric data from Ifri n'Ammar (Morocco) and the chronostratigraphy of the Middle Paleolithic in the western Maghreb. J. Hum. Evol. 59, 672–679.

Robbins, L.H., Murphy, M.L., Brook, G.A., Ivester, A.H., Campbell, A.C., Klein, R.G., Milo, R.G., Stewart, K.M., Downey, W.S., Stevens, N.J., 2000. Archaeology, palaeoenvironment, and chronology of the Tsodilo Hills white paintings rock shelter, northwest Kalahari Desert, Botswana. J. Archaeol. Sci. 27, 1085–1113.

Robert, A., Soriano, S., Rasse, M., Stokes, S., Huysecom, E., 2003. First chrono-cultural reference framework for the West African Paleolithic: new data from Ounjougou, Dogon Country. Mali. J. Afr. Archaeol. 1, 151–169.

Rohli, R.V., Vega, A.J., 2008. Climatology. Jones and Bartlett Publishers, Sudbury.

Rose, J.I., Usik, V.I., Marks, A.E., Hilbert, Y.H., Galletti, C.S., Parton, A., Geiling, J.M., Cerny, V., Morley, M.W., Roberts, R.G., 2011. The Nubian complex of Dhofar, Oman: an African Middle Stone Age industry in southern Arabia. Plos One 6, 1–22.

Rossignol-Strick, M., 1985. Mediterraniean Quaternary sapropels, an immediate response of the African monsoon to variation of insolation. Palaeogeogr. Palaeoclimatol. Palaeoecol. 49, 237–263.

Rostek, F., Bard, E., Beaufort, L., Sonzogni, C., Ganssen, G., 1997. Sea surface temperature and productivity records for the past 240 ka in the Arabian Sea. Deep-Sea Res. 44, 1461–1480.

Saji, N.H., Goswami, B.N., Vinayachandran, P.N., Yamagata, T., 1999. A dipole mode in the tropical Indian Ocean. Nature 401, 360–363.

Sandel, B., Arge, L., Dansgaard, B., Davies, R.G., Gaston, K.J., Sutherland, W.J., Svenning, J.-C., 2011. The influence of late Quaternary climate change velocity on species endemism. Science 334, 660–664.

Schneider, R.R., Muller, P.J., Ruhland, G., Meinecke, G., Schmidt, H., Wefer, G., 1995. Late Quaternary surface temperatures and productivity in the east equatorial South Atlantic: response to changes in trade/monsoon wind forcing and surface water advection. In: Wefer, G., Berger, W.H., Siedler, G., Webb, D.J. (Eds.), The South Atlantic: Present and Past Circulation. Springer Verlag, Berlin, pp. 527–551.

Scholz, C.A., Johnson, T.C., Cohen, A.S., King, J.W., Peck, J.A., Overpeck, J.T., Talbot, M.R., Brown, E.T., Kalindekafe, L., Amoako, P.Y.O., Lyons, R.P., Shanahan, T.M., Castañeda, I.S., Heil, C.W., Forman, S.L., McHargue, L.R., Beuning, K.R., Gomez, J., Pierson, J., 2007. East African megadroughts between 135 and 75 thousand years ago and bearing on early-modern human origins. Proc. Natl. Acad. Sci. 104, 16416–16421.

Please cite this article in press as: Blome, M.W., et al., The environmental context for the origins of modern human diversity: A synthesis of regional variability in African climate 150,000–30,000 years ago, Journal of Human Evolution (2012), doi:10.1016/j.jhevol.2012.01.011

Schwarcz, H.P., Blackwell, B., Goldberg, P., Marks, A.E., 1993. Uranium series dating of carbonates from Bir Tarfawi and Bir Sahara East. In: Wendorf, F., Schild, R., Close, A.E. (Eds.), Egypt During the Last Interglacial: The Middle Paleolithic of Bir Tarfawi and Bir Sahara East. Plenum Press, New York, pp. 205–217.

Schwarcz, H.P., Rink, W.J., 2000. ESR dating of the Die Kelders Cave 1 site, South Africa. J. Hum. Evol. 38, 121–128.

Shea, J.J., 2008. The Middle Stone Age archaeology of the Lower Omo Valley Kibish Formation: excavations, lithic assemblages, and inferred patterns of early *Homo sapiens* behavior. J. Hum. Evol. 55, 448–485.

Shea, J.J., 2011. *Homo sapiens* is as *Homo sapiens* was? Curr. Anthropol. 52, 1–35.

Sicre, M.A., Ternois, Y., Paterne, M., Boireau, A., Beaufort, L., Martinez, P., Bertrand, P., 2000. Biomarker stratigraphic records over the last 150 years off the NW African coast at 25°N. Org. Geochem. 31, 577–588.

Skinner, A.R., Hay, R.L., Masao, F., Blackwell, B.A.B., 2003. Dating the Naisiusiu Beds, Olduvai Gorge, by electron spin resonance. Quatern. Sci. Rev. 22, 1361–1366.

Smith, J.R., Hawkins, A.L., Asmerom, Y., Polyak, V., Giegengack, R., 2007. New age constraints on the Middle Stone Age occupations of Kharga Oasis, Western Desert. Egypt. J. Hum. Evol. 52, 690–701.

Sorin, L., Vaks, A., Bar-Matthews, M., Porat, R., Frumkin, A., 2010. Late Pleistocene paleoclimatic and paleoenvironmental reconstruction of the Dead Sea area (Israel), based on speleothems and cave stromatolites. Quatern. Sci. Rev. 29, 1201–1211.

Stager, J.C., Ryves, D.B., Chase, B.M., Pausata, F.S., 2011. Catastrophic drought in the Afro-Asian monsoon region during Heinrich event 1. Science 331, 1299–1302.

Stiner, M.C., Munro, N.D., Surovell, T.A., Tchernov, E., Bar-Yosef, O., 1999. Paleolithic population growth pulses evidenced by small animal exploitation. Science 283, 190–194.

Stokes, S., Haynes, G., Thomas, D.S.G., Horrocks, J.L., Higginson, M., Malifa, M., 1998. Punctuated aridity in southern Africa during the last glacial cycle: the chronology of linear dune construction in the northeast Kalahari. Palaeogeogr. Palaeoclimatol. Palaeoecol. 137, 305–322.

Stone, J.R., Westover, K.S., Cohen, A.S., 2011. Late Pleistocene paleohydrography and diatom paleoecology of the central basin of Lake Malawi, Africa. Palaeogeogr. Palaeoclimatol. Palaeoecol. 303, 51–70.

Street, F.A., Grove, A.T., 1979. Global maps of lake-level fluctuations since 30,000 yr BP. Quatern. Res. 12, 83–118.

Stuut, J.B.W., Lamy, F., 2004. Climate variability at the southern boundaries of the Namib (southwestern Africa) and Atacama (northern Chile) coastal deserts during the last 120,000 yr. Quatern. Res. 62, 301–309.

Surovell, T.A., Finley, J.B., Smith, G.M., Brantingham, P.J., Kelly, R., 2009. Correcting temporal frequency distributions for taphonomic bias. J. Archaeol. Sci. 36, 1715–1724.

Szabo, B.J., Haynes, C.V., Maxwell, T.A., 1995. Ages of Quaternary pluvial episodes determined by uranium series and radiocarbon dating of lacustrine deposits of eastern Sahara. Palaeogeogr. Palaeoclimatol. Palaeoecol. 113, 227–242.

Thomas, D.S.G., Bailey, R., Shaw, P.A., Durcan, J.A., Singarayer, J.S., 2009. Late Quaternary highstands at Lake Chilwa, Malawi: frequency, timing and possible forcing mechanisms in the last 44 ka. Quatern. Sci. Rev. 28, 526–539.

Thomas, D.S.G., Shaw, P.A., 2003. Late Quaternary environmental change in central southern Africa: new data, synthesis, issues and prospects. Quatern. Sci. Rev. 21, 783–797.

Tierney, J.E., Russell, J.M., Huang, Y., Sinninghe Damsté, J.S., Hopmans, E.C., Cohen, A.S., 2008. Northern Hemisphere controls on tropical southeast African climate during the past 60,000 years. Science 322, 252–255.

Tishkoff, S.A., Reed, F.A., Friedlaender, F.R., Ehret, C., Ranciaro, A., Froment, A., Hirbo, J.B., Awomoyi, A.A., Bodo, J.M., Doumbo, O., Ibrahim, M., Juma, A.T., Kotze, M.J., Lema, G., Moore, J.H., Mortensen, H., Nyambo, T.B., Omar, S.A., Powell, K., Pretorius, G.S., Smith, M.W., Thera, M.A., Wambebe, C., Weber, J.L., Williams, S.M., 2009. The genetic structure and history of Africans and African Americans. Science 324, 1035–1044.

Tisserand, A., Malaizé, B., Jullien, E., Zaragosi, S., Charlier, K., Grousset, F., 2009. African monsoon enhancement during the penultimate glacial period (MIS 6.5~170 ka) and its atmospheric impact. Paleoceanography 24, PA2220. doi:10.1029/2008PA001630.

Tjallingii, R., Claussen, M., Stuut, J.B.W., Fohlmeister, J., Jahn, A., Bickert, T., Lamy, F., Röhl, U., 2008. Coherent high- and low-latitude control of the northwest African hydrological balance. Nat. Geosci. 1, 670–675.

Toggweiler, J.R., Russell, J., 2008. Ocean circulation in a warming climate. Nature 451, 286–288.

Trauth, M.H., Deino, A.L., Bergner, A.G.N., Strecker, M.R., 2003. East African climate change and orbital forcing during the last 175 kyr BP. Earth Planet. Sci. Lett. 206, 297–313.

Trauth, M.H., Larrasoaña, J.C., Mudelsee, M., 2009. Trends, rhythms, and events in Plio-Pleistocene African climate. Quatern. Sci. Rev. 28, 399–411.

Tribolo, C., Mercier, N., Selo, M., Valladas, H., Joron, J.L., Reyss, J.L., Henshilwood, C., Sealy, J., Yates, R., 2006. TL dating of burnt lithics from Blombos Cave (South Africa): further evidence for the antiquity of modern human behaviour. Archaeometry 48, 341–357.

Tribolo, C., Mercier, N., Valladas, H., 2005. Chronologie des technofaciès Howiesons Poort et Still Bay (Middle Stone Age, Afrique du Sud): bilan et nouvelles données de la luminescnece. Bull. Soc. Préhist. Fr. 102, 855–866.

Trinkaus, E., 2005. Early modern humans. A. Rev. Anthropol. 34, 207–230.

Tryon, C.A., Faith, J.T., Peppe, D.J., Fox, D.L., McNulty, K.P., Jenkins, K., Dunsworth, H., Harcourt-Smith, W., 2010. The Pleistocene archaeology and environments of the Wasiriya Beds, Rusinga Island, Kenya. J. Hum. Evol. 59, 657–671.

Tryon, C.A., Roach, N.T., Logan, M.A.V., 2008. The Middle Stone Age of the northern Kenyan Rift: age and context of new archaeological sites from the Kapedo Tuffs. J. Hum. Evol. 55, 652–664.

Vaks, A., Bar-Matthews, M., Ayalon, A., Halicz, L., Frumkin, A., 2007. Desert speleothems reveal climatic window for African exodus of early modern humans. Geology 35, 831–834.

Valladas, H., Wadley, L., Mercier, N., Froget, L., Tribolo, C., Reyss, J.L., Joron, J.L., 2005. Thermoluminescence dating on burnt lithics from Middle Stone Age layers at Rose Cottage Cave. S. Afr. J. Sci. 101, 169–174.

Van Andel, T.H., 1989. Late Pleistocene sea levels and the human exploitation of the shore and shelf of southern South Africa. J. Field Archaeol. 16, 133–155.

Van Campo, E., Duplessy, J.C., Rossignol-Strick, M., 1982. Climatic conditions deduced from a 150 kyr oxygen isotope-pollen record from the Arabian Sea. Nature 296, 56–59.

Van Neer, W., 1989. Contribution to the Archaeozoology of Central Africa. In: Annales Sciences Zoologiques, vol. 259. Musee Royal de l'Afrique Centrale (Tervuren).

Van Noten, F., 1977. Excavations at Matupi Cave. Antiquity 51, 35–40.

Van Peer, P., Fullagar, R., Stokes, S., Bailey, R.M., Moeyersons, J., Steenhoudt, F., Geerts, A., Vanderbeken, T., De Dapper, M., Geus, F., 2003. The Early to Middle Stone Age transition and the emergence of modern human behaviour at site 8-B-11, Sai Island, Sudan. J. Hum. Evol. 45, 187–193.

Verdu, P., Austerlitz, F., Estoup, A., Vitalis, R., Georges, M., Thery, S., Froment, A., Le Bomin, S., Gessain, A., Hombert, J.M., Van der Veen, L., Quintana-Murci, L., Bahuchet, S., Heyer, E., 2009. Origins and genetic diversity of pygmy hunter-gatherers from western Central Africa. Curr. Biol. 19, 312–318.

Vermeersch, P.M., 2002. Palaeolithic Quarrying Sites in Upper and Middle Egypt. Leuven University Press, Leuven.

Vermeersch, P.M., Paulissen, E., Stokes, S., Charlier, C., Van Peer, P., Stringer, C.B., Lindsay, W., 1998. A Middle Paleolithic burial of a modern human at Taramsa Hill, Egypt. Antiquity 72, 475–484.

Vogel, J.C., 2001. Radiometric dates for the Middle Stone Age in South Africa. In: Tobias, P.V., Raath, M., Maggi-Cecchi, J., Doyle, G. (Eds.), Humanity from African Naissance to Coming Millenia: Colloquia in Human Biology and Paleoanthropology. Florence University Press, Florence, pp. 261–268.

Vogel, J.C., Fuls, A., Visser, E., 1986. Pretoria radiocarbon dates III. Radiocarbon 28, 1133–1172.

Vogel, J.C., Partridge, T.C., 1984. Preliminary radiometric ages for the Taung tufas. In: Vogel, J.C. (Ed.), Late Cainozoic Palaeoclimates of the Southern Hemisphere. A.A. Balkema, Rotterdam, pp. 507–514.

Vogelsang, R., 1998. Middle Stone Age Fündstellen in Sudwest-Namibia. Heinrich Barth Institut, Köln.

Voight, B., Gabriel, B., Lassonczy, K., Ghod, M., 1990. Quaternary events at the Horn of Africa. Berl. Geowiss. Abh. 120, 679–694.

Walter, R., Buffler, R.T., Bruggemann, J.H., Guillaume, M.M.M., Berhe, S.M., Negassi, B., Libeskal, Y., Cheng, H., Edwards, R.L., Von Cosel, R., Néraudeau, D., Gagnon, M., 2000. Early human occupation of the Red Sea coast of Eritrea during the last interglacial. Nature 405, 65–69.

Wang, Q., Tobias, P.V., Roberts, D.L., Jacobs, Z., 2008. A re-examination of a human femur found at the Blind River Site, East London, South Africa: its age, morphology, and breakage pattern. Anthropol. Rev. 71, 43–61.

Wefer, G., Berger, W.H., 1991. Isotope paleontology: growth and composition of extant calcareous species. Mar. Geol. 100, 207–248.

Weisrock, A., Wengler, L., Mathieu, J., Ouammou, A., Fontugne, M., Mercier, N., Reyss, J.-L., Valladas, H., Guery, P., 2006. Upper Pleistocene comparative OSL, U/Th, and ^{14}C datings of sedimentary sequences and correlative morphodynamical implications in the south-western anti-atlas (Oued Noun, 29°N, Morocco). Quaternaire 17, 45–59.

Weldeab, S., Lea, D.W., Schneider, R.R., Andersen, N., 2007. 155,000 years of West African monsoon and ocean thermal evolution. Science 316, 1303–1307.

Wendorf, F., Close, A., Schild, R., 1987. Middle Paleolithic occupations at Bir Tarfawi, Egypt. Afr. Archaeol. Rev. 5, 4963.

Wendorf, F., Schild, R., Close, A.E., 1989. The Prehistory of Wadi Kubbaniya. In: Stratigraphy, Paleoeconomy and Environment, vol 2. Southern Methodist University Press, Dallas.

Wendorf, F., Schild, R., Close, A.E., 1993. Middle Palaeolithic occupations at Bir Tarfawi and Bir Sahara East, Western Desert of Egypt. In: Krzyzaniak, L., Kobusiewicz, M., Alexander, J. (Eds.), Environmental Change and Human Culture in the Nile Basin and Northern Africa until the Second Millennium B.C. Museum Archeologiczne W. Poznianu, Poznan, pp. 103–112.

White, T.D., Asfaw, B., DeGusta, D., Gilbert, H., Richards, G.D., Suwa, G., Howell, F.C., 2003. Pleistocene *Homo sapiens* from Middle Awash, Ethiopia. Nature 423, 742–747.

Woltering, M., Johnson, T.C., Werne, J.P., Schouten, S., Sinninghe Damsté, J.S., 2011. Late Pleistocene temperature history of southeast Africa: a TEX_{86} temperature record from Lake Malawi. Palaeogeogr. Palaeoclimatol. Palaeoecol. 303, 93–102.

Wrinn, P.J., Rink, W.J., 2003. ESR dating of tooth enamel from Aterian levels at Mugharet el 'Aliya (Tangier, Morocco). J. Archaeol. Sci. 30, 123–133.

Yellen, J.E., Brooks, A.S., Helgren, D.M., Tappen, M., Ambrose, S.H., Bonnefille, R., Feathers, J.K., Goodfriend, G., Ludwig, K., Renne, P., Stewart, K., 2005. The archaeology of Aduma Middle Stone Age Sites in the Awash Valley, Ethiopia. Paleoanthropology 10, 25–100.

Yuan, Y., Zhou, W., Yang, H., Li, C., 2008. Warming in the northwestern Indian Ocean associated with the El Niño event. Adv. Atmos. Sci. 25, 246–252.

Zhao, M., Beveridge, N.A.S., Shackleton, N.J., Sarnthein, M., Eglinton, G., 1995. Molecular stratigraphy of cores off northwest Africa; sea surface temperature history over the last 80 ka. Paleoceanography 10, 661–675.

Please cite this article in press as: Blome, M.W., et al., The environmental context for the origins of modern human diversity: A synthesis of regional variability in African climate 150,000–30,000 years ago, Journal of Human Evolution (2012), doi:10.1016/j.jhevol.2012.01.011